

University of Mosul

Collage of Veterinary Medicine



Comparison between Two Biological Dressing for Induced Cutaneous Wound Healing in Feline

Mustafa Mohammed Zaki Danoon

MSc. / Thesis

Veterinary Medicine / Veterinary Surgery

Supervised By

Assistant Professor Dr.

Sahar Mohammed Ibrahim

2024 A.D.

1446A.H.

Comparison between Two Biological Dressing for Induced Cutaneous Wound Healing in Feline

A Thesis Submitted

By

Mustafa Mohammed Zaki Danoon

To

The Council of the College of Veterinary Medicine

University of Mosul

In

Partial Fulfillment of the Requirements

For the Degree of Master

In

Veterinary Medicine / Veterinary Surgery

Supervised By

Assistant Professor Dr.

Sahar Mohammed Ibrahim

2024 A.D.

1446 A.H.



قُلِ اللَّهُمَّ مَالِكَ الْمُلْكِ تُؤْتِي
الْمُلْكَ مَنْ تَشَاءُ وَتَنْزِعُ الْمُلْكَ
مِمَّنْ تَشَاءُ وَتُعِزُّ مَنْ تَشَاءُ
وَتُذِلُّ مَنْ تَشَاءُ بِيَدِكَ الْخَيْرُ
إِنَّكَ عَلَى كُلِّ شَيْءٍ قَدِيرٌ



□ سورة ال عمران

الآية (٢٦)

Supervisor Certification

I certify that this thesis entitled “**Comparison between Two Biological Dressing for Induced Cutaneous Wound Healing in Feline**” was prepared under my supervision at the College of Veterinary Medicine / University of Mosul, as a partial fulfillment of the requirements for the degree of Master in Veterinary Medicine/Veterinary surgery.

Signature:

Name: **Assist. Prof. Dr. Sahar Mohammed Ibrahim**

Date: 30/06/2024

Linguist Certification

I certify that this thesis entitled “**Comparison between Two Biological Dressing for Induced Cutaneous Wound Healing in Feline**” has been linguistically reviewed and corrected for language and expression mistakes; therefore, it becomes ready for the defense as for as the integrity of the writing and expression.

Signature:

Name: **Lect. Huda Abdullah Abdulateef**

Date: 04/ 07/ 2024

Statistic Certification

I certify that this thesis entitled “**Comparison between Two Biological Dressing for Induced Cutaneous Wound Healing in Feline**” has been statistically reviewed and corrected for statistic and expression mistakes; therefore, it becomes ready for the defense as for as the integrity of the writing and expression.

Signature:

Name: **Assistant Professor Dr. Osama Basheer Shukur**

Date: 04 /07/ 2024

Department of Surgery and Theriogenology Certification

Based on the supervisor and linguistics recommendations, I forward this thesis for the defense.

Signature:

Name: **Prof. Dr. Mohammed Abdul-elah Rahawy**

Date: 14 / 07 /2024

Postgraduate Committee Director Certification

Based on the supervisor, linguistics and the Head of the Department of Surgery and Theriogenology recommendations, I forward this thesis for the defense.

Signature:

Name: **Prof. Dr. Raad Abdulghany Al-Sanjary**

Date: 31 / 07 /2024

Examination Committee Decision

We, the members of the Evaluation and Discussion Committee, have reviewed this thesis and discussed the student **Mustafa Mohammed Zaki Danoon** in its contents on 26 / 8 /2024, and certify that the deserves the degree of Master in Veterinary Medicine/ Veterinary Surgery.

Signature

Assistant Professor

Dr. Nazhad Hussin Qader

Member

Signature

Assistant Professor

Dr. Shahbaa Khalil Ibrahim

Member

Signature

Professor

Dr. Osama Hazem Ismail

Chairman

Signature

Assistant Professor

Dr. Sahar Mohammed Ibrahim

Member and Supervisor

College Council Decision

The College of Veterinary Medicine Council was met, the meeting, on / /2024, and decided to award him a degree of Master in Veterinary surgery.

Signature

Professor

Dr. Raad Abdulghany Al-Sanjary

Assistant Dean for Scientific Affairs

Signature

Professor

Dr. Dhafer Mohammad Aziz

Dean

Acknowledgment

I thank and praise the Almighty God for blessing everything in my life including the ceaseless efforts I spent to pursue my postgraduate studies.

I extend my thanks and gratitude to the Deanship of the College of Veterinary Medicine, represented by the Dean, and his two assistants, for the support and facilities they provided for this study.

I am very indebted and grateful to my supervisor, **Assist. prof. Dr. Sahar Mohammed Ibrahim** for her great help, support, endless advice, patience, and suggestions for completing this thesis in the most comprehensive, clear, and accurate way.

I would like to express my appreciation to all the academic and technical staff in the Department of Surgery and Theriogenology at the College of Veterinary Medicine / the University of Mosul, for their tremendous support and patience that contributed to the success of this work.

In addition, I would like to provide infinite thanks for special ones and the dearest to my heart, my father and my mother. I will never forget my sincere thanks to my dear wife, children, and brothers for their support during my studies. May God reward them success and his ongoing bless.

Abstract

The study was planned to compare between acellular ovine skin and acellular bovine pericardium as biological dressing to repair induced cutaneous wound in feline. Eighteen local breed adult cats were divided into two equal groups. A full-thickness skin wounds of 4x4 cm dimensions were created on the backs of all felines. In the first group, acellular ovine skin of 3x3 cm patch was used to dress these full-thickness back wounds whereas acellular bovine pericardium of a same size was used to cover these induced wounds in the second group. Grossly, the wounds healing was assessed daily post dressing in both groups, in addition to the histopathological examination, immunohistochemical study and ultrasonography at days 7, 14, and 21 post-wounding. The mechanical properties of both biological dressing before and after decellularization was depended also.

The clinical outcomes showed a significant difference ($P < 0.05$) between both groups in pliability, color and adherence of biological dressing to the underling wound bed. The results of physical planimetry measurements for the wound size that performed on days 0, 7, 14, and 21 following dressing exhibited presence of reduction in the wound size area especially in the first group rather than second group. In addition, the contraction percentage was increased and reached up to 65% of wound size. Also, the percentage of total wound healing was increased from day 0 to day 21 that reached over 85%.

The histopathological manifestations revealed presence of significant differences in most of the observed histopathological parameters between both groups during the whole time period of study. In the first group, the dressing of wounds with acellular ovine skin on day 7 was much better which characterized by existence of well-developed

granulation tissue, good angiogenesis, less inflammatory response and infiltration of polymorphonuclear and mononuclear inflammatory cells as compare with dressing of wounds by acellular bovine pericardium in second group. Besides, the doppler ultrasound examination revealed presence of good blood perfusion since day 10 that became more detectable on day 12 in first group and day 14 in second group, then continue to increase until reached its peak on day 21.

The immunohistochemistry results of vascular endothelium growth factor expression showed variable intensity expression and visualization of VEGF in both groups. However, in the first group the expression and intensity of VEGF was appeared more than second group. Furthermore, testing of mechanical properties of both acellular tissues exhibited hug improvement in their mechanical characters after decellularization especially maximum load and modulus of elasticity. In a nutshell, acellular ovine skin was much better than acellular bovine pericardium as a biological dressing for extensive wound healing in feline.

List of Contents

	Contents	Page Number
Chapter One	Introduction	1-5
1-1	Hypothesis	4
1-2	Aims of Study	5
Chapter Two	Review of Literature	6-27
2-1	Skin	6
2-1-1	Anatomy of Skin	6-8
2-1-2	Feline Skin	9-13
2-1-3	Mechanical properties of Skin	13
2-2	Wounds	14-15
2-3	Wound Healing	15-17
2-4	Skin Substitutions	17-18
2-4-1	Traditional Dressings	19
2-4-2	Bioactive Dressing (Biomaterials)	19-21
2-4-2-1	Acellular Bovine pericardium	21-22
2-4-2-2	Acellular Ovine Skin	22-23
2-5	Decellularization	23-24
2-5-1	Physical Methods for Decellularization	24-25
2-5-2	Chemical Methods for Decellularization	25-26
2-5-3	Biological Methods for Decellularization	26-27
Chapter Three	Materials and Methods	28-42
3-1	Animals	28
3-2	Preparation of Acellular Ovine Skin	28-29
3-3	Preparation of Acellular Bovine pericardium	30
3-4	Mechanical Evaluation	31-33
3-4-1	Uniaxial Stretching Test	33-34
3-5	Experimental Design	34-35

3-6	Preoperative Preparation	35
3-7	Anesthetic Protocol	35
3-8	Surgical Procedure	36-38
3-9	Post-operative Care	38
3-10	Wound Healing Assessment	38
3-10-1	Macroscopic Examination	38-39
3-10-2	Physical Evaluation	39
3-10-2-1	Planimetry	40
3-10-3	Microscopic Evaluation	40
3-10-3-1	Histopathological assessment	40-41
3-10-3-2	Immunohistochemistry of VEGF	41
3-11	Doppler Ultrasound Evaluation	42
3-12	Statistical Analysis	42
Chapter Four	Results	43-78
4-1	Mechanical Results	43-47
4-2	Macroscopical Results	47
4-2-1	Cross Results	47-50
4-2-2	Wound Bed Results	50-55
4-2-3	Planimetry	55-57
4-3	Microscopical Results	57
4-3-1	Histopathological Results	57-68
4-3-2	Immunohistochemistry Results	69-75
4-4	Physical Results	75
4-4-1	Doppler Ultrasound Results	75-78
Chapter Five	Discussion	79-93
Chapter Six	Conclusions and Recommendations	93-94
6-1	Conclusions	93
6-2	Recommendations	94
	References	95-122

List of Figures

Figure No.	Title	Page
Figure 1	Illustration for skin histology and anatomy	9
Figure 2	Photographic image of acellular ovine skin following complete decellularization	29
Figure 3	Photographic image shows horizontal orbital shaker machine	29
Figure 4	Histological section of acellular ovine skin patch	29
Figure 5	Photographic image of acellular bovine pericardium following complete decellularization.	30
Figure 6	Histological section of acellular bovine pericardium dressing	31
Figure7	Photographic image for the stripes of both acellular ovine skin and bovine pericardium samples	32
Figure 8	Photographic image shows testing the mechanical properties of both acellular tissues	32
Figure 9	Photographic image shows Alfa Universal testing machine	33
Figure 10	Photographic image shows the tearing of both acellular tissues	34
Figure 11	Illustration for the experimental design.	35
Figure 12	Photographic image shows the induced wound of on the back of the cat	36
Figure13	Photographic images for suturing of acellular ovine skin	37
Figure14	Photographic images for suturing of acellular bovine pericardium	37
Figure15	Photographic images for four- layers bandaging of the induced wounds	38
Figure16	Photographic images for doppler ultrasonographic examination	42
Figure 17	Diagrams shows the maximum load (Newton) of ovine skin before and after decellularization	44
Figure 18	Diagrams shows the maximum load (Newton) of bovine pericardium before and after decellularization	44
Figure 19	Diagrams shows the Modulus of elasticity (mm) of ovine skin before and after decellularization.	45

Figure 20	Diagrams shows the Modulus of elasticity (mm) of bovine pericardium before and after decellularization	45
Figure 21	Diagrams shows comparison between the maximum load (newton) of both decellularized ovine skin and decellularized bovine pericardium after decellularization.	46
Figure 22	Diagrams shows comparison between the Modulus of elasticity (mm) of both decellularized ovine skin and decellularized bovine pericardium after decellularization.	46
Figure 23	Diagrams of the comparison in clinical scoring between two experimental groups in day 7 post dressing.	48
Figure 24	Diagrams of the comparison in macroscopic gross scoring between two experimental groups in day 14 post dressing.	48
Figure 25	Diagrams of the comparison in macroscopic gross scoring between two experimental groups in day 21 post dressing.	49
Figure 26	Photographic image for acellular ovine skin after 7 days following dressing	51
Figure 27	Photographic image for acellular bovine pericardium after 7 days	51
Figure 28	Photographic image for acellular ovine skin after 14 days	52
Figure 29	Photographic image for acellular bovine pericardium after 14 days	52
Figure 30	Photographic image for acellular ovine skin after 21 days	53
Figure 31	Photographic image for acellular bovine pericardium after 21 days	53
Figure 32	Diagrams of the comparison in macroscopic gross scoring between two experimental groups in day 7 post dressing.	54
Figure 33	Diagrams of the comparison in macroscopic gross scoring between two experimental groups in day 14 post dressing.	54
Figure 34	Diagrams of the comparison in macroscopic gross scoring between two experimental groups in day 21 post dressing.	55

Figure 35	Diagrams of the comparison in wound planimetry dimensions between two experimental groups in day 7 post dressing.	56
Figure 36	Diagrams of the comparison in wound planimetry dimensions between two experimental groups in day 14 post dressing.	56
Figure 37	Diagrams of the comparison in wound planimetry dimensions between two experimental groups in day 21 post dressing.	57
Figure 38	Histopathological section of first group at day 7 after dressing in a cat skin wound	57
Figure 39	Histopathological section of first group at day 7 after dressing in a cat skin wound	58
Figure 40	Histopathological section of second group at day 7 after dressing in a cat skin wound	58
Figure 41	Histopathological section of second group at day 7 after dressing in a cat skin wound.	59
Figure 42	Histopathological section of first group at day 14 after biomaterial dressing in a cat skin wound.	60
Figure 43	Histopathological section of first group at day 14 after dressing in a cat skin wound	60
Figure 44	Histopathological section of first group at day 14 after dressing in a cat skin wound	61
Figure 45	Histopathological section of first group at day 14 after dressing in a cat skin wound	61
Figure 46	Histological section of second group at day 14 after dressing in a cat skin wound	62
Figure 47	Histological section of second group at day 15 after dressing in a cat skin wound.	62

Figure 48	Histological section of second group at day 14 after dressing in a cat skin wound.	63
Figure 49	Histological section of first group at day 21 after dressing in a cat skin wound.	64
Figure 50	Histological section of first group at day 21 after dressing in a cat skin wound.	64
Figure 51	Histological section of first group at day 21 after dressing in a cat skin wound	65
Figure 52	Histological section of second group at day 21 after dressing in a cat skin wound	66
Figure 53	Histological section of second group at day 21 after dressing in a cat skin wound.	66
Figure 54	Diagrams of the comparison in inflammatory response scoring between two experimental groups in days 7, 14 and 21 post dressing.	67
Figure 55	Diagrams of the comparison in granulation tissue formation scoring between two experimental groups in days 7, 14 and 21 post dressing.	67
Figure 56	Diagrams of the comparison in re-epithelization scoring between two experimental groups in days 7, 14 and 21 post dressing.	68
Figure 57	Diagrams of the comparison in blood perfusion formation scoring between two experimental groups in days 7, 14 and 21 post dressing.	68
Figure 58	Immunohistochemical staining for VEGF of first group at day 7 after dressing in a cat skin wound.	70
Figure 59	Immunohistochemical staining for VEGF of second group at day 7 after dressing in a cat skin wound.	70

Figure 60	Immunohistochemical staining for VEGF of first group at day 14 after dressing in a cat skin wound.	71
Figure 61	Immunohistochemical staining for VEGF of second group at day 14 after dressing in a cat skin wound.	71
Figure 62	Immunohistochemical staining for VEGF of first group at day 21 after dressing in a cat skin wound.	72
Figure 63	Immunohistochemical staining for VEGF of second group at day 21 after dressing in a cat skin wound.	72
Figure 64	Diagrams shows VEGF expression within decellularized ovine skin on days 7, 14, 21 post dressing.	73
Figure 65	Diagrams shows VEGF expression within decellularized bovine pericardium on days 7, 14, 21 post dressing.	73
Figure 66	Diagrams show comparison of VEGF between first and second group on days 7 post dressing	74
Figure 67	Diagrams show comparison of VEGF expression between first and second group on days 14 post dressing.	74
Figure 68	Diagrams show comparison of VEGF expression between first and second group on days 21 post dressing.	75
Figure 69	Ultrasonographic image for 1 st group (AOS) after 12 days of dressing.	76
Figure 70	Ultrasonographic image for 1 st group (AOS) after 14 days of dressing.	76
Figure 71	Ultrasonographic image for 1 st group (AOS) after 18 days of dressing.	77
Figure 72	Ultrasonographic image for 2 nd group (ABP) after 12 days of dressing.	77
Figure 73	Ultrasonographic image for 2 nd group (ABP) after 14 days of dressing.	78
Figure 74	Ultrasonographic image for 2 nd group (ABP) after 18 days of dressing.	78

List of Tables

Table no.	Title	Page
Table .1	Macroscopical criteria for evaluation of acellular ovine skin and acellular bovine pericardium dressing performance.	39
Table .2	Gross criteria for evaluation of wound bed healing.	39
Table .3	Histopathological parameters for semi-qualitative assessment for dressing performance.	41
Table .4	Immunohistochemistry scoring of VEGF.	41
Table .5	Show the mechanical properties of decellularized ovine skin and decellularized bovine pericardium before and after decellularization.	43
Table .6	Comparison in clinical scoring between two experimental groups in days 7, 14, 21 post dressing.	50
Table .7	Show the expression of VEGF within beds of both transplanted acellular ovine skin and acellular bovine pericardium during the period of study.	69

List of Abbreviations

Abbreviation	Total name
ABP	Acellular Bovine Pericardium
AOS	Acellular Ovine Skin
DAB	Dako-Envision + System-Hrp
EGF	Epidermal Growth Factor
EGTA	Ethylene Glycol Tetra Acetic Acid
EDTA	Ethylenediaminetetraacetic Acid
ECM	Extracellular Matrix
H&E	Hematoxylin And Eosin
IHC	Immunohistochemistry
MHC	Major Histocompatibility Complex
PBS	Phosphate Buffered Saline
PDGF	Platelet-Derived Growth Factor
SDS	Sodium Deoxycholate Solution
SWC	Surgical Wound Classification
TWH	Total Wound Healing
VEGF	Vascular Endothelial Growth Factor
WC	Wound Contraction

Chapter One

Introduction

Cutaneous wounds are still representing as one of the most common daily cases in small animal practice (Corr, 2009; Kožár *et al.*, 2018; Angelou *et al.*, 2022). Skin and its associated appendages representing the largest body organ that accounting about 15% of the entire mature body weight. Its position as the first defensive shield between the body and the atmosphere enables it achieving a lot of dynamic roles, especially protection against various invaders and factors, thermoregulation and prevention water and electrolytes losses (Kolarsick *et al.* 2011; Wong *et al.*, 2016; Dąbrowska *et al.*, 2018). Its position and huge proportion predisposing it to be the first tissue that face any invasion or injury especially large extensive wounds that are still representing an economical and physiological challenges for both human and veterinary world due to their extended healing time, need for a continues complex management and being more vulnerable for various complications (Davidson, 2015; Pavletic, 2018; Levitan *et al.*, 2021). In addition, the most serious impact is its life threatening potential because wounds larger than 10% of body surface area can cause a potentially life-threatening losing in extracellular fluid (Percival, 2002). This particularly found in feline family because cats are one of the most problematic behavioral animals that are more curious and cautious about investigating things (Crowell-Davis, 2007; Bradshaw, 2017; Bradshaw 2018; Windschnurer *et al.*, 2022).

This curious nature makes cats more vulnerable for being injured with many kinds of wounds particularly those with extensive skin loss that needs to adapt successful wound management to prevent complications (Balsa and Culp, 2015; Cavanaugh, 2024). Also, to get the perfect swift healing as it is the crucial process for restoring skin integrity especially in

cats. This is because their cutaneous healing process is not an easy and fast process as in other animals. Besides, it is entirely different from what is happening with other domestic animals because of the deficiencies in many wound healing features, especially poor inflammatory response and weakened granulation tissue formation that deprived blood vascularization and diminish contraction (Volk & Bohling., 2013; Pavletic *et al.*, 2018; Nolff, 2021). This actually leads to poor quality healing response (Nolff *et al.*, 2017). Besides, many studies revealed that there are great differences in macroscopic appearance of wounds, skin perfusion, and even in microscopic cell structure of feline wounds that make extended wound healing and “pseudo-healing” phenomena much more happening in cats comparable with other species especially dogs (Angelou *et al.*, 2022; Chatzimisios *et al.*, 2023; Cavanaugh, 2024). Furthermore, some researchers even mentioned that total time to wound closure in cat can extended up to 39-75 days in some conditions (Nolff *et al.*, 2018; Bohling *et al.*, 2004)

Moreover, the normal histology and anatomy of cat's skin is relatively different from that of other species that's in turn influence deeply on kind of its healing process. Additionally, feline skin is very flexible and more moveable over most of parts of body surface. Besides, the blood circulation of skin especially within the trunk region is much less than that of other mammals as a result of their relatively low mass of tertiary blood vessels that's in turn leading to low degree of cutaneous perfusion (Langley-Hobbs *et al.*, 2013; Hollenbeck *et al.*, 2023). All these anatomical, histological and physiological variations associated with feline skin make healing of extensive skin loss wounds in cat is a challenging issue that require using special alternative therapeutic options to deal

efficiently and successfully with such kind of wounds (Balsa and Culp, 2015; Cavanaugh, 2024).

Although, dealing and treatment of various wounds is a common daily practice in veterinary clinics but extensive wounds are more challenging cases that necessitate suitable open wound therapy to guarantee their effective management (Nolff, 2021; Dermisiadou *et al.*, 2023). Surgical rebuilding after excision of large volumes of tissue as it happens in association with treatment of severe trauma, infection or even neoplastic lesions represents huge challenging tricky task for the surgeon. This is because; accomplishing the quick uncomplicated wound healing is always required for large volume wounds because failure of wound repair is potentially disastrous (Bohling *et al.*, 2006).

The purpose of extensive wound care and dressing is to generate a suitable situation for healing to happen initiates the beginning of healing, adjust the exudate, contract pain, provide mechanical support, and avoid contamination (Aisa and Parlier 2022; Li *et al.*, 2023; Mirani *et al.*, 2023). Therefore, there is significant request for finding and supplying new revolutionary materials and products that can speed up healing process (Corr, 2009; Davidson, 2015). A variety of different biodegradable, biocompatible natural and synthetic materials are continuously driven into biomedical field, especially for wound dressing and treatment (Granick *et al.*, 2020; Prete *et al.*, 2023), making biomaterial market as one of the most rapidly growing medical field (Das & Baker 2016; AL-Bayati & Hameed 2018; Luze, *et al.*, 2022; Niculescu *et al.*, 2022; Albahrawy *et al.*., 2023, Bhoopathy *et al.*, 2024).

Biological viable scaffolds that derived from pericardium, skin, small intestine and submucosa that can be harvested from human and nonhuman sources like porcine, equine, or even bovine is nowadays

constitutes the basic sources for biomaterial industry (Deng *et al.*, 2022; Kaur *et al.*, 2022). These derived biologic materials, which could be either degradable or permanent, are usually subjected to a series of procedures to achieve complete decellularization and preserve their extracellular matrix components only without any antigenic or inflammatory properties (Hillebrandt *et al.*, 2019; Choudhury *et al.*, 2020; Sokol *et al.*, 2020).

Using of natural biomaterials for promoting wound healing has become a very trendy trial due to their highly positive influence on the stages of wound healing. This can be done through supplying the appropriate healing atmosphere and acting as scaffold that facilitate bridging for the many healing aspects including cell movement, propagation, and differentiation, and thus progress tissue regeneration and repairing process. Furthermore, most of these materials display multifunctional role that participate during diverse stages of wound healing course (Shi *et al.*, 2010; Kim and Evans, 2012; Deng *et al.*, 2022; Fadilah *et al.*, 2023).

1-1: Hypothesis

Our hypothesis implies that using of acellular ovine skin and acellular bovine pericardium for dressing large cutaneous wounds in cats could speed up wound healing thus decreasing the consuming healing time, enhancing the ending cosmetic appearance and improving the chance for the return to the full and regular routine.

1-2: Aims of Study

The main aim of this study to compare between effect of acellular ovine skin and acellular bovine pericardium as biological dressing on healing of induced cutaneous wounds in feline through using the following parameters: -

1. Microscopical (histopathological and immunohistochemical) manifestation associated with using of acellular ovine skin and acellular bovine pericardium for induced full-thickness wounds.
- 2- Macroscopical and planimetry evaluations associated with using of acellular ovine skin and acellular bovine pericardium for induced full-thickness wounds.
3. Mechanical properties of acellular ovine skin and acellular bovine pericardium before and after decellularization.
4. Doppler ultrasonography for assessment blood perfusion associated with using of acellular ovine skin and acellular bovine pericardium

Chapter Two

Review of Literature

2-1: Skin

Skin is the major tissue constituting the body, is made up of three layers and many various crucial cells and elements including protein, water, lipids, and several minerals and chemicals. The crucial function of the skin is to protect the living body from biological, chemical, physical harmful agents. Besides, the thermoregulatory mechanism of body temperature and the inhibition of water and electrolytes losses. Furthermore, skin also performs many vital nervous sensory roles through its various sensory receptors such as touch, pressure, pain, vibration, temperature and itching. Additionally, the skin has an important cutaneous immunological property through its important anatomical sites, especially its appendages like hair follicles and sweat glands and even postcapillary venules that serve as distinct portal locations for immune cells for creating tertiary lymphoid tissues (Kabashima *et al.*, 2019; Maranduca *et al.*, 2020).

2-1-1: Anatomy of Skin

Skin considered as the major organ of the living body, in adults, it accounting for about 15% of the whole-body weight. Histologically, skin has three main distinct layers: the epidermis, the dermis, and the hypodermis (subcutaneous fat) (Figure 1). In addition to its associated appendages such as sebaceous glands, sweat glands and hair follicles that are situated in its deepest layers (Wickett and Visscher, 2017).

The first highest layer of skin is the epidermis. The epidermis histology consists of stratified squamous epithelium that has four to five distinct cellular layers dependent on its position: (Kolarsick *et al.* 2011; Wong *et al.*, 2016; Yadav *et al.*, 2019)

Stratum Basalis (Basal cell layer): It is the deepest and nearest layer to the dermis. It is the active layer that has continuous mitotic activity. The cells of this layer are melanocytes, keratinocytes, and stem cells. Keratinocytes are the main cells that forming this layer. When they grow and become mature, they move outward/upward to generate the remaining layers.

Stratum Spinosum (prickle cell layer): This layer has the most thickness of the epidermis that comprises many layers up to 8-10 that connected to each other by desmosomes that permit cells to persist firmly connected to one another that look like "spines" structurally.

Stratum Granulosum (granular cell layer): This layer comprises of many sheets of cells that have lipid-rich granules. The cells of this layer start to immortalize and losing their nuclei during their movement away from the nutrient sources positioned in the deeper layer.

Stratum Lucidum: This layer is solitary present in the thick skin of palms and soles that consists of regularly dead cells.

Stratum Corneum (keratin layer): Is the outermost layer of the epidermis. This keratinized layer serves as the defensive layer of the epidermis. Due to its lipid and keratinization contents, this layer permits the controlling of water loss by avoiding interior fluid evaporation

The second skin layer is dermis, which lies beneath to the epidermis. It consists of dense layer of connective tissue containing collagen and elastin fibers that is responsible for skin's elasticity and strength. Separately, the dermis also contains blood vessels, nerve endings, and glandular structures such sweat and sebaceous glands and hair follicles. The dermal connective tissue is chiefly consisting of both collagen and elastic fiber bundles and the amorphous extracellular matrix ECM in between them. This ECM represents the ground substance that consist of glycosaminoglycans, such as glycoproteins, hyaluronic acid and

proteoglycans. The dermis is separated into two divided layers: the upper papillary dermis and the down reticular dermis. The papillary dermis lies deep to the epidermis; it consists of highly vascular loose connective tissue. However, the reticular layer which establishes most bulk of the dermis thickness is consisting of dense connective tissue (Wickett and Visscher, 2017).

Collagen fibers are the major abundant element of the dermis. Precisely, type I and type III collagen fiber bundles. In addition, elastic fibers, which is responsible for stretching, slipping and withdrawing of fibers also represent a significant physical part within dermis. Elastic fibers have two main structural components elastin and fibrillin microfibrils.

The hypodermis which is also termed as subcutaneous fascia is the third and deepest layer consisting mainly of adipose tissue with other skin appendages like sensory neurons, hair follicles, and blood vessels (Khavkin and Ellis, 2011; Yousef *et al.*, 2023; Agarwal and Krishnamurthy, 2019).

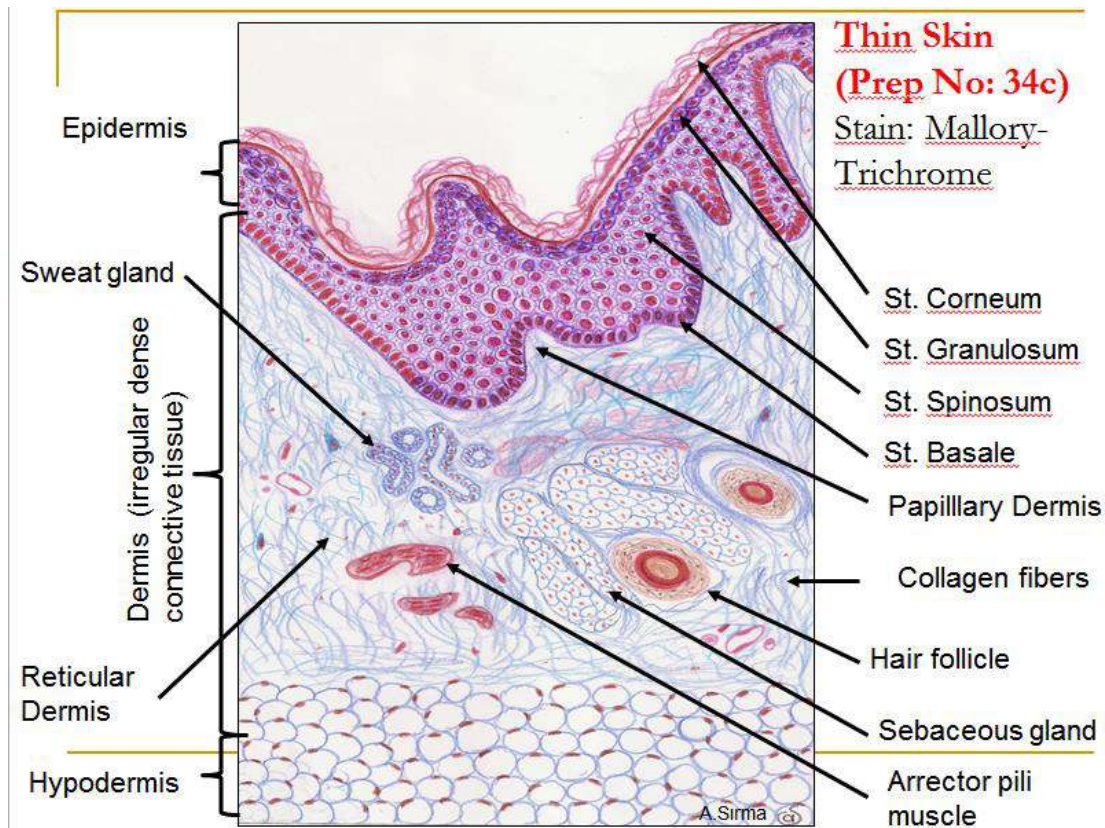


Figure 1: Illustration for skin histology and anatomy

Forum software by XenForo® © 2010-2019 XenForo Ltd Read more at:
<https://forum.facmedicine.com/threads/histology-of-skin.25430>

2-1-2: Feline Skin

The integumentary system of cats contains the skin and its appendages like hair, glands, digital pads, and claws (Linder, 2020; Kumar, 2024). Generally feline skin is highly elastic and pliable. It is relatively waterproof and permeable thus enables the absorption of different medicines and oils. Anatomically, although the skin of cat consists of three layers just like other animals, it is much thinner than that of other animals as a result of the less thickness of all its three layers (epidermis, dermis and subcutis). The dermal layer represents the most thickness of skin ranging

from 0.5-5.0 mm depending on its location within the body (Bohling *et al.*, 2006; Foss *et al.*, 2008).

The epidermis of the skin captivates ultraviolet radiation by the melanocytes and helps in vitamin D biosynthesis. The dermal papillae usually extended into the epidermis and surrounded by rete ridges of the epidermal layer. These two structures join with each other and fixing the epidermis (Kumar, 2024).

The epidermis thickness is 0.4-2.0 mm and it consists of five layers of living keratinocytes and forms rete ridges that are most clear on the foot pads. The upper most layer, the stratum corneum is thicker that build a more solid, lamellar design, particularly on the foot pads. It consists of several layers of flat, cornified non-nuclear cell implanted in a keratohyalin matrix that offers the fence against the entry of pathogens and harmful chemicals and pathogens. Its thickness is about 3–35 μm depending on the body region. Then, the stratum lucidum, which is typically and only found in the foot pads and nose that cannot be recognized as a separate layer by most histologists is a very thin translucent layer comprises a thin layer of flattened cells with no apparent cytological features that can differentiate it from stratum corneum. However, the stratum granulosum is finely established on the foot pads and is typically tinny or absent on the nose. The stratum granulosum consists of 2-3 layers of flattened epithelial cells that are rich with keratohyalin granules within their cytoplasm. The fourth epidermal layer is stratum spinosum (or prickly cell layer), which has 2-4 rows of cells and even up to 40 rows in very thick skin. Then finally, the stratum basale, which is the innermost epidermal layer, resting on the basement membrane consists of single layer of cells that is in a continuous mitosis to maintain the stem cell population while adding new cells that progressively passage to the surface.

On the other hand, the basement membrane zone within the dermo-epidermal junction is fairly distinct and non-convoluted except areas of glabrous skin (mucocutaneous junctions, foot pads and planum nasale) where it has more evident basement membrane zone and rete ridges (Affolter and Moore, 1994; Epaulard *et al.*, 2014). The most dominant cells within the epidermal layer that representing about 85% of all its cells are keratinocytes while other cell types population which comprise approximately 15% is Merkel cells, melanocytes and Langerhans cells (Epaulard *et al.*, 2014; Kumar, 2024).

Whereas the dermal layer, which represents the thickest vascularized second skin layer beneath the epidermis has a thickness of about 0.5-5.0 mm. (Bohling *et al.*, 2006; Foss *et al.*, 2008). It is detached from the epidermis by a tinny basement membrane. The dermis is a connective tissue structure that has two layers, superficial and a deeper layer. First superficial layer (papillary layer) forms a finger- like projections below the epidermis and it comprises of loose collagenous tissue holding abundant vascular plexuses and nerve endings. Still, the deeper dermis is called the reticular one, based on appearance of collagen fibers within the matrix. Many cell kinds inhabit the dermis, including fibroblasts, myofibroblasts, macrophages (histiocytes), and mast cells that is more abundant (Epaulard *et al.*, 2014; Kumar, 2024).

On the other side, the third skin layer i.e. subcutaneous layer in cat has a completely different vital role in wound healing as comparable with other species. This is because it represents the supportive layer of the skin, acting as the stretchy linking between the underlying fixed fascia and the movable skin, and supplying blood and nerve circulations to the covering dermis (Scott *et al.*, 2001; Bohling *et al.*, 2006; Foss *et al.*, 2008). Also, subcutaneous tissue considered as the primary source for cellular

precursors for granulation tissue so its injury could influence deeply on rate of granulation, wound contraction and damages epithelialization (Bohling *et al.*, 2006; Bohling, 2004). Likewise, the subcutaneous layer is mainly varying in thickness according to body condition and body site (Langley-Hobbs *et al.*, 2013). The hypodermis primarily contains irregular bundles of elastic and collagen fibers and various types of connective tissue cells (Kumar, 2024).

Furthermore, the normal histology and anatomy of cat's skin is relatively different from that of other species that's in turn influence deeply on kind of its healing process. Likewise, feline skin is very flexible and more moveable over most of parts of body surface. Besides, the blood circulation of skin especially within the trunk region is much less than that of other mammals as a result of their relatively low mass of tertiary blood vessels that's in turn leading to low degree of cutaneous perfusion (Langley-Hobbs *et al.*, 2013).

Most of the cat's body surface is sheltered by hair coat. Consequently, its epidermis is much thinner than that of human skin because there is reversed relationship between the concentration of hair coat and the width of the epidermis. However, this thick huge concentration of hair follicles provides an extra attaching mechanism between epidermis and the underlying dermis (Kumar, 2024).

Cat's hair coat has a selective benefit in thermal regulation, coverup, defense from predators, and a barrier to infectious agents, besides its color and quality determine their breed (White, 2019). Feline has compound medullated hair follicles consist of many primary and secondary hair follicles with an angle of 30-60 to the skin surface. The primary hairs are consisting of one large central hair and a cluster of 2-5 primary hairs while the secondary hairs, which surrounds the primary one is about 5 to 20 hairs.

Primary hair follicles have one single hair, sweat glands, sebaceous glands and arrector pili muscles while secondary hair follicles have sebaceous glands only (Affolter & Moore 1994; Kierszenbaum and Tres 2015). The skin has many kinds of glands. Sweat glands that are responsible for small portion of thermoregulation located only on the foot pads whereas sebaceous gland that are linked with the hair follicles secrete an oily material known as sebum that become hardens when contact air. It skins the hairs, thus defending the fur and making it silky (Foss *et al.*, 2008).

2-1-3: Mechanical Properties of Skin

Skin is a complex multifunctional structure that shelters the entire body surface. Determination of the skin mechanical characters has important applied and scientific values (Žak *et al.*, 2011). To license body motion, skin wants to be adequately flexible to permit massive twists in all directions. Yet, at the same time stile has the ability to returning back to its original state. When skin is considered entire, including its three constituting layers, it can be called as viscoelastic, anisotropic, nonlinear, non-homogenous leading to a capacity to withstand excessive deformations. The dermal layer plays the most vital role in terms of mechanical properties (Žak *et al.*, 2011); especially its stratum cornium which is the hardest skin layer.

Mechanical behavior of this layer can differ significantly depending on hydration, temperature, humidity and chemical treatment (Wu *et al.*, 2006). The entire mechanical behavior of skin is greatly correlated to the presence of elastin and collagen fibers in the dermis. It has been proposed that the dermal elastic fibers are the main responsible for the mechanical behavior (Wenger *et al.*, 2007). Conversely, the hypodermal layer is the softest layer among the three layers and equally conveys the loads from upper skin layer to the underlying layers (Groves, 2012).

2-2: Wounds

Wounds can be defined as an injury or damage of the skin or mucous membrane or other body tissues continuity leading to exposing of the deeper tissues to danger of infection. Wounds are caused by mechanical, thermal, chemical, biological, radial and other factors. Determination the kind of wound is very essential before using any kind of treatment or therapy because each kind of wound is somehow different from other as a result of its structure, position, biology and even its physiology that require completely different therapeutic approach (Pope, 2009; Irfan-Maqsood, 2018). When damage to the skin occurs, various invaders can easily enter body to cause either local infection and inflammation known as (wound infection) or systemic infection such as septicemia. However, the most associated danger of wound is the fluid loss accompanying these wounds as wounds that are larger than 10% of body surface area can cause an actual life-threatening factor because of the loss of extracellular fluid. Therefore, the most important goal with any wound kind is to accomplish its healing as swiftly as possible because wounds represent one of the most daily practical cases that face any veterinarian (Percival, 2002; Gupta, 2021).

Although, there is no typical cataloguing for wounds, there are many various categorizing that wounds can be classified according to them that also help in their describing. The most important features that can be based on to categorize wounds are: time after injury, the nature of the injury that caused the wounds, involvement of tissues and its depth (Rosselli, 2024). Nevertheless, these classifications are helpful in determination the capability of these wounds to heal with or without surgical interference. Yet, the surgical wound classification (SWC) system that was firstly established by National Academy of Sciences and National Research Council at 1964 is considered as the most precise one as it

was established to reflect the severity of bacterial population within the surgical field. This classifying system categorize wounds into main four classes. Each class has its own postoperative scores for the risk of infection that starts with 1% to 5% and ends with 17%, and even more than 27%.

- Class 1 wounds (clean wounds): These kinds of wounds are not infected, they do not display any signs of being inflamed, and are characteristically closed.
- Class 2 wounds (clean-contaminated): These wounds usually have little level of contamination. These kinds of wounds include access into the digestive, respiratory, urinary and genital tracts but with controlled conditions.
- Class 3 wounds (contaminated): These wounds are characteristically occurred due to failure in the sterile conditions or escape from the gastrointestinal tract.
- Class 4 wounds (dirty or infected): These kinds of wounds are generally happening due to insufficient handling of clear infection, and traumatic wounds.

The scientific significance of the correct wound sorting represents in its capacity to assistance for guess the possibility of surgical site contaminations, postoperative problems besides its ability to predict quality of life, morbidity and even mortality (Wilkins and Unverdorben, 2013; Onyekwelu *et al.*, 2017).

2-3: Wound Healing

Wound healing is an energetic physiological procedure for reestablishing the anatomical function of the living tissue. Meanwhile damage of tissue is very common, the body is finely accommodated to start

the mechanism for repair and protection to provoke the healing process cascade. Typical wound healing process is greatly impacted by kind, location and extent of injury, intrinsic and extrinsic factors. Wound healing has three highly précised programmed stages: inflammatory, proliferation, and remodeling phase that must happen in the correct sequence and time (Doyle and McCutcheon, 2015; Perry *et al.*, 2019).

Hemostasis and Inflammatory phase (Immediately after injury up to 4-6 days). It is characterized by hemostasis and inflammatory features. As soon as injury happens, a powerful vasoconstrictor prostaglandin and thromboxane A₂ are released. A clot will be formed by combination of collagen, blood platelets, thrombin, and fibronectin. All these factors together liberate various cytokines and growth factors that induce the inflammatory response. The fibrin clot will concentrate the growth factors and cytokines, besides acting as a scaffold for incoming inflammatory cells, such as neutrophils, monocytes, fibroblasts, and endothelial cells. New blood vessels formation within wound bed is essential for correct wound healing. The granulation phase formation requires nutrients supplementation by the blood capillaries, so any failure, a chronically unhealed wound will develop (Gonzalez et al., 2016).

Proliferative Phase: Day 4-14, characterized by epithelization, blood perfusion, and formation of ECM. Epithelial cells within the skin edge starts multiplying and sending out their projections to rebuild a defensive wall against extra bacterial attack and fluid losses. Epithelization starts just after wounding due to inflammatory cytokines that impact on fibroblast. In turn, fibroblasts manufacture and release other cytokines which activate adjacent keratinocytes to travel, multiply, and distinguish. The final level of the proliferative phase is the synthesis of granulation tissue. Fibroblasts that moved into the injured site from the adjacent tissue, become

stimulated, and begin manufacturing collagen fibers and proliferate. Platelet-derived growth factor (PDGF) and epidermal growth factor (EGF) from blood platelets and macrophages are the chief key signals to fibroblasts to initiate producing a temporary matrix consist of collagen fiber type III, glycosaminoglycans, and fibronectin (Ellis et al., 2018).

Maturation and Remodeling (Day 8 up to 1 year). The main property of this stage is the deposition of collagen fibers in an ordered and well-organized network. Net collagen fiber formation will continue for at least 4 - 5 weeks after wounding. The amplified rate of collagen fiber synthesis during wound healing process is not only coming from an elevation in the number of fibroblasts but also from the rise in their activity to produce collagen fibers. Then, with progress of time the wound will gaining more tensile strength, depending on its collagen fiber thickness/orientation. Following first week, the wound has only 4 percent of its ultimate strength, but its tensile strength will be up to 80 percent at 3 months and beyond (George *et al.*, 2006).

2-4: Skin Substitutions

Skin substitutions mean diverse group of either synthetic, biologic or biosynthetic ingredients that can offer momentary or permanent coverage for extensive skin wounds. The aim of these skin substitutes is to simulate the functions of the normal skin in generating a suitable situation for healing to occur, inspiring the beginning of healing, regulating the exudate, diminishing pain, providing mechanical support, and avoiding contamination (Mirani *et al.*, 2023; Abdulghani and Mitchell, 2019). Therefore, there is significant request for finding and supplying new revolutionary materials and products that can speed up healing process (Corr, 2009; Davidson, 2015). A variety of different biodegradable, biocompatible natural and synthetic materials are continuously driven into

biomedical field (Granick *et al.*, 2020; Prete *et al.*, 2023), making biomedical market as one of the most rapidly growing field (Niculescu *et al.*, 2022; Albahrawy *et al.*, 2023, Bhoopathy *et al.*, 2024).

Using of natural biomaterials for promoting wound healing has become a very trendy trial due to their highly positive influence on the stages of wound healing. This is through supplying the appropriate atmosphere and acting as scaffold that facilitate bridging for the many healing aspects including cell movement, propagation, and differentiation thus progress tissue regeneration and repair. Furthermore, most of these materials display multifunctional role that participate during diverse phases of the wound healing process (Shi *et al.*, 2010; Deng *et al.*, 2022; Fadilah *et al.*, 2023; Kim and Evans, 2012). The chief aim of wound management is to enable the possible rapidest healing of the wound while diminishing patient distress and scarring (Aisa and Parlier, 2022). To perform the most efficient wound handling it is highly recommended to diminish formation of scar tissue, lessen production of necrotic tissue production and spoil the infiltration of microbes (Schultz *et al.*, 2003).

For wound management, diverse medications are usually used and developed. However, they can be classified into two chief groups: traditional dressings (passive dressing) and bioactive dressing (biomaterial). Traditional old dressing such as gauze and conventional dressing means these substances that positioned in direct contact with the wounded injured tissues to achieve coverage, hemostasis, and defense while bioactive dressing aims to perform more extra goals in addition to traditional one like sustain suitable moisture and temperature environment, elimination of exudates and necrotic material, defend against exogenous pathogens, and finally to allow oxygen permeability, cause zero trauma (Bianchera *et al.*, 2020; Riha *et al.*, 2021; Prete *et al.*, 2023).

2-4-1: Traditional Dressings

Conventional dressings were the traditional approach for dealing with many kinds of wounds for years. Yet, this handling procedure is not recommended any more as a result of many factors including high risk of associated infections, its adverse influences on the healing atmosphere and causing to amplified pain and suffering for the patient. Besides, gauze and cotton gauze dressing that are used in a direct contact during the first dealing in a wound treatment have very high absorption capacity causing rapid dehydration that in turn. This leads to bleeding and damage to newly formed epithelium when they are being detached from the wound surface (Gupta and Edwards, 2019; Parkale *et al.*, 2021; Perte *et al.*, 2023).

2-4-2: Bioactive Dressing (Biomaterials)

Although biomaterials market is one of the oldest biomedical technologies, it is still usable in current clinical application. The term “biomaterial” indicates the capability of these active materials to become combined into native tissues and being part of it. Today, this term involves an ever-expanding list of materials and classes obtained from both human and animal tissue and artificial products originated from naturally sources organic elements (Abdulghani and Mitchell 2019; Cao and Ding 2022).

Biomaterial skin substitutes from various origins like autogenic, allogenic, or even xenogenic bases have developed a novel and different therapeutic choice. A wide variety of such materials that differ in their cellular property and structure are certified and driven directly into clinical use. These alternatives can be positioned directly onto a prepared wound bed to hasten or even stimulate healing process through encouraging cellular immigration, revascularization through their structural scaffold that acting as material to enable these processes. Besides, these

biomaterials release many bioactive molecules including growth factors and cytokines (Bianchera *et al.*, 2020; Riha *et al.*, 2021).

Biomaterials exhibit a significant impact on various wound healing stages including cell propagation, immigration, and differentiation, thereby contributing advanced avenues for tissue regeneration and repair through their multifunctionality properties (Li *et al.*, 2023). Scaffolds represent the new trend of biomaterials industry involving the creation of 3D structures because extensive wounds are incapable to regenerate themselves. Thus, the synthesis of scaffolds is crucial to encourage the normal physiology of healing process by presenting the necessary mechanical support for the growth of new tissue. A scaffold is a physical outline that offers support and solidity to living tissue. It cooperates with cells to initiate the normal physiological events needed for the healing and regeneration of the tissue. It helps in the delivery of biochemical factors enabling proper cell attachment and movement (Lam *et al.*, 2002; Smandri *et al.*, 2020).

Biomaterial categories and processing procedures are significant for determining the properties of the resulting scaffolds. These scaffolds can be gained from synthetic, natural, or hybrid polymers. Then, they are amended to be suitable to be functioning with many agents aimed at enhancing cellular reactions and hastening the wound healing course (Prete *et al.*, 2023).

The bio-derivative substitution in regenerative medicine profits directly from the architecture structure of tissue especially the extra cellular matrix (ECM) design. This ECM can be derived from cell, tissue and even organ although tissue ECM is the most dominant one. These bio-derived materials can be obtained from many biological sources. However, the immunological features associated with using such kind of derivatives represents the most serious problem facing these valuable resources that

implies the necessity for removal of their cells using decellularization technique (Wong *et al.*, 2014; Moura *et al.* 2022).

ECM itself is a critical natural biomaterial consists of collagens and other particles that form a fibrous matrix. The different types of collagens found within ECM based on the kind of tissue itself such as skin, heart, small intestine and urinary bladder, which in turn furtherly impact on the functions of ECM (Goh and Holmes, 2017; Rowley *et al.*, 2019). The bioactive tissues following decellularization process usually hold many structural elements like collagen, elastin, fibronectin, growth factors, etc., that offer a micro-environment analogous to the extracellular matrix (ECM) for contact, growth, immigration, and cells differentiation (Cramer and Badylak, 2020; Zhang *et al.*, 2022).

2-4-2-1: A Cellular Bovine Pericardium

Bovine pericardium is a collagen fibers-rich biological tissue that is one of the ideal materials used to accomplish critical heart disease such as heart valve diseases, ventricular septal disorders and aortic annulus root infections. In addition its huge flexibility make it the perfect replacement substitute in many surgical fields for the construction of a variety of bio prostheses materials such as vascular grafts, heart valves, vascular graft and patches for vaginal or abdominal or vaginal wall reparation besides, repair or replacement in the surgery of pericardial closure, acquired/congenital cardiac defects, and blood vessels (Goissis *et al.*, 2011; Zouhair *et al.*, 2020; Zhao *et al.*, 2021; Mendoza-Novelo *et al.*, 2011). Other application includes its use for treatment deep intrabody defects (Stavropoulos *et al.*, 2011).

The great characters that enable pericardial membrane to be used are the slight rates of associated infection, complications and fibrotic adherence, however, immunogenicity and cytotoxicity could be considered

as the main significant limitations for the long-standing performance of these pericardial alternatives. Therefore, the decellularization of pericardium could be considered as the solution to overcome all these drawbacks that might be applied to yield biological scaffolds with improved less immunogenicity and unchanged viable and biomechanical properties with respect to original tissues (Zouhair *et al.*, 2020).

Up to now, several forms of acellularized bovine pericardial scaffolds have been used in tissue bioengineering to treat certain conditions such as rebuilding of pelvic and ventricle defects or closure of soft tissue conditions including various abdominal, diaphragmatic, umbilical defects or for intra-cardiac and blood vessel repair. Recently, the decellularized bovine pericardia was also used as a dura matter fixer for some brain surgery procedures (Alizadeh *et al.*, 2019; Al-Saiegh *et al.*, 2024).

2-4-2-2: Acellular Ovine Skin

Currently, there is a huge trend towards using of biomaterials derived from allogenic or xenogeneic ECM for clinical uses as templates to enable tissue regenerative process due to their active role to swiftly initiate vascular supply that enable the effective transport of vital oxygen and cellular nutrients during regeneration (Lun *et al.*, 2010; Irvine *et al.*, 2011; Karnik *et al.*, 2019). Nevertheless, these biomaterials that can be derived from many sources especially porcine and bovine bases have some limitations based on cultural and religious considerations. Also, the danger for transmitting some disease such as bovine spongiform encephalopathy restricts the clinical use of bovine derived material (Silvipriya *et al.*, 2015; Schmidt *et al.*, 2016). On the other side, biomaterials originated from sheep and goat is broadly accepted by all cultures and religious societies (Abdullah *et al.*, 2018; Silvipriya *et al.*, 2015). Besides, their lower risk for disease transmission (Fauzi *et al.*, 2016; Caetano *et al.*, 2018).

Numerous commercial extracellular matrix-based biomaterials obtained from ovine tissue are now become very popular trend in biomaterial market (Bohn *et al.*, 2016; Ghodbane *et al.*, 2016; Rashtbar *et al.*, 2018; Alizadeh *et al.*, 2020; Xin *et al.*, 2024). Collagen is the chief constituent of the extracellular matrix and it plays a key role in wound healing process. Collagen derived from animals, such as bovine, rat or porcine is quite expensive while ovine is less expensive. Therefore, they become available for academic use in many research criteria especially cancer field as the acellularized ovine skin models enable the adhesion and growth of various cancer cell lines (breast, pancreatic, and melanoma cells). Recently, decellularized extracellular matrices are employed as biomaterials to develop scaffolds/hydrogels (Kumar *et al.*, 2022).

2-5: Decellularization

Decellularization can be clarified as is a technical procedure to obtain and preserve the extracellular matrix structure of any tissue without its associated cells to decrease immunological reaction toward the original whole tissue by removing its immunogenic materials (Tan *et al.*, 2021; Zhang *et al.*, 2022). The decellularization approaches contain applying either enzymatic, chemical and physical techniques or even their mixture (Koo *et al.*, 2022). Although decellularization is a best technique to gain valuable biological scaffolds, some disturbance of the original ECM structure can be expected and the complete avoidance is not possible. For decellularization, enzyme like trypsin is used to detached and isolate cells from the structural proteins while the crosslinking step, which include the chemical and physical procedures is recommended to enhance the mechanical properties especially the residual strength of natural biomaterials (Fernández-Pérez and Ahearne 2019; Yang *et al.*, 2022).

Scaffolds composed of extracellular matrix (ECM) from biological resources are broadly used in extended clinical applications for repairing and reconstruction of tissues such as gastrointestinal tract, urinary tract, cardiovascular structures and musculoskeletal tissues and even central nervous system. These kinds of biologic scaffold containing extracellular matrix properties are obtained through decellularization of various mammalian tissues (Zhang *et al.*, 2022).

All adapted methods for decellularization unfortunately disturb the architecture, surface landscape and even orientation of ECM to some degree. Therefore, a precise balance between preserving the original structure of ECM and the elimination of cellular contents especially DNA, membrane lipids, mitochondria, and cytosolic protein particles is a critical point. However, radical removal of all cellular components is not possible. These residues of cellular elements can initiate a revers inflammatory reaction and prevent constructive remodeling. Hence, choosing the ideal decellularization method is not an easy task as a result of the diversity of tissues and organs in addition to its dependence on many tissue factors including tissue shape and thickness, cell density, lipid contents, and matrix density (Crapo *et al.*, 2011; Keane *et al.*, 2015). Methods of decellularization can be categorized into many criteria, but they can be described as physical, chemical, and biological or their combinations (Crapo *et al.*, 2011; Gilpin and Yang, 2017; Choudhury *et al.*, 2020; Cao and Ding, 2022).

2-5-1: Physical Methods for Decellularization

A lot of studies have tried using many physical procedures to obtained decellularized tissue that can be used with various tissues (Rabbani *et al.*, 2021; Guimaraes *et al.*, 2019; Miranda *et al.*, 2021; Moffat *et al.*, 2022). In general physical procedures include many procedures

including thermal shock (freeze-thaw cycle) temperature (Keane *et al.*, 2015), mechanical loading and hydrostatic pressure (Funamoto *et al.*, 2010), Electroporation (Phillips *et al.*, 2010), ultrasonic, agitation in solution (Oliveira *et al.*, 2013), pressure gradient (Sierad *et al.*, 2015) vacuum assisted (Butler *et al.*, 2017) supercritical fluid (Gilpin and Yang, 2017) immersion and agitation perfusion (He and Callanan, 2013).

In general, various physical decellularization methods could disrupt cellular membrane, liberation of the cell contents that enable the elimination of these contents from the ECM. However, some of these adapted physical methods cannot eliminate cell debris, especially in these processes that do not use fluid flow such as ultrasound or electroporation. Therefore, it is essential to use a tissue washing step with a suitable detergent. Though each physical method can be used separately with appropriate result, physical approaches are frequently inadequate to accomplish whole decellularization for all kinds of tissues that must be accompanied with other chemical methods (Gilbert, 2012; Keane *et al.*, 2015; Rabbani *et al.*, 2021).

2-5-2: Chemical Methods for Decellularization

Various chemicals are usually examined for their capability to decellularize various biological tissues. These chemical materials are normally designated in order to solubilize cellular membranes and to carriage out these cells components from the tissue by means of either tension or perfusion. The chemical substances that are normally used are classified into numerous general classes including acidic and alkaline solutions, detergents, solvents, and ionic solutions (Gilbert, 2012, Crapo *et al.*, 2011; Hrebikova *et al.*, 2015; McCrary *et al.*, 2020).

For example, acids like peracetic acid is commonly decellularize tissues through removing remaining nucleic acids with slight influence on

the ECM composition and construction as it destroys and eliminates collagen fibers without affecting on glycosaminoglycans (Yamanaka *et al.*, 2020). However, bases such calcium hydroxide is a strong harsh agent that applied for hair removing from dermis samples during the primary stages of decellularization (Sarvazyan, 2020). Nevertheless, bases can entirely eradicate growth factors from the matrix and decline its mechanical properties more significantly than acids. (Carpo *et al.*, 2011). Additionally, hypotonic and hypertonic liquids can also be used for decellularization, hypertonic agent via separates DNA from proteins and hypotonic by cell lysis with simple osmotic affects leading to slight changes in matrix molecules and construction (Kim *et al.*, 2016).

Conversely, other chemical agents like detergents, which include many chemical agents such as ionic, non-ionic, and zwitterionic detergents lysis cell membranes and separate DNA from proteins. Using multiple detergents together can upsurges ECM protein loss (Farrokhi *et al.*, 2018). The list of detergents still possesses many agents such as Triton X-100 and sodium dodecyl sulfate (SDS), which is more effective comparable to Triton X-100 for eradicating nuclei from organs and dense tissues such as kidney and temporomandibular joint with minimal impact on tissue mechanics (Tebyanian *et al.*, 2017; Cai *et al.*, 2021). Yet, alcohols such as ethanol, isopropanol and glycerol help in tissue decellularization via dehydrating and lysing cells (Choudhury *et al* 2020). Furthermore, other solvents like acetone and tributyl phosphate (TBP) can also be used to remove lipids during decellularization, especially decellularization of dense tissues such as tendon (Carpo *et al.*, 2011; El Soury *et al.*, 2021).

2-5-3: Biological Methods for Decellularization

Numerous biologically derivative agents such as enzymatic and non-enzymatic can be utilized for decellularization of tissues. Enzymatic agent

like trypsin, nucleases, lipase, collagenase, lipase, dispose are highly specific for removing cell residues or unwanted ECM elements. Nevertheless, whole cell elimination by enzymatic approach alone is difficult (Khosravimelal *et al.*, 2020; Ramm *et al.*, 2020). Endonucleases enzymes like benzonase could be more effective than exonucleases because they cut sequence of nucleotides thus be more effectively splint DNA in the preparation for its elimination (Moore *et al.*, 2015). Trypsin can be used efficiently to interrupt tissue ultrastructure and progress penetration of subsequent decellularization agents. Consequently, exposure to trypsin considered as a basic initial step in any tissue decellularization protocol particularly for whole removal of cell nuclei from the dense tissues (Giraldo-Gomez *et al.*, 2016; Rahman *et al.*, 2018). Non-enzymatic agents is another biological method to produce decellularization through using chelating agents such as ethylene glycol tetra acetic acid (EGTA) and ethylenediaminetetraacetic acid (EDTA) and aid in cell to indirect disturbances between protein-protein interactions; however, they are week and in capable to remove cells so they mixed with other enzymes such as trypsin (Greco *et al.*, 2015; Emami *et al.*, 2021). Further, toxins such as latrunculin can be used to remove DNA and other intracellular materials from dense tissue (Carpó *et al.*, 2011; Neishabouri *et al.*, 2022).

Chapter Three

Materials and Methods

3-1: Animals

Eighteen (N=18), of 1-2 years old with an average weight of $2-3 \pm 0.3$ kg local breed cats were acclimatized one week earlier before the beginning of this experiment. All the surgical operative and accompanying handling procedures were done following the ethical standards line and rules for animal utilization protocols. To ascertain the healthiness of our experimental cat, all animals were inspected to be free from any infectious disease and pathological conditions.

3-2: Preparation of Acellular Ovine Skin

Ovine skin was derived from the patriot abattoir and directly saved inside an ice-cold box contain sterile phosphate buffered saline (PBS, pH 7.4) enriched with broad-spectrum antibiotic (Amikacin-1 mg/ml), and a proteolytic inhibitor (0.02% EDTA). In the preparation room, shaving of skin was done to remove all skin hair while all the adherent debris and blood were washed out thoroughly using sterile PBS. De-epithelization of skin sample was done using 0.25% trypsin and 2Molar sodium chloride solution for eight hours followed by using of 2% of sodium deoxycholate for 48 hours to decellularize the dermis (Figure 2). During both de-epithelization and decellularization processes and in order to ascertain best contact of skin with chemicals and to obtained the better result, the samples were subjected to continuous agitation in a horizontal orbital shaker at the rate of 220 (rotations per minute) (Figure 3). To be sure of the complete removal of all cells from the processed skin samples, a microscopic inspection following staining with Hematoxylin and Eosin (H&E) was achieved (Figure 4). Then the prepared acellular bovine skin sample was washed with sterile PBS solution for six times (2 hours each) to eliminate

all the residual chemicals and finally stored at -20°C in PBS solution containing 0.1% amikacin solution (Kumar *et al* 2013; Singh *et al.*, 2022).



Figure 2: Photographic image of acellular ovine skin following complete decellularization.



Figure 3: Photographic image shows horizontal orbital shaker machine.

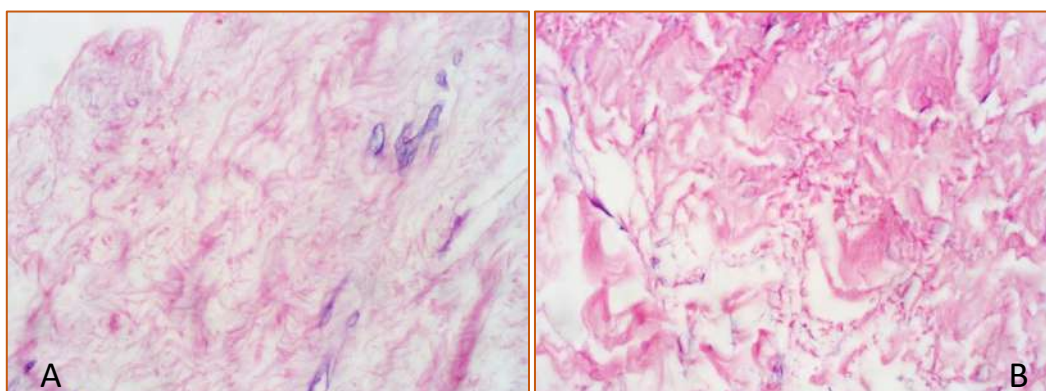


Figure 4: Histological section of acellular ovine skin patch shows efficiently eliminate the cellular part of the tissue, absent of nucleus.

H&E, 100x (A), 400x (B).

3-3: Preparation of Acellular Bovine Pericardium

To prepare a cellular bovine pericardium, the pericardium membrane was obtained from the neighboring abattoir and instantly saved within an ice-cold solution of sterile phosphate buffered saline (PBS, pH 7.4) enhanced with broad-spectrum antibiotic (Amikacin-1 mg/ml).

Next, inside the preparation room, all the adherent debris, fats, and blood were removed and washed out thoroughly using sterile gauze and PBS. Decellularization (Figure 5) of bovine pericardium was accomplished using new modified approach through complete immersion of pericardium membrane inside 2% of sodium deoxycholate solution (SDS) for 9 hours with continuous agitation in a horizontal orbital shaker at the rate of 220 (rotations per minute) to ensure optimal contact of the membrane with chemicals. To ascertain a cellularity of the processed pericardium samples, a microscopic inspection following staining with Hematoxylin and Eosin (H&E) was completed (Figure 6). Then the prepared acellular bovine pericardium was washed for two hours with sterile PBS solution for six times to remove any remaining substances and finally stored at 4°C in PBS solution containing 0.1% amikacin solution (Kumar *et al* 2013; Singh *et al.* 2022).



Figure 5: Photographic image of acellular bovine pericardium following complete decellularization.

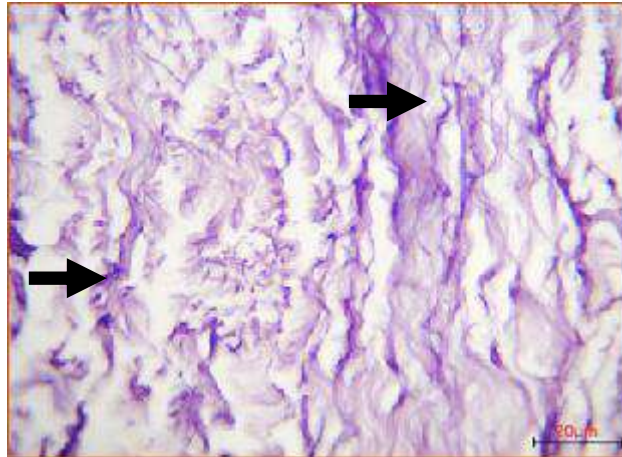


Figure 6: Histological section of acellular bovine pericardium dressing Shows efficiently eliminates the cellular part of the tissue and presence of the collagen bundles (black arrow), (400x H&E).

3-4: Mechanical Evaluation

The mechanical properties (maximum load and modulus of elasticity) of both acellular ovine skin and acellular bovine pericardium were examined before and after decellularization to discover the effect of decellularization process on the mechanical properties of these biodegradable dressing materials.

Stripes of both acellular tissue's samples of the same geometric dimensions (Figure 7) (Žak *et al.*, 2011) were excised and kept at a room temperature in 0.9 % normal saline solution until the time of testing (no longer than 5 hours) (Žak *et al.*, 2011), then subjected to biomechanical test (Figure 8). This test was completed at the Strength of Material Laboratory, Faculty of Engineering, Mosul University. The samples were tested using an Alfa Universal Testing Machine (Model UTM-001 Turkey) with 20kN capacity (Figure 9).

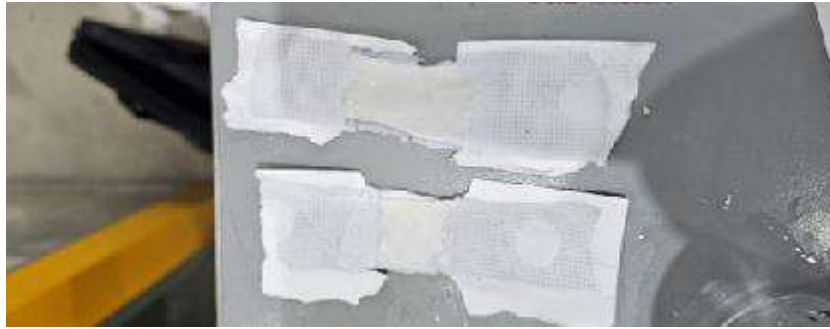


Figure7: Photographic image for the stripes of both acellular ovine skin and bovine pericardium samples of the same geometric dimensions to perform mechanical test.

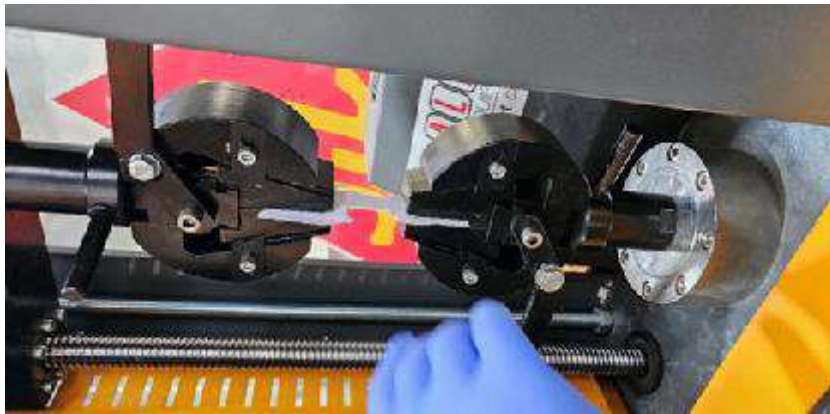


Figure8: Photographic image shows testing the mechanical properties of both acellular tissues



Figure9: Photographic image shows Alfa Universal Testing Machine (Model UTM-001 Turkey) with 20kN capacity.

3-4-1: Uniaxial Stretching Test

Uniaxial stretching analysis was carried out on both a cellular stripes to find out the following properties including the maximum load (N) and the ultimate modulus of elasticity (mm) (maximum extension) (Zak *et al.*, 2011; Kalra *et al.*, 2016).

The tests elaborate uniaxial stretching of the tested samples at a fixed rate of 5 mm/min until they tear (Zak *et al.*, 2011). To achieve this aim, the samples were secured strongly between the two holding grips of the machine using gauze to avoid slipping, the machine preloaded to 0.005 N,

held for 120s, and then a persistent rise in force was subjected until the examples break and can no longer hold more strain (Figure 10) (Bermudez *et al.*, 2011).



Figure10: Photographic image shows the tearing of both acellular tissue sampler after completing the mechanical testing.

3-5: Experimental Design

Eighteen (N=18) cat were divided randomly into equal groups of 9 for each. A 4x4 cm square of full-thickness skin defect was created in the back region of all cats. In the 1st experiment group, a 3x3 cm segment of fenestrated acellular ovine skin was implanted onto the skin defect and sutured with 2.0 Nylon using simple interrupted. On the other side, fenestrated acellular bovine pericardium was used to repair the induced back defect in the second group. The full thickness dressing area was examined clinically, grossly, physically, and subjected to mechanical and histological examinations on days 7, 14 and 21 following dressing (Figure 11).

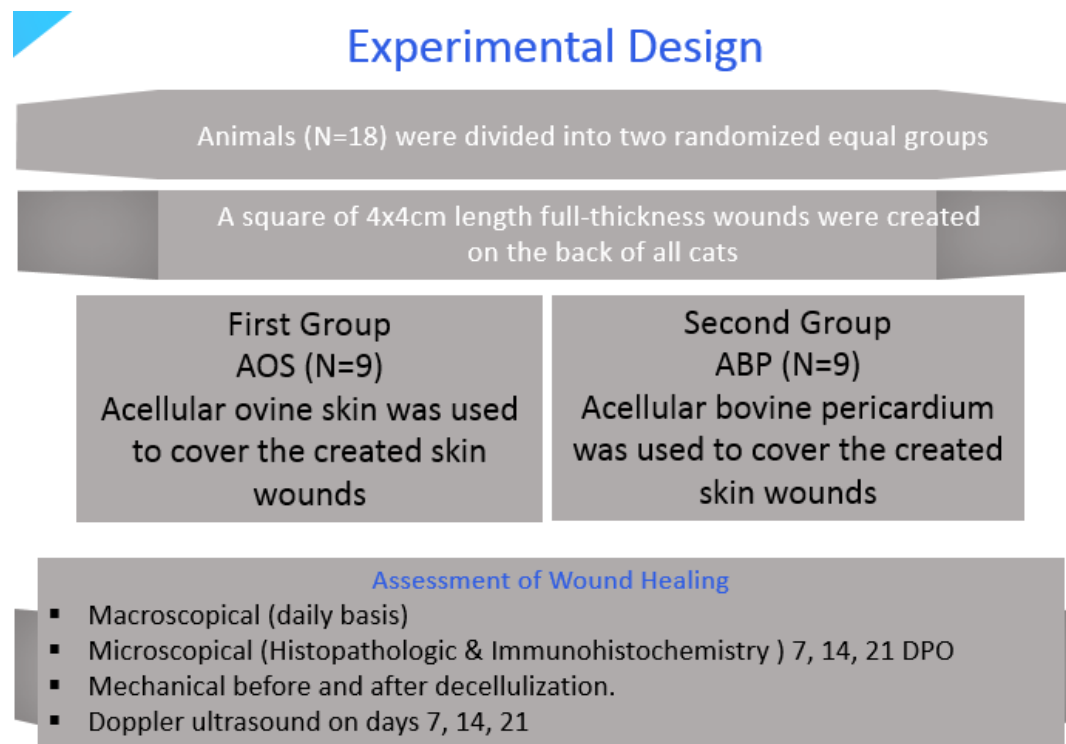


Figure 11: Illustration of the experimental design.

3-6: Preoperative Preparation

All experimental cats were deprived from food and water prior to surgery. The site of operation on the back of each animal was prepared strictly for aseptic intervention through clipping and shaving of hair firstly then application of antiseptic solution 5% of povidone iodine and 70% ethyl alcohol.

3-7: Anesthetic Protocol

All surgical procedures were achieved under general anesthesia using intramuscular mixture of 15 mg/kg of Ketamine Hydrochloride (Narketan®-10, Troy Laboratories PTY Limited, Australia) and 1mg/kg of Xylazine (ILium Xylazil-100, Troy Laboratories PTY Limitd, Australia) (Dzikiti *et al.*, 2007).

3-8: Surgical procedure

Animals were positioned in sternal recumbence then the experimental wounds outline was determined using skin marker and caliper. Then a 4x4 cm square full-thickness skin wounds without removing the panniculus muscle was excised with a #15 scalpel blade on the center of the trunk, just beneath the caudal border of the scapula (Figure 12).

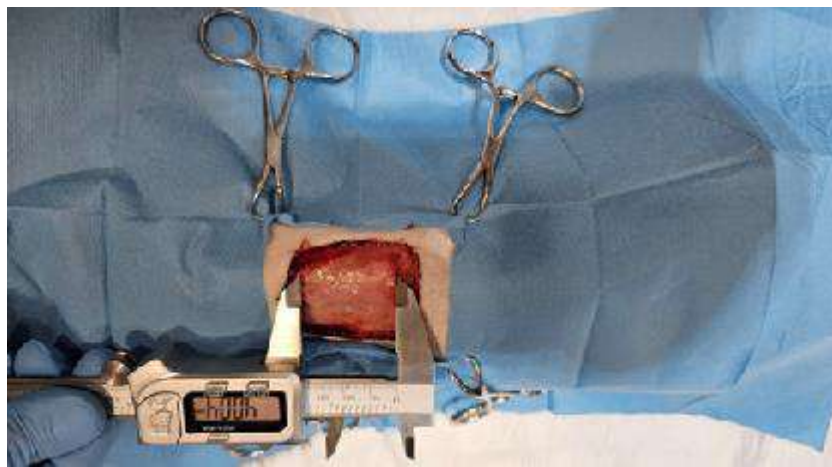


Figure 12: Photographic image shows the induced wound of 4x4 cm on the back of the cat.

Following the defect creation, a 3x3cm segment of acellular ovine skin was used to cover the induced skin defects and sutured into the edges of that wound by 2.0 Nylon (Ethilon*, Ethilon. LLC.) using simple interrupted in the 1st group (Figure 13). In the meantime, cellular bovine pericardium sheets were used for the 2nd group (Figure 14). Finally, the wounds were bandaged and covered with a four-layer padded bandage as follows, the contact layer was covered with a sterile, low-adherent, semi-occlusive pad The second bandage layer consisted of cotton pad, third layer using cotton roll gauze, applied in multiple layers crossing over the body to prevent the bandages from slipping, and the fourth of a self-adhesive bandage for 3days (Figure 15).

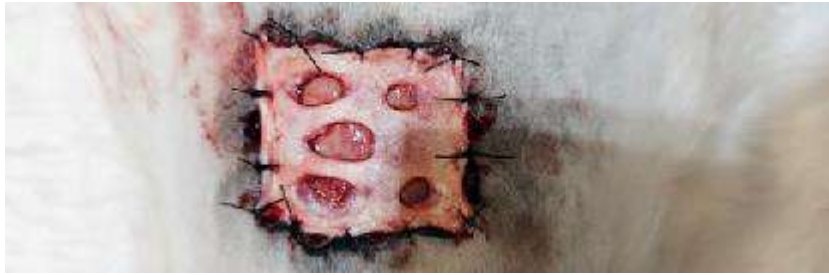


Figure13: Photographic images for suturing of acellular ovine skin onto induced wounds using 2/0 Nylon simple interrupted technique.



Figure14: Photographic images for suturing of acellular bovine pericardium onto induced wounds using 2/0 Nylon simple interrupted technique.





Figure15: Photographic images (A, B, C and D) for four- layers bandaging of the induced wounds following complete suturing.

3-9: Post-Operative Care

A daily basis inspection of the skin wounds was accomplished for any gross signs of wound dehiscence or complications. Penicillin (40000 IU/kg for five days) and ketoprofen (2.2 mg/kg for three days) were administered to the cats. The sutures were removed after the 7day of the operation.

3-10: Wound Healing Assessment

The progress of wound healing process was based on the following criteria.

3-10-1: Macroscopic Examination

To evaluate the progress of skin wound healing process daily, clinical and gross observation were achieved on 7, 14, and 21days post surgeries. They were assessed by clinical and gross inspection based on

several parameters as shown in **Table1** (Başaran *et al.*, 2006) and **Table 2** (Tsioli *et al.*, 2016; Tsioli *et al.* , 2018).

Table .1: Macroscopical criteria for evaluation of acellular ovine skin and acellular bovine pericardium dressing performance			
Clinical parameters	Scores		
	0	1	2
Adherence	Detached from wound	Lightly adherent	Strongly adherent
Color	Blackened	Mat gray or brown	Normal
Pliability	Very rough	Slightly hardened	Pliable and smooth

Table .2: Gross criteria for evaluation of wound bed healing					
Macroscopic Parameters	Scores				
	0	1	2	3	4
Exudate	Absent	Mild	Moderate	Sever	More Sever
Pus	Absent	Mild	Moderate	Sever	More Sever
Edema	Absent	Mild	Moderate	Sever	More Sever
Hemorrhage	Absent	Mild	Moderate	Sever	More Sever

3-10-2: Physical Evaluation

Progress of cutaneous wounds healing following using of acellular ovine skin and acellular bovine pericardium was also assessed using physical criteria including doppler ultrasonography to detect the presence of blood perfusion and planimetry measurements to determine wound size and wound contraction rates.

3-10-2-1: Planimetry

The dimensions of full-thickness wound area in centimeters were measured daily using electrical caliper since the first day following dressing till end of day 21 to assess the percentages for total wound contraction and total wound healing using the following formulas (Bohling *et al.*, 2004; Bohling *et al.*, 2006).

Percent of Wound Contraction (WC) was calculated using 2 steps

$$1-: \text{Total wound on day } n \text{ as \% of original} = \frac{\text{total wound area day } n}{\text{original wound area (day 0)}} \times 100$$

$$2-: \% \text{ of wound contraction on day } n = 100 - \text{total wound on day } n \text{ as \% of original}$$

Percent of Total Wound Healing (TWH) was calculated as

$$1- : \text{Open wound day } n \text{ as \% of original} = \frac{\text{open wound area day } n}{\text{original wound area (day 0)}} \times 100$$

$$2-: \% \text{ total wound healing day } n = 100 - \text{open wound day } n \text{ as \% of original}$$

3-10-3: Microscopical Evaluation

Progress of cutaneous wounds healing following using of acellular ovine skin and acellular bovine pericardium was furtherly monitored using microscopic criteria including both histopathological and immunohistochemistry.

3-10-3-1: Histopathological Assessment

The histopathological features associated with cutaneous skin wound healing was evaluated on 7, 14 and 21 days following dressing using skin samples collected from the wounds' corners along with 1–2 mm of the surrounding normal skin. The transplanted tissues were preserved with 10% neutral-buffered formalin for 48 hours for fixation. Then, these

samples were embedded in paraffin, sectioned, stained with hematoxylin–eosin, and examined using light microscopy. Each histological section was assessed microscopically for evaluation of the healing features as shown in Table 3 (Başaran *et al.*, 2006; Sultana *et al.*, 2009; Gupta and Kumar, 2015; Tsioli *et al.*., 2018).

Table 3: Histopathological parameters for semi-qualitative assessment for dressing performance.				
Criteria	1	2	3	4
Granulation tissue	Absent	Discrete	Moderate	Intense
Re-epithelization	Absent	Discrete	Moderate	Intense
Severity of inflammation	Sever	Moderate	Few	Absent
Blood prefusion	Absent	Discrete	Moderate	Intense

3-10-3-2: Immunohistochemistry of VEGF

Assessment of VEGF visualization and localization was used to investigate tissue viability based on subjective modified scoring criteria described by (Fedchenko and Reifenrath, (2014), and Sojo *et al.*, (2005) (Table 4). Five microscopic fields were examined for each histological criterion per slide and the mean \pm S.E.M was calculated for each parameter based on the different staining intensity observed.

Table 4: Immunohistochemical scoring of VEGF					
Criteria	0	1	2	3	4
VEGF	Negative absent	Very Weak +	Low Positive ++	Moderate Positive +++	Strong Positive ++++

Immunohistochemical scoring of VEGF. (0) absent; (1) (+) very weak immunoreactivity; (2) (++) low positive immunoreactivity; (3) (+++) moderate positive immunoreactivity; (4) (++++ high immunoreactivity.

3-11: Doppler Ultrasound Evaluation

The linear transducer of 4-13 MHz doppler ultrasound evaluation was used (Clarius / Canadian) to detect presence of cutaneous blood perfusion associated with using both xenografts for dressing of full-thickness. It started to be taken since day 12 post surgery to avoid the separation of the dressing from the underline bed and continued until end of experiment on day 21 post dressing (Figure 16) (Cosgrove and Lassau, 2010; Angelou *et al.*, 2022).



Figure16: Photographic images for doppler ultrasonographic examination following dressing to assess cutaneous circulation.

3-12: Statistical Analysis

The obtained data of this study was presented as mean \pm SEM. The comparison between the two groups was done using t-test while the scored data of the three times periods was evaluated using One-way ANOVA and Duncan's multiple range test that considered significant when P values were less than 0.05 ($P < 0.05$) (Pearson *et al.*, 2011).

Chapter Four

Results

4-1: Mechanical Results

The results of mechanical properties of both a cellular ovine skin and a cellular bovine pericardium exhibited hug improvement in their values especially (maximum load and modulus of elasticity) following decellularization (Table 5) (Figures 17-20). Furthermore, acellular bovine pericardium elasticity was much better comparable to acellular ovine skin that made it tear partially and gradually throughout the time of mechanical testing while acellular ovine skin showed less elasticity that manifested as a sudden and complete tearing during mechanical testing. On the other hand, the tensile strength of a cellular ovine skin was much higher than that of acellular bovine pericardium (Figure 21 and 22).

Table 5: Show the mechanical properties of decellularized ovine skin and decellularized bovine pericardium before and after decellularization.

KIND OF TISSUE	Mechanical characters			
	Maximum load (Newton)		Modules of elasticity (mm)	
	Before decellularization	After decellularization	Before decellularization	After decellularization
Ovine skin	386.3±23.1 B	598.6±53.4 Aa	26.25±3.6 B	33.25±1.7 Ab
Bovine pericardium	103±0.8 B	211.3±4.3 Ab	27.25±3.09 B	36.5±2.2 Aa

Data were presented as means \pm S.E.M. Different capital letters mean there was significant differences between groups at $p \leq 0.05$. While the different small letters mean there was significant differences between periods at $p \leq 0.05$.

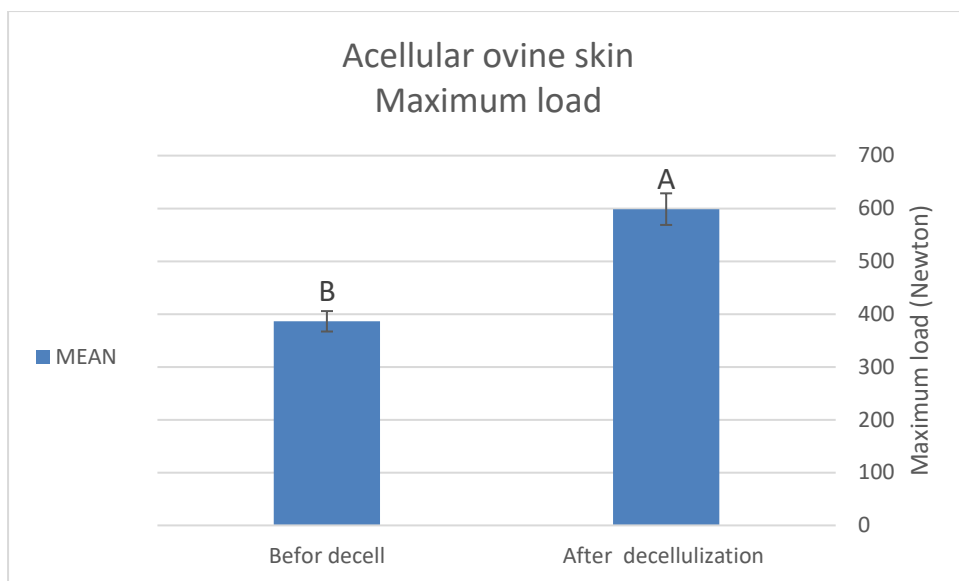


Figure 17: Diagrams show the maximum load (Newton) of ovine skin before and after decellularization. Data were expressed as means \pm S.E.M. Different letters indicate significant difference.

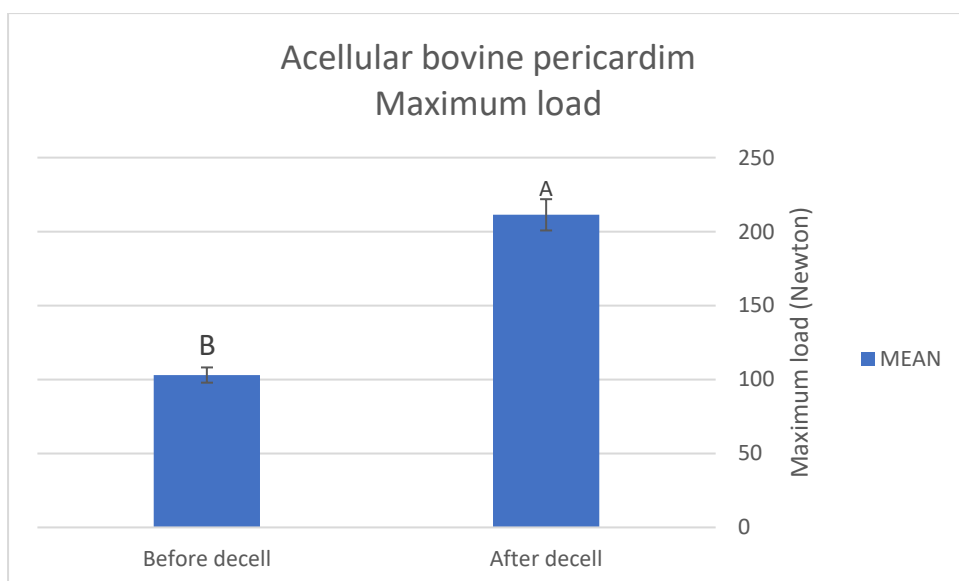


Figure 18: Diagrams show the maximum load (Newton) of bovine pericardium before and after decellularization. Data were expressed as means \pm S.E.M. Different letters indicate significant difference.

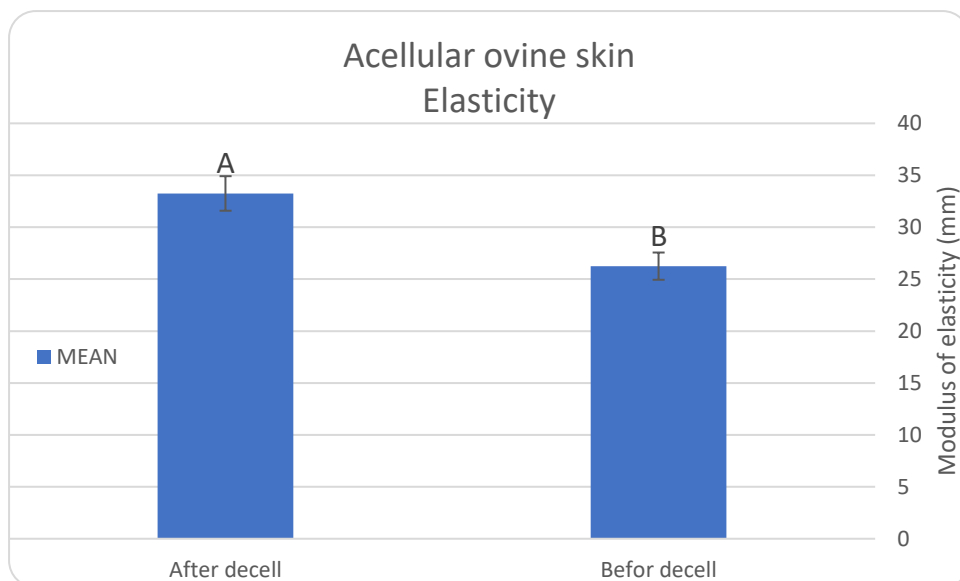


Figure 19: Diagrams show the Modulus of elasticity (mm) of ovine skin before and after decellularization. Data were expressed as means \pm S.E.M. Different letters indicate significant difference.

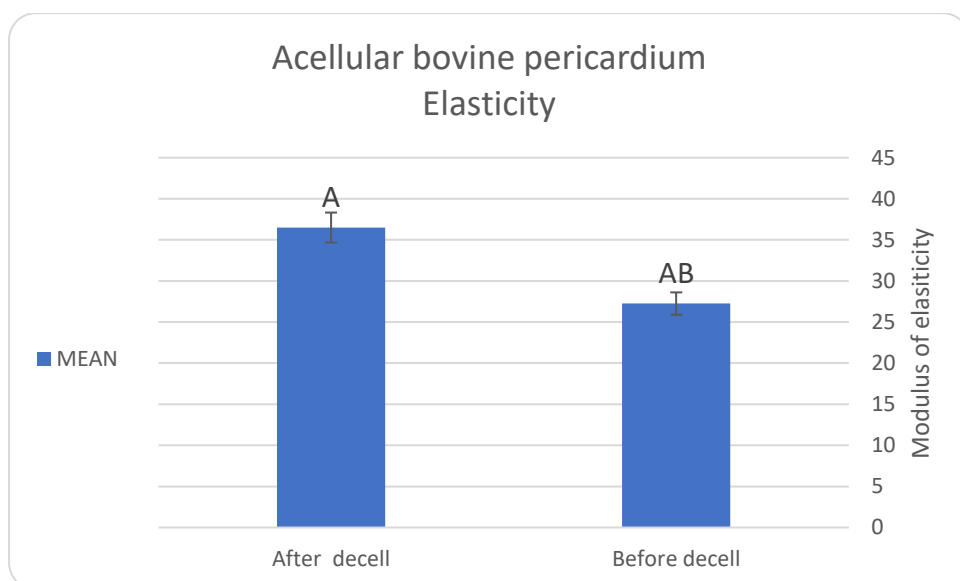


Figure 20: Diagrams show the Modulus of elasticity (mm) of bovine pericardium before and after decellularization. Data were expressed as means \pm S.E.M. Different letters indicate significant difference.

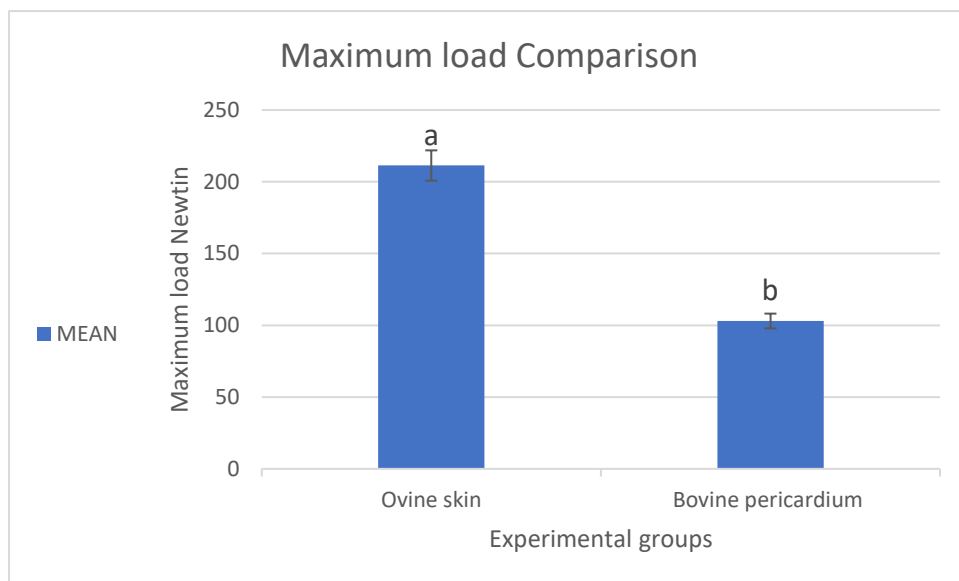


Figure 21: Diagrams show comparison between the Maximum load (Newton) of both decellularized ovine skin and decellularized bovine pericardium after decellularization. Data were expressed as means \pm S.E.M. Different letters indicate significant difference.

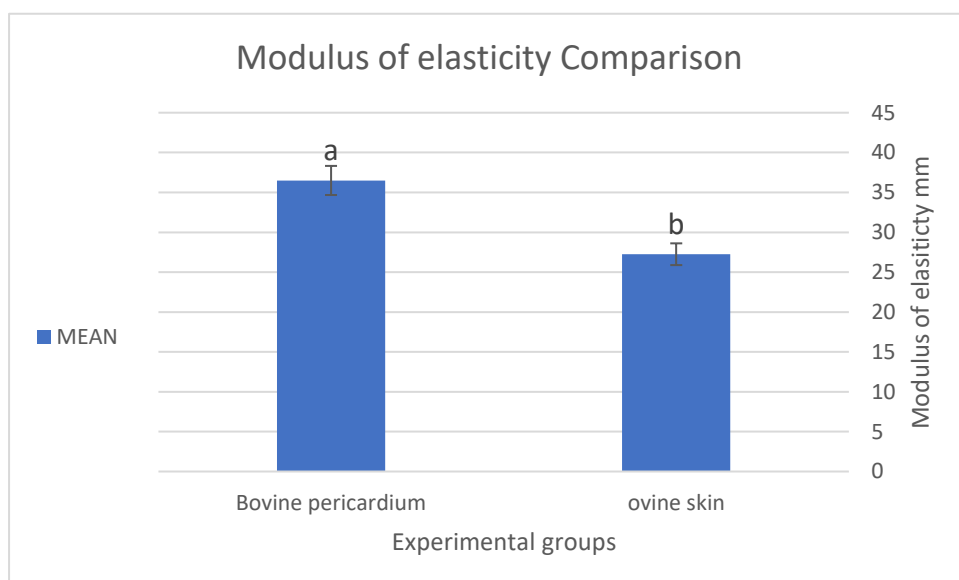


Figure 22: Diagrams show comparison between the Modulus of elasticity (mm) of both decellularized ovine skin and decellularized bovine pericardium after decellularization. Data were expressed as means \pm S.E.M. Different letters indicate significant difference

4-2: Macroscopic Results

4-2-1: Cross Results

4-2-1-1: Pliability of decellularized xenografts

The clinical observations showed that the pliability of acellular ovine skin was good since 1st day until day 9 post dressing then became stiffer gradually till its shedding on day 19 while acellular bovine pericardium elasticity was normal till day 5 then it started to be stiffer gradually until its detached (Figure 23-25).

4-2-1-2: Color of decellularized Xenografts

The color of acellular bovine pericardium dressing (n=9) was normal since the 1st dressing day till day nine when it started to become greyer in comparison to acellular ovine skin, which started to lose its normal color since day seven, then both xenografts dressing gradually became darker (Figures 23-25).

4-2-1-3: Adherence of the decellularized Xenografts with Wound Bed

In both groups, acellular dressing started to be partially and loosely adhered to the recipient bed on day 3 post dressing in all cat. However, acellular ovine skin adhesion was much better than that of acellular bovine pericardium and continued until day 15, while it continued up to day 7 in pericardium group. Then, these dressing started to be detached from the underlining bed on day 15 for acellular ovine skin and on days 8 up to 14 for acellular bovine pericardium (Figures 23-25).

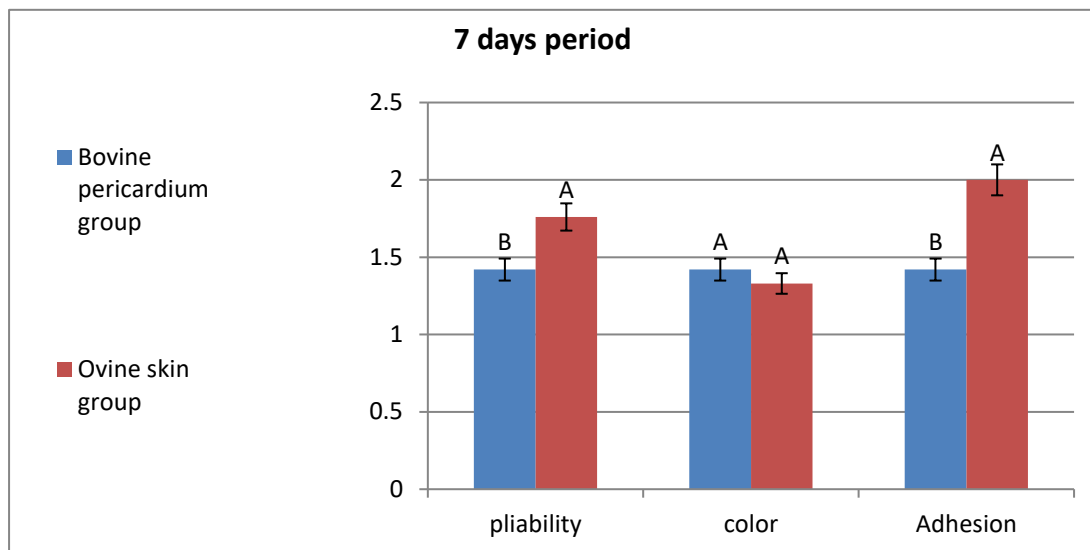


Figure 23: Diagram of the comparison in clinical scoring between two experimental groups in day 7 post dressing. Different letters indicate significant difference. One-way ANOVA, Duncan's multiple comparison test. Data were presented as means \pm S.E.M.

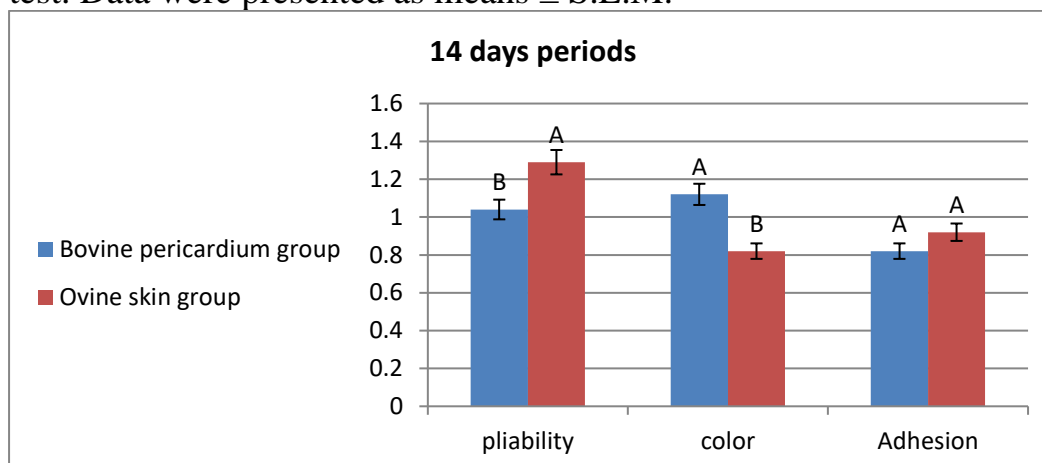


Figure 24: Diagram of the comparison in clinical scoring between two experimental groups in day 14 post dressing. Different letters indicate significant difference. One-way ANOVA, Duncan's multiple comparison test. Data were presented as means \pm S.E.M.

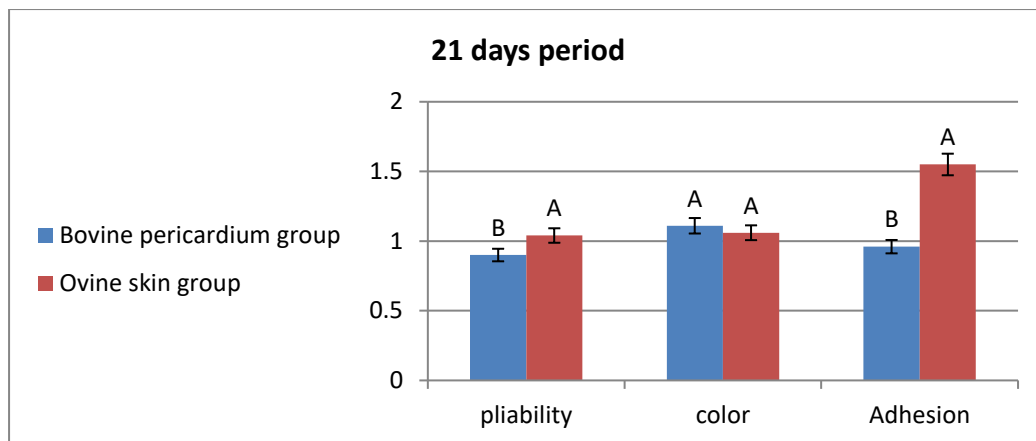


Figure 25: Diagram of the comparison in clinical scoring between two experimental groups in day 21 post dressing. Different letters indicate significant difference. One-way ANOVA, Duncan's multiple comparison test. Data were presented as means \pm S.E.M.

The statistical examination exhibited significant difference in the observed clinical criteria between both experimental groups during the whole periods of study (Table 6).

Periods	Criteria Groups	Pliability	Color	Adhesion
7 days	Bovine pericardium G.	1.42± 0.11 A	1.42±0.11 A	1.42±0.11 B
	Ovine skin G.	1.76±0.09 A	1.33±0.10 A	2±0.0 A
14 days	Bovine pericardium G.	1.04±0.12 C	1.12±0.11 B	0.82±0.09 C
	Ovine skin G.	1.29±0.13 B	0.82±0.08 C	0.92±0.11 C
21 days	Bovine pericardium G.	1.68±0.87 A	1.11±0.07 B	0.96±0.10 C
	Ovine skin G.	1.04±0.13 C	1.06±0.09 B	1.55±0.10 B
<i>p</i> -Value		<0.001	0.028	<0.001

Table 6: Comparison in clinical scoring between two experimental groups in days 7, 14, 21 post dressing. Different letters indicate significant difference. One-way ANOVA, Duncan's multiple comparison test. Data were presented as means ± S.E.M.

4-2-2: Wound Bed Results

In both groups, there was some degree of exudate and edema especially in 2nd group (ABP) comparable to 1st group (AOS). Besides, the statistical analysis of gross observations displayed a significant difference between both experimental group ($P \leq 0.05$). Nonetheless, the progress of wound healing was slower in ABP as compare to AOS group. Besides there were remarkable differences in wound area and its morphology between both groups as shown in (Figures 26-31).



Figure 26: Photographic image for acellular ovine skin after 7 days and days following dressing onto full-thickness skin wounds in cat.



Figure 27: Photographic image for acellular bovine pericardium after 7 days following dressing onto full-thickness skin wounds in cat.



Figure 28: Photographic image for acellular ovine skin after 14 days following dressing onto full-thickness skin wounds in cat.



Figure 29: Photographic image for acellular bovine pericardium after 14 days following dressing onto full-thickness skin wounds in cat.



Figure 30: Photographic image for acellular ovine skin after 21 days following dressing onto full-thickness skin wounds in cat.



Figure 31: Photographic image for acellular bovine pericardium after 21 days following dressing onto full-thickness skin wounds in cat.

The statistical analysis of the gross data i.e. exudate, pus, edema and hemorrhage exhibited significant decrease along the period of study and showed significant difference between both experimental group during the whole periods of study (Figures 32-34).

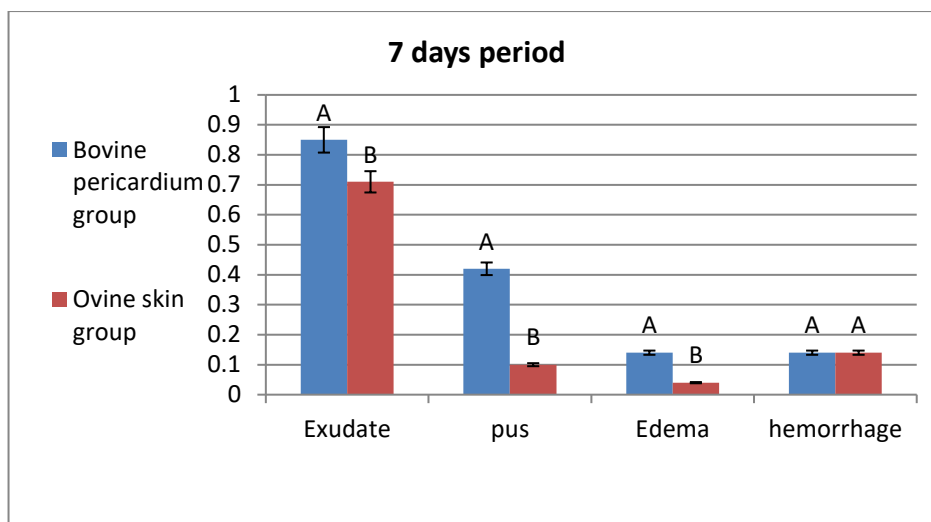


Figure 32: Diagram of the comparison in macroscopic gross scoring between two experimental groups in day 7 post dressing. Different letters indicate significant difference. One-way ANOVA, Duncan's multiple comparison test. Data were presented as means \pm S.E.M.

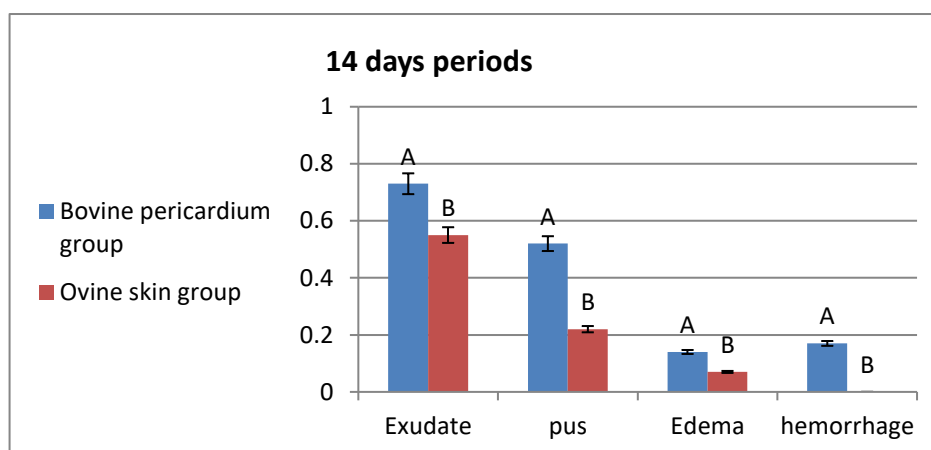


Figure 33: Diagram of the comparison in macroscopic gross scoring between two experimental groups in day 14 post dressing. Different letters indicate significant difference. One-way ANOVA, Duncan's multiple comparison test. Data were presented as means \pm S.E.M.

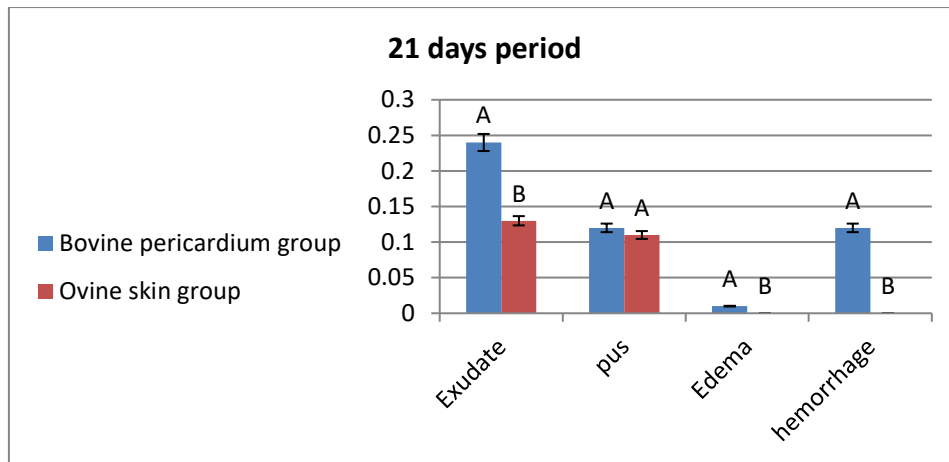


Figure 34: Diagram of the comparison in macroscopic gross scoring between two experimental groups in day 21 post dressing. Different letters indicate significant difference. One-way ANOVA, Duncan's multiple comparison test. Data were presented as means \pm S.E.M.

4-2-3: Planimetry

The dimensions of the full-thickness cutaneous wounds started to decrease since the next day following dressing. Besides, the rates of wound contraction and total healing on days 7, 14 and 21 following dressing exhibited progress significant decrease in their measurements during the whole period of study (Figures 35-37).

4-2-3-1: Contraction

The contraction percentage increased gradually from day 0 to day 21 ($p < 0.001$). The mean contraction percentage of the 1st group was (48.2%) while for the 2nd group was (40.75%). On day 14, a big elevation in contraction was observed in both groups. On day 21, the contraction percentage was up to 65% in AOS and 55% ABP groups. A significant difference was noted in both experimental groups during all measurement days.

4-2-3-2: Total Wound Healing

The main percentage of total wound healing in acellular ovine skin group was (61.51%), which was greater than that of acellular bovine

pericardium group (55.19%). On day 7, the mean total healing in the 1st group was greater (21.8 %) than in the 2nd group (15.2%). The total wound healing percentage increased in both groups at all measurement times from day 0 to day 21 ($p < 0.001$). Total wound healing reached 85% in AOS and 74% in ABP on day 21.

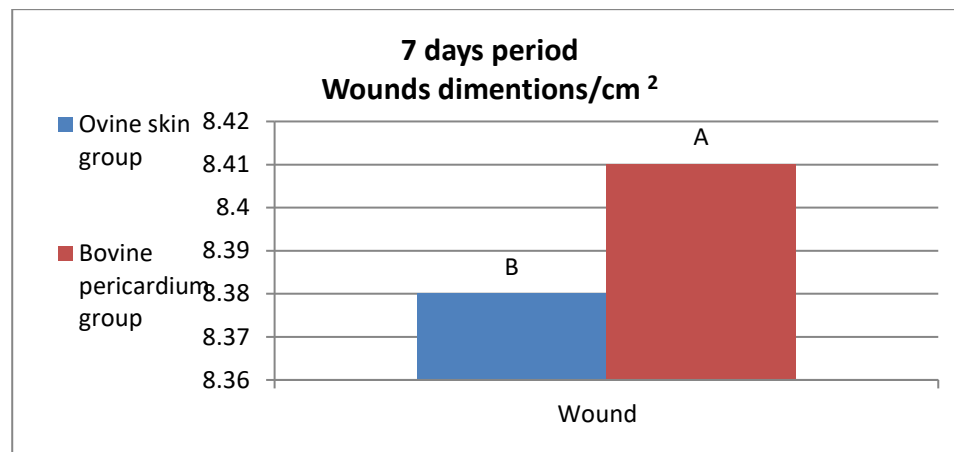


Figure 35: Diagram of the comparison in wound planimetry dimensions between two experimental groups in day 7 post dressing. Different letters indicate significant difference. One-way ANOVA, Duncan's multiple comparison test. Data were presented as means \pm S.E.M.

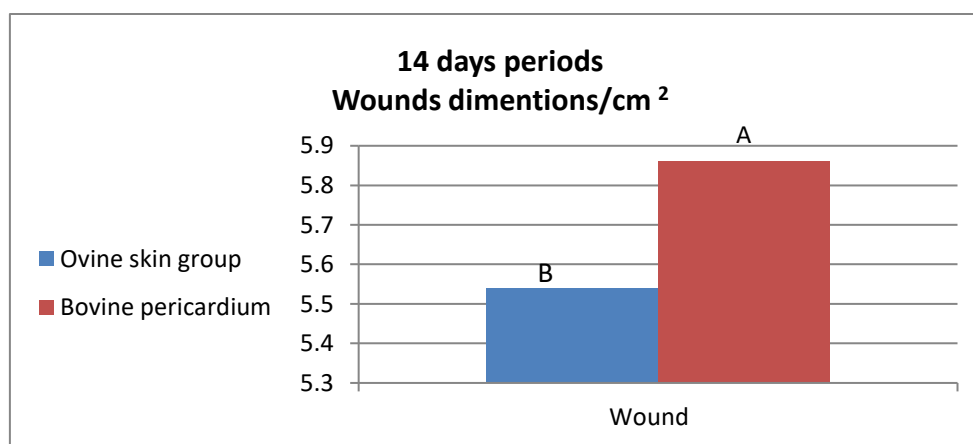


Figure 36: Diagram of the comparison in wound planimetry dimensions between two experimental groups in day 14 post dressing. Different letters indicate significant difference. One-way ANOVA, Duncan's multiple comparison test. Data were presented as means \pm S.E.M.

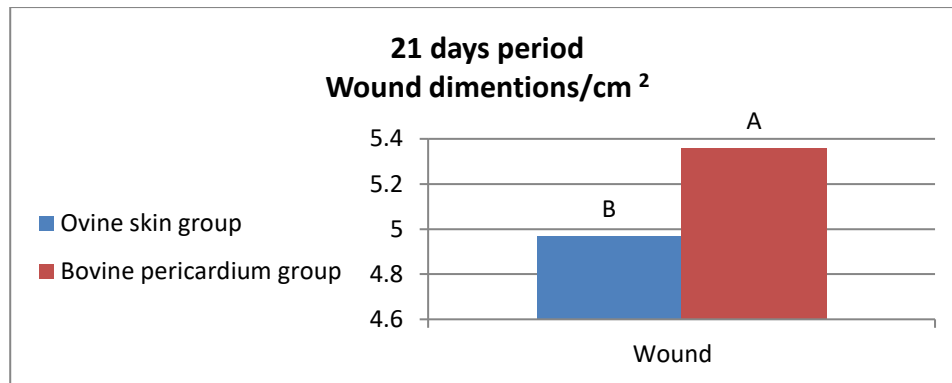


Figure 37: Diagram of the comparison in wound planimetry dimensions between two experimental groups in day 21 post dressing. Different letters indicate significant difference. One-way ANOVA, Duncan's multiple comparison test. Data were presented as means \pm S.E.M.

4-3: Microscopic Results

4-3-1: Histopathological Results

4-3-1-1: Day 7

The histopathological examination for the 1st acellular ovine skin exhibited presence of closely contact between the dressing and wound beds skin margins with severe diffuse infiltration of polymorph nuclear inflammatory cells and mononuclear inflammatory cells (Figures 38-39).

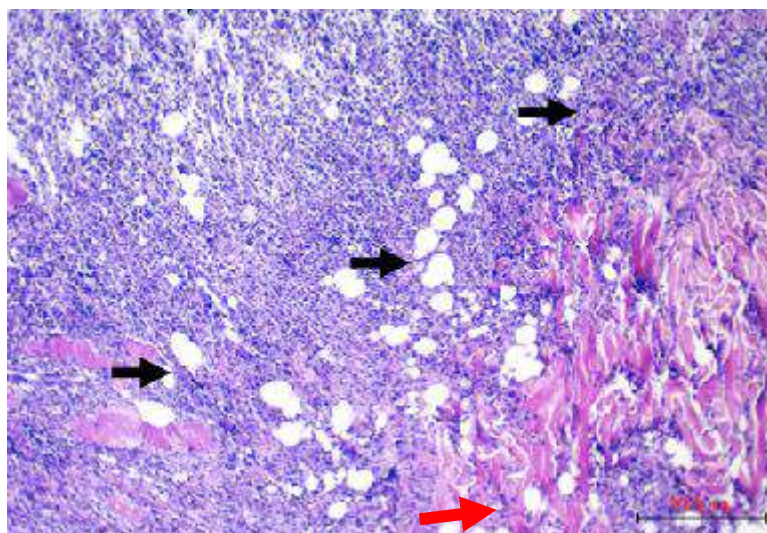


Figure 38: Histopathological section of first group at day 7 after dressing in a cat skin wound, shows severe diffuse infiltration of inflammatory cells inside of the wound (black arrows) associated with congesting of blood vessels (red arrows), (10x H&E).

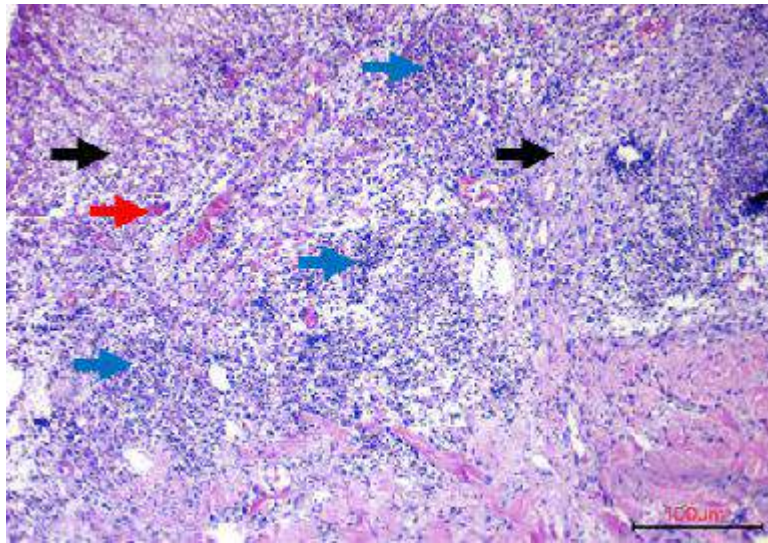


Figure 39: Histopathological section of ovine skin biomaterial dressing at day 7 after dressing in a cat skin wound, shows granulation tissue formation (black arrows), severe infiltration of inflammatory cells inside of the wound (blue arrows) associated with congesting of blood vessels (red arrows), (10x H&E).

On the other side, the histological section of acellular bovine pericardium patch at day 7 after dressing exhibited presence of extensive infiltration of inflammatory cells between skin and patch associated with edema and hemorrhage (Figures 40-41).

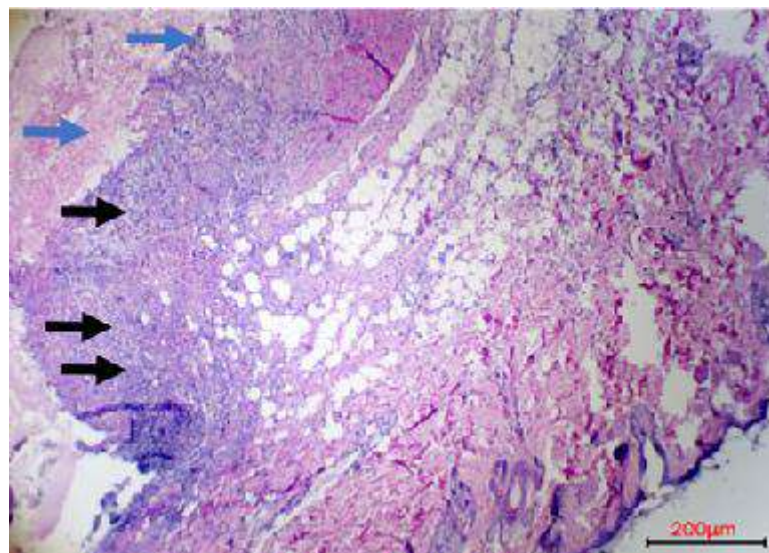


Figure 40: Histopathological section of second group at day 7 after dressing in a cat skin wound, shows the granulation tissue (black arrow) with inflammatory reaction and exudates at wound edges (blue arrow), (4x H&E).

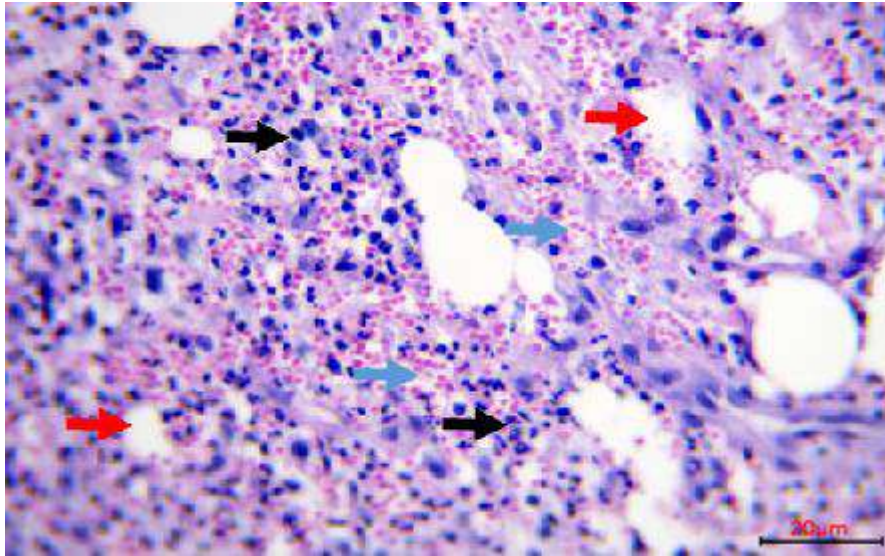


Figure 41: Histopathological section of second group at day 7 after dressing in a cat skin wound, shows infiltration of mononuclear inflammatory cells (black arrows) associated with edema (red arrow), and haemorrhage (blue arrow) in the bovine pericardium patch, (40x H&E).

4-3-1-2: Day 14

While the histological section of acellular ovine skin patch at day 14 after dressing exhibited that the ovine dressing is closely interwoven with the skin wound bed and attached very well to the skin tissue with infiltration of fibroblast between them, presence of well-developed granulation tissue. Besides, well fibrous tissue and collagen fibers distributed between the patch and skin, formation of blood capillaries (blood perfusion), well re-epithelialization and no heavy inflammatory response with few inflammatory cells (Figures 42-45).

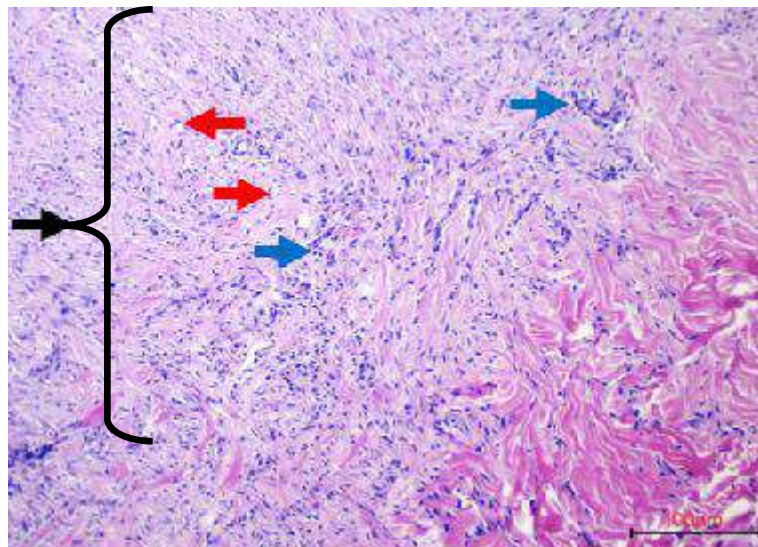


Figure 42: Histopathological section of first group at day 14 after biomaterial dressing in a cat skin wound, shows well granulation tissue with proliferated fibrous tissue closely interwoven with the skin (black arrow), with formation of new blood capillaries (red arrows) and few inflammatory cells (blue arrows), (10x H&E).

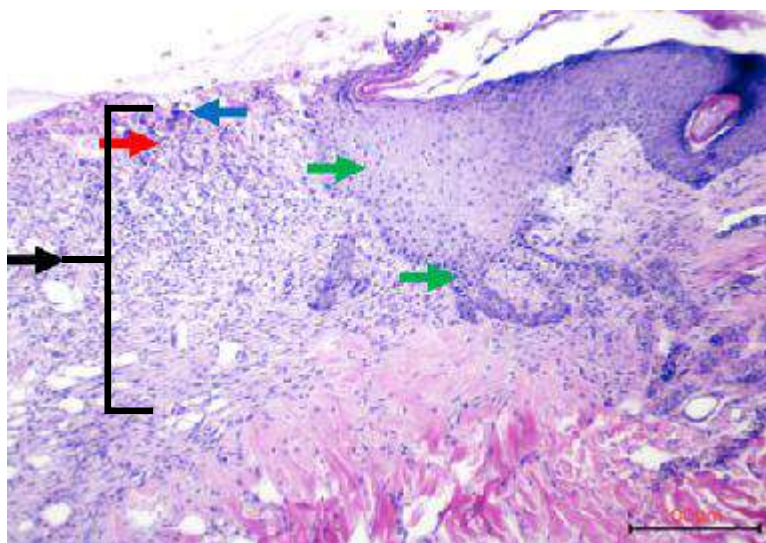


Figure 43: Histopathological section of first group at day 14 after dressing in a cat skin wound, shows the ovine dress with well-developed granulation tissue (black arrows), with well vascularized (blood perfusion) (red arrow), few infiltrations of inflammatory cell (blue arrows), and well re-epithelialization (green arrow), (4x H&E).

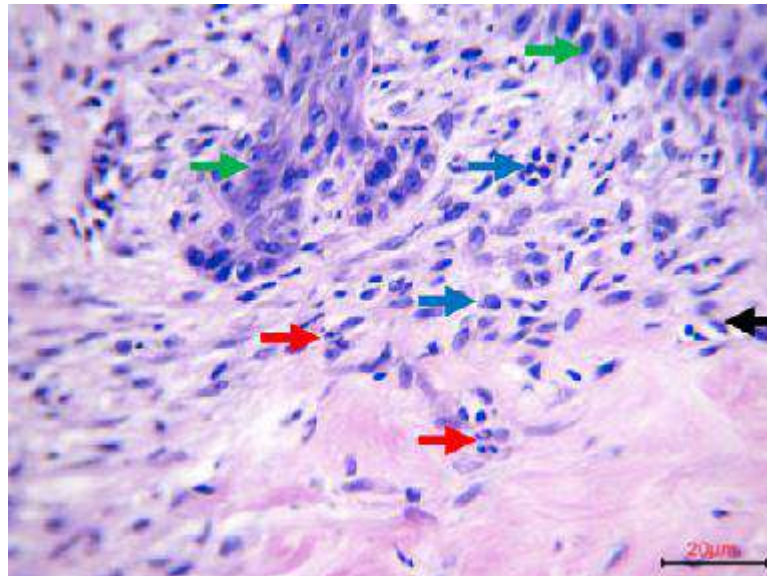


Figure 44: Histopathological section of first group at day 14 after dressing in a cat skin wound, shows well-developed granulation tissue (black arrows), with well vascularized (blood perfusion) (red arrow), few infiltrations of inflammatory cell (blue arrows), and well re-epithelialization (green arrow), (40x H&E).

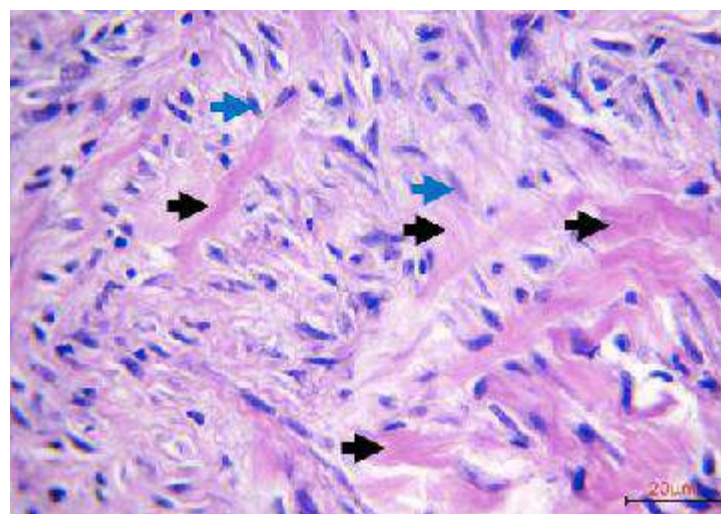


Figure 45: Histopathological section of first group at day 14 after dressing in a cat skin wound, shows well granulation tissue with mature connective tissue (black arrows) and proliferated fibroblasts (blue arrows) (40x H&E).

Also, for acellular bovine pericardium after 14 days, there was good closely interwoven between skin and pericardium with focal infiltration of mononuclear inflammatory, formation of blood capillaries (blood perfusion) re-epithelialization (Figures 46- 48).

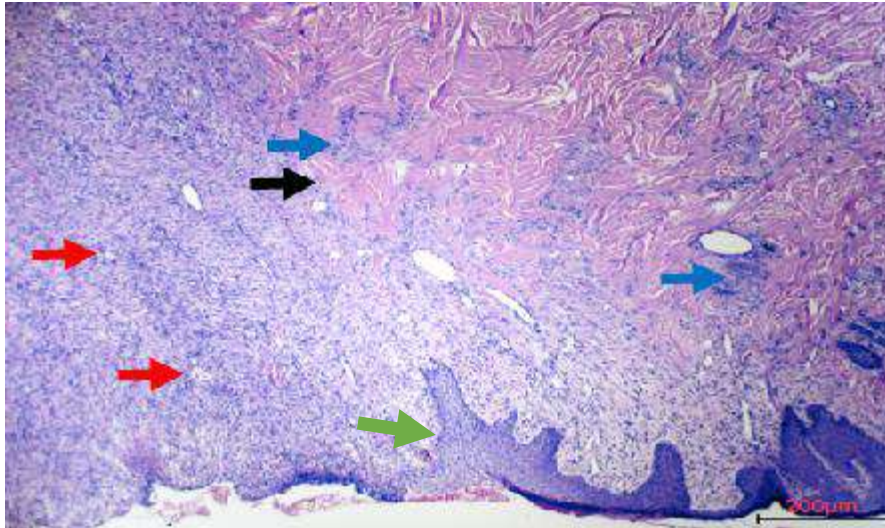


Figure 46: Histopathological section of second group at day 14 after dressing in a cat skin wound, shows the pericardium dress is closely interwoven with the skin (black arrow), focal infiltration of inflammatory cells between the dress and skin (blue arrows), formation of blood capillaries (blood perfusion) (red arrows) and re-epithelialization (green arrow), (4x H&E).

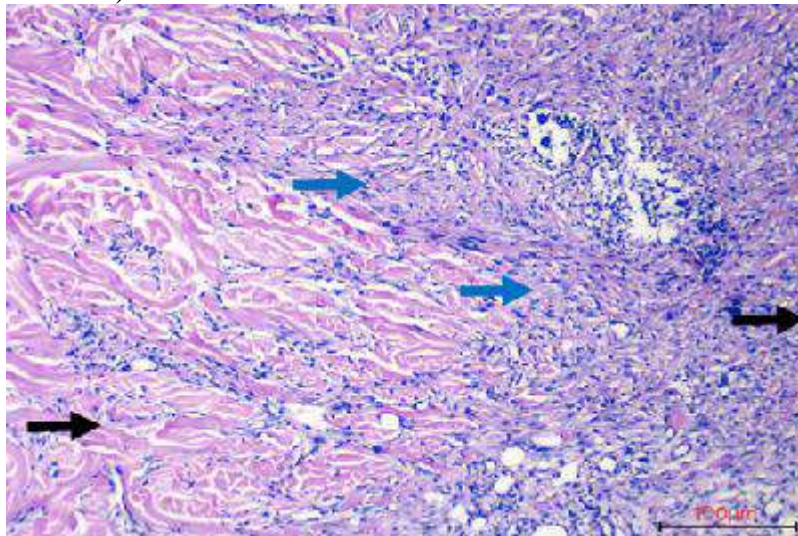


Figure 47: Histopathological section of second group at day 14 after dressing in a cat skin wound, shows extensive infiltration of inflammatory cells (black arrows), immature fibrous tissue and collagen fibers are between the dress and skin (blue arrows), (10x H&E).

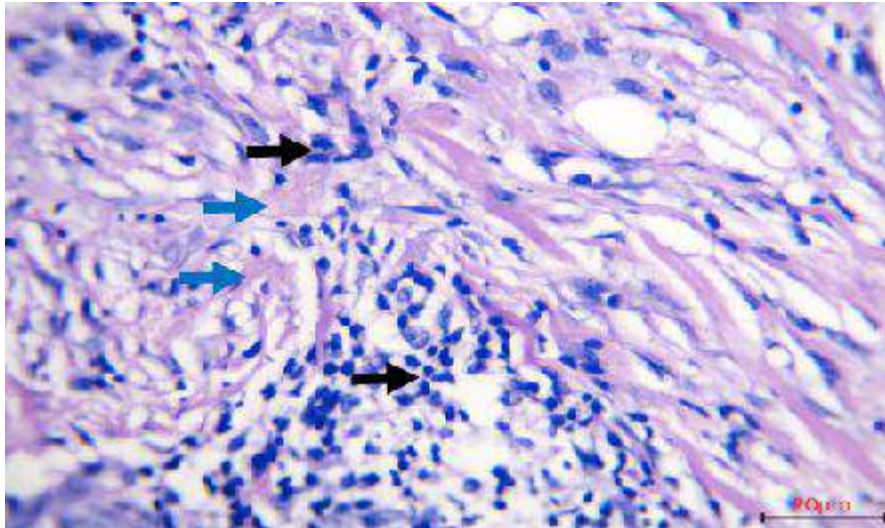


Figure 48: Histopathological section of second group at day 14 after dressing in a cat skin wound, shows focal infiltration of mononuclear inflammatory cells with fibroblasts (black arrows) immature fibrous tissue and collagen fibres are between the dressing and skin (blue arrows), (40x H&E).

4-3-1-3: Day 21

The histological section of acellular ovine skin patch at day 21 after dressing exhibited strict interwoven with the skin with re-epithelialization and regeneration of wound edges. The regenerating epithelium displayed the polarity of normal basal cells and well differentiation of squamous cells, epidermal outlines and dermo-epidermal junction started to regain its architecture structure. Besides, the tissue construction especially the epidermal outlines and dermo-epidermal junction showed healthier histological manifestations with good tissue architecture, and structural integrity along with more deposition of collagen fibres. Few of inflammatory cells were found with distribution of fibrosis and fibroblast cells (Figures 49- 51).

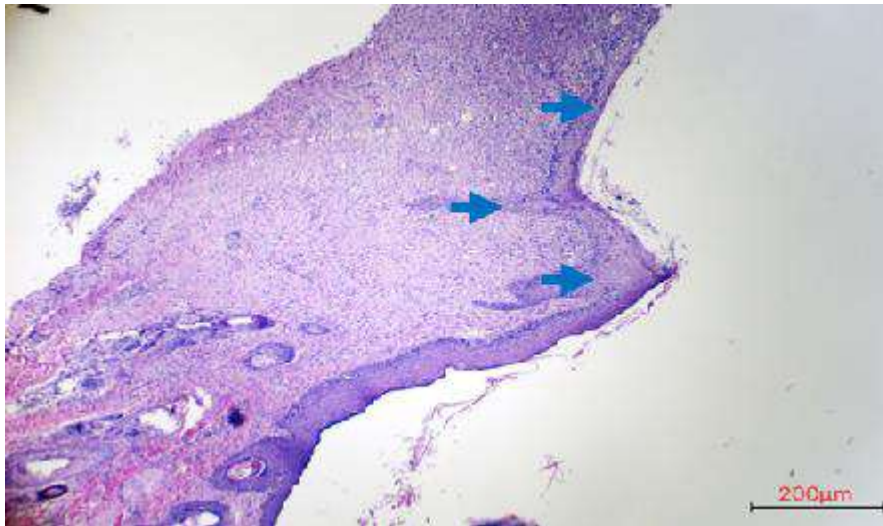


Figure 49: Histopathological section of first group at day 21 after dressing in a cat skin wound, re-epithelialization and regeneration wound edges (blue arrows), (4x H&E).

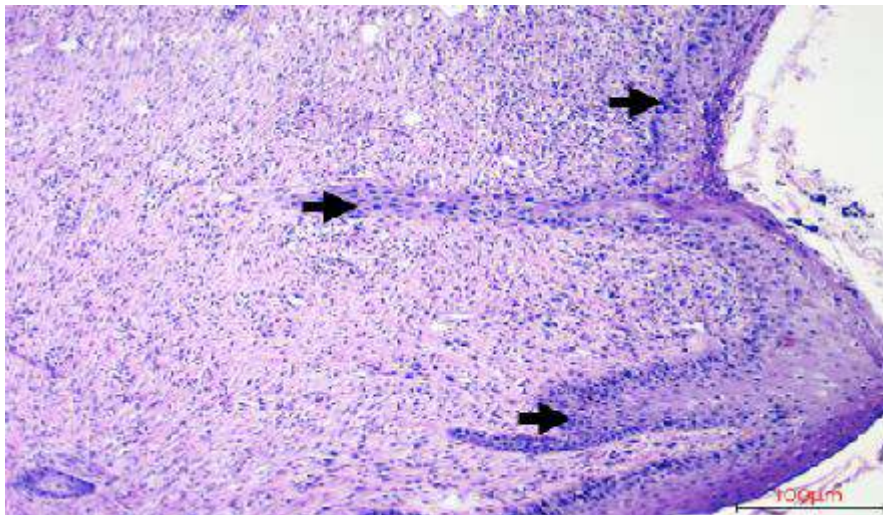


Figure 50: Histopathological section of first group at day 21 after dressing in a cat skin wound. The regenerating epithelium shows the polarity of normal basal cells and the differentiation of squamous cells (black arrows), (4x H&E).

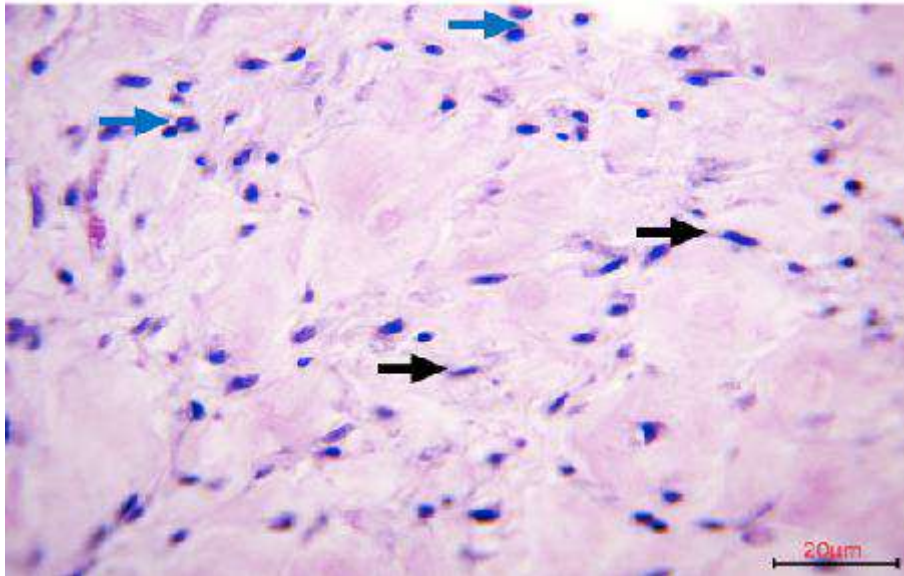


Figure 51: Histopathological section of ovine skin patch dress at day 21 after dressing in a cat skin wound, shows the granulation tissue involves more collagen fibers and fibroblast (black arrows) and few inflammatory cells (blue arrows), (40x H&E).

On the other hand, the histopathological examination of acellular bovine pericardium after 21 days, showed the more prominent interwoven between skin and pericardium with re-epithelialization as rebuilding of epidermis over the pericardium graft, formation of fibrous tissue and infiltration of cluster of mononuclear inflammatory cells between the dress and skin focal and less edema and increased formation of blood capillaries (blood perfusion). Besides, epidermal integrity and dermal and epidermal junction started to regain its architecture with more deposition of collagen fibres (Figures 52-53).

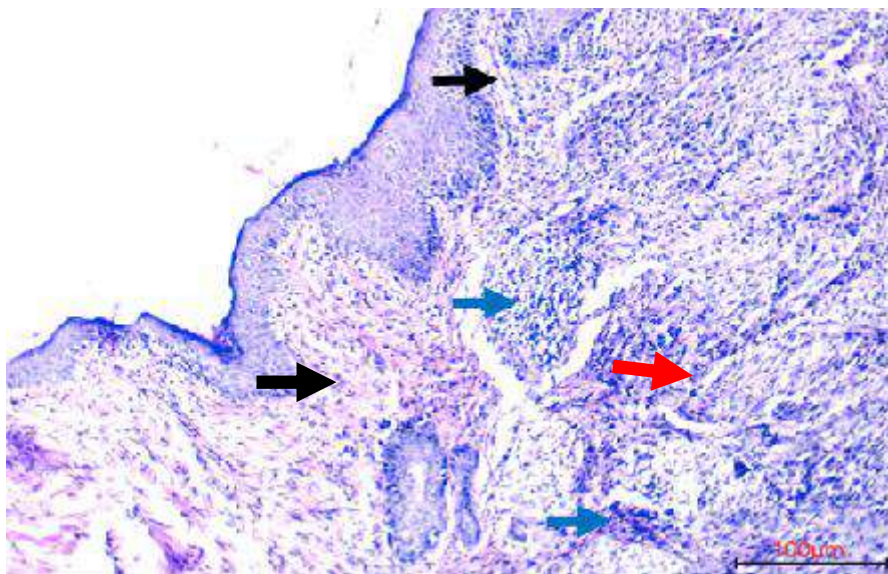


Figure 52: Histopathological section of second group at day 21 after dressing in a cat skin wound, shows re-epithelialization as rebuilding of epidermis over the pericardium dress (black arrow), formation of fibrous tissue (red arrow) and infiltration of cluster of mononuclear inflammatory cells between the dress and skin (blue arrows), (4x H&E).

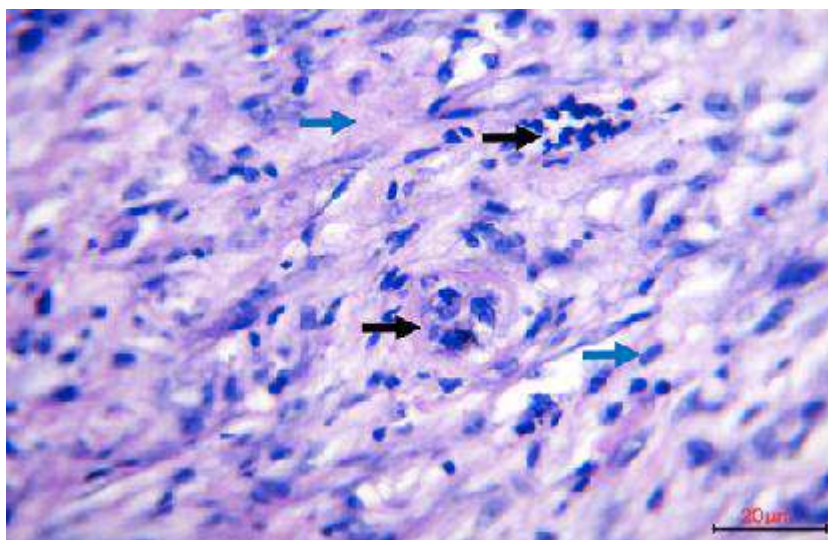


Figure 53: Histopathological section of second group at day 21 after dressing in a cat skin wound, shows the diffuse mononuclear cells (lymphocytes, macrophages, giant cells) (black arrows), infiltration of granulation tissue into the dressing with a lots of fibroblast cells (blue arrows), (40x H&E).

Furthermore, statistical analysis showed significant difference ($P < 0.05$) between both decellularized ovine skin and bovine pericardium and among different times for the microscopic criteria including inflammatory infiltration, granulation tissue re-epithelization and blood perfusion (Figures 54-57).

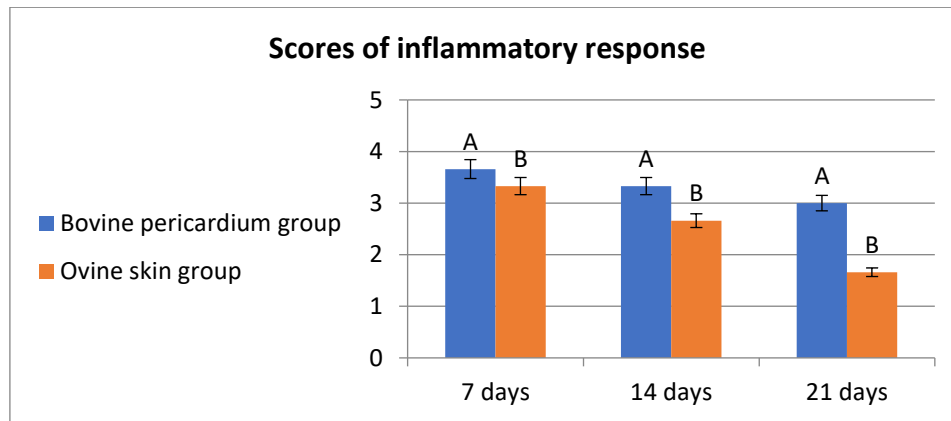


Figure 54: Diagram presentation of the comparison in inflammatory response scoring between two experimental groups in days 7, 14 and 21 post dressing. Different letters indicate significant difference. One-way ANOVA, Duncan's multiple comparison test. Data were presented as means \pm S.E.M.

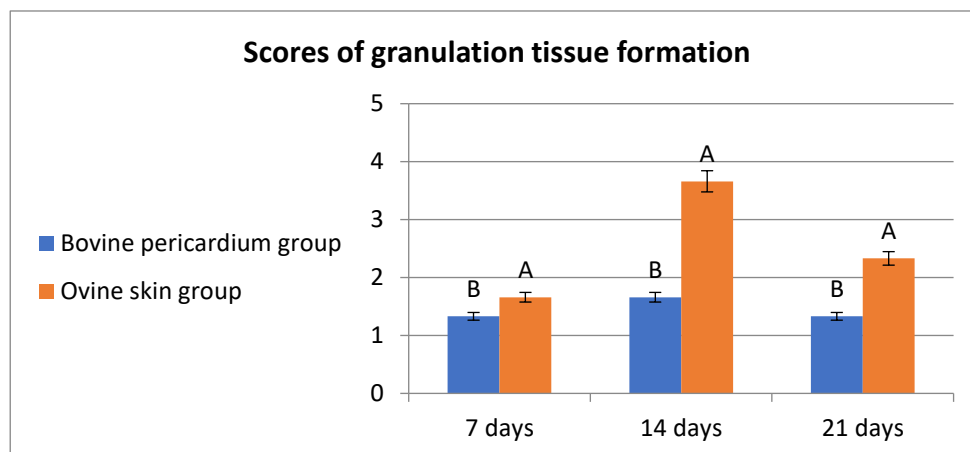


Figure 55: Diagram presentation of the comparison in granulation tissue formation scoring between two experimental groups in days 7, 14 and 21 post dressing. Different letters indicate significant difference. One-way ANOVA, Duncan's multiple comparison test. Data were presented as means \pm S.E.M.

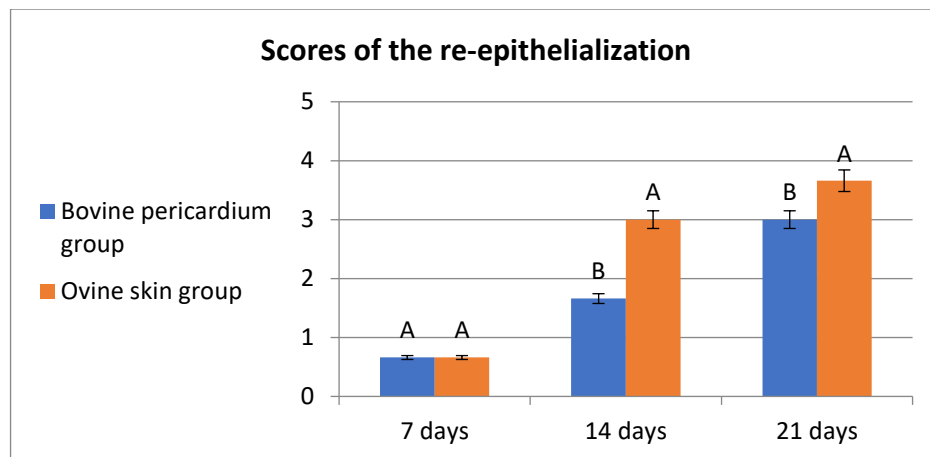


Figure 56: Diagram presentation of the comparison in re-epithelialization scoring between two experimental groups in days 7, 14 and 21 post dressing. Different letters indicate significant difference. One-way ANOVA, Duncan's multiple comparison test. Data were presented as means \pm S.E.M.

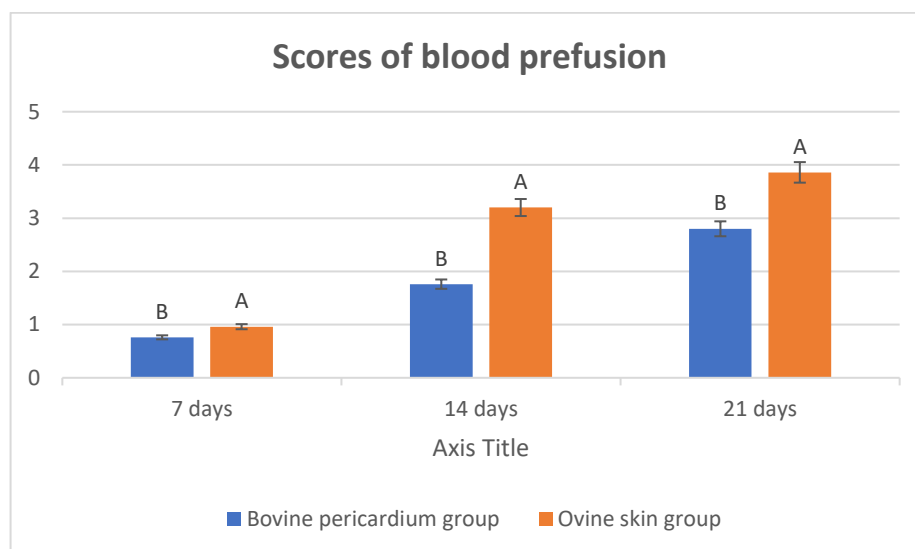


Figure 57: Diagram presentation of the comparison in blood perfusion formation scoring between two experimental groups in days 7, 14 and 21 post dressing. Different letters indicate significant difference. One-way ANOVA, Duncan's multiple comparison test. Data were presented as means \pm S.E.M.

4-3-2: Immunohistochemistry Results

The results of vascular endothelium growth factor expression showed its presences within the angioblast cells. The overall trend detected that both exogenous patch dressings bed showed variable intensity expression and visualization of VEGF. However, decellularized ovine skin showed more staining intensity than decellularized bovine pericardium, which showed mild staining intensity. Furthermore, the intensity of staining and expression was gradually increasing with time. It was mild on day 7 post dressing, then became moderate on day 14, and became strong on day 21 in both groups; however, that expression was more obvious with ovine skin more than bovine pericardium (Figures 58- 63).

Statistical analysis showed significant difference ($P < 0.05$) in VEGF localization between both decellularized ovine skin and bovine pericardium and among different times within each experimental group (Table 7), (Figures 64-68).

Table 7: Show the expression of VEGF within beds of both transplanted acellular ovine skin and acellular bovine pericardium during the period of study.			
Protein	7 days	15 days	21 days
VEGF expression	2.1±0.14	3.26±0.22	4.19±0.16
Ovine skin	Ac	Ab	Aa
VEGF expression	0.8±0.04	2.5±0.61	3.5±0.55
Bovine pericardium	Bc	Bb	Ba

Data were presented as means \pm S.E.M. Different capital letters indicate significant difference between groups, small letters indicate significant difference within groups.

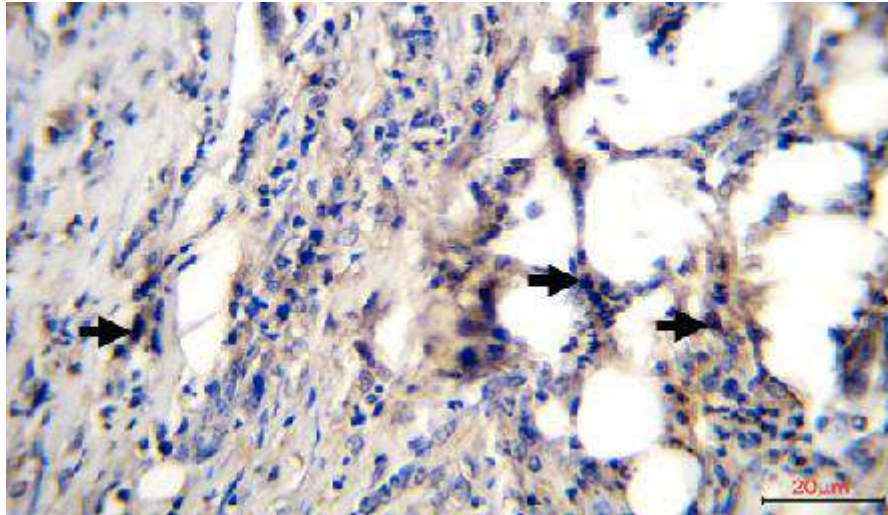


Figure 58: Immunohistochemical staining for VEGF of first group at day 7 after dressing in a cat skin wound, shows weak positive (+) VEGF expression that appear as nuclear brown stain in the Angioblasts cells within the tissue (arrows), (IHC. 40x).

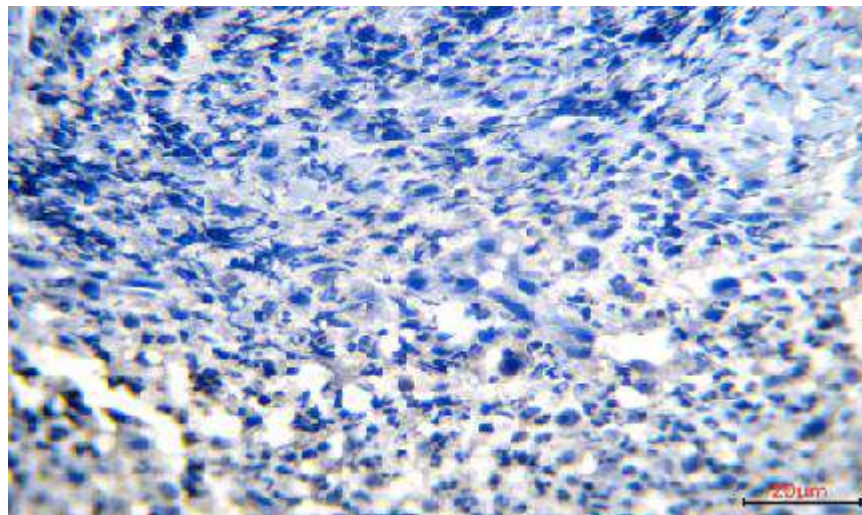


Figure 59: Immunohistochemical staining for VEGF of second group at day 7 after dressing in a cat skin wound, shows (+) weak positive VEGF expression that appears as nuclear brown stain in the Angioblasts cells within the tissue (arrows), (IHC. 10x)

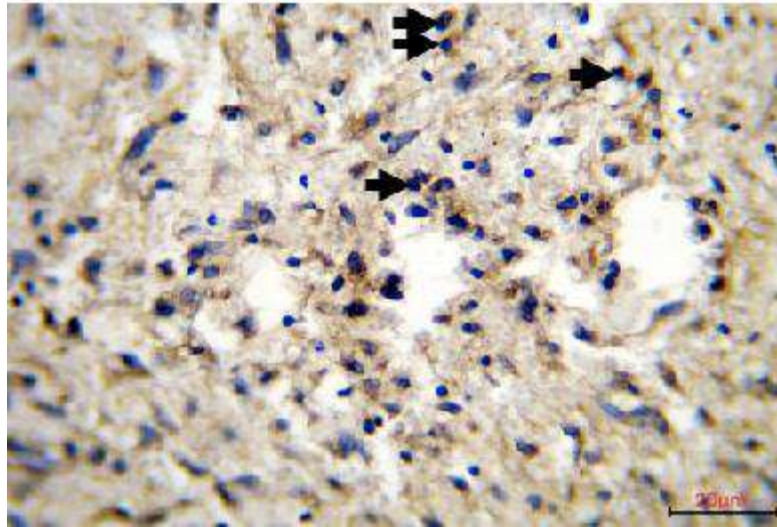


Figure 60: Immunohistochemical staining for VEGF of first group at day 14 after dressing in a cat skin wound, shows mild positive (++) VEGF expression that appears as nuclear brown stain in the Angioblasts cells within the tissue (arrows), (IHC. 40x).

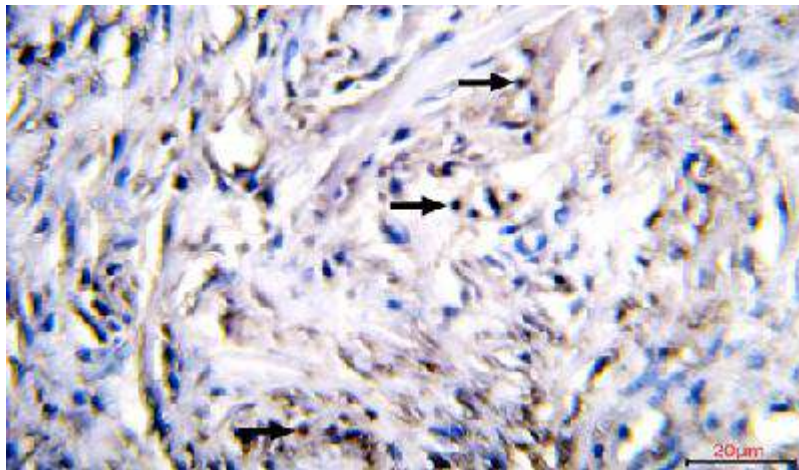


Figure 61: Immunohistochemical staining for VEGF of second group at day 14 after dressing in a cat skin wound, shows moderate positive (+++) VEGF expression that appears as nuclear brown stain in the Angioblasts cells within the tissue (arrows), (IHC. 40x).

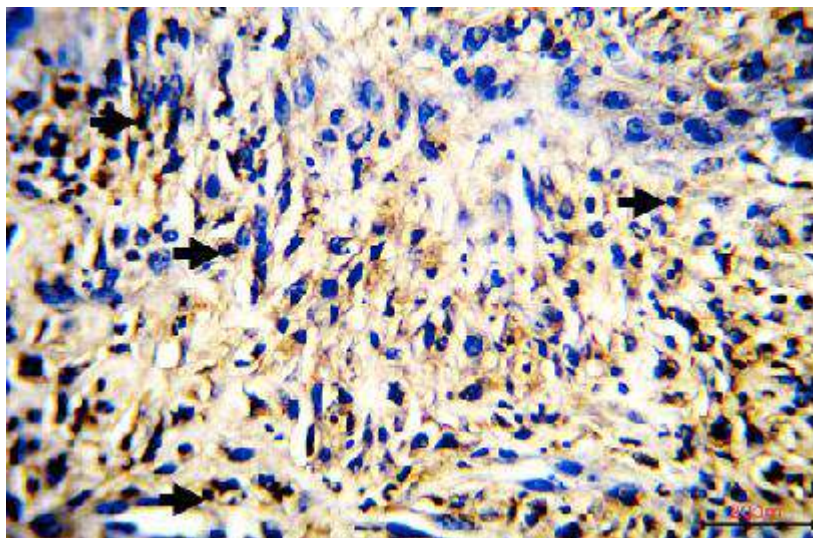


Figure 62: Immunohistochemical staining for VEGF of first group at day 21 after dressing in a cat skin wound, shows sever positive (++++) VEGF expression that appears as nuclear brown stain in the Angioblasts cells within the tissue (arrows), (IHC. 40x).

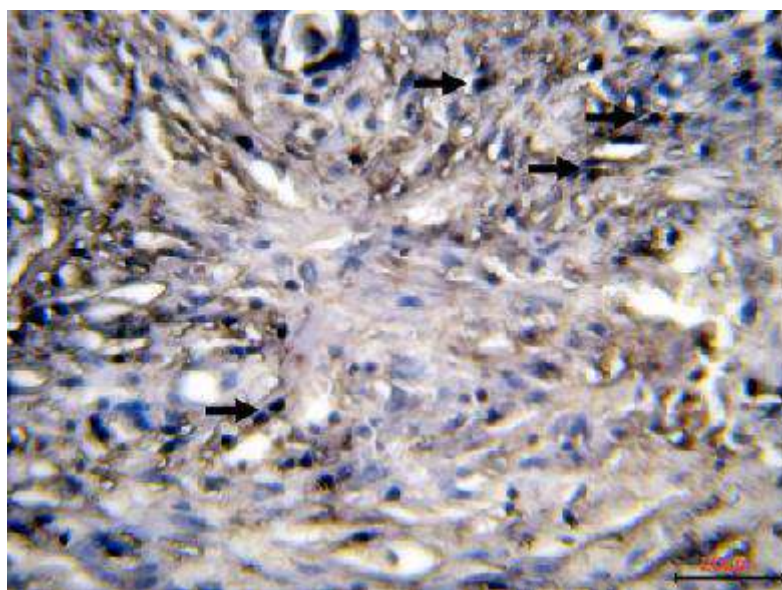


Figure 63: Immunohistochemical staining for VEGF of second group at day 21 after dressing in a cat skin wound, shows moderate positive (++++) VEGF expression that appears as nuclear brown stain in the Angioblasts cells within the tissue (arrows), (IHC. 400x).

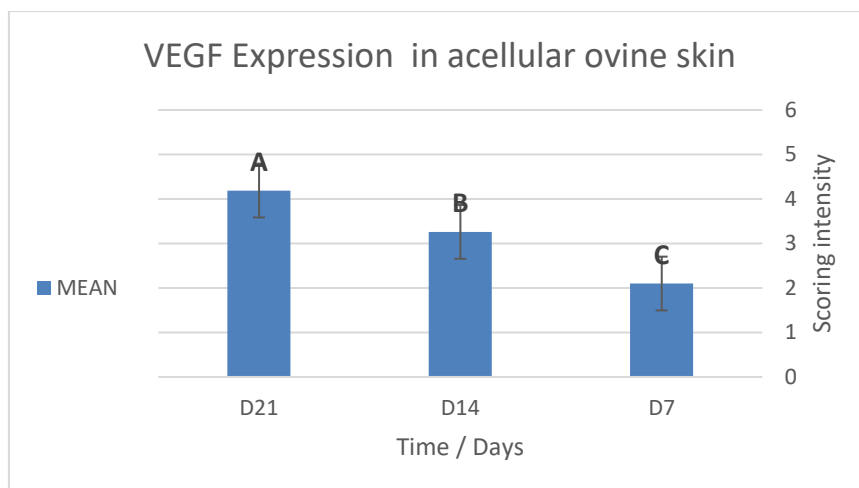


Figure 64: Diagrams show VEGF expression of wounds in first group on days 7, 14, 21 post dressing. Data were expressed as Means \pm S.E.M. Different letters indicate significant difference.

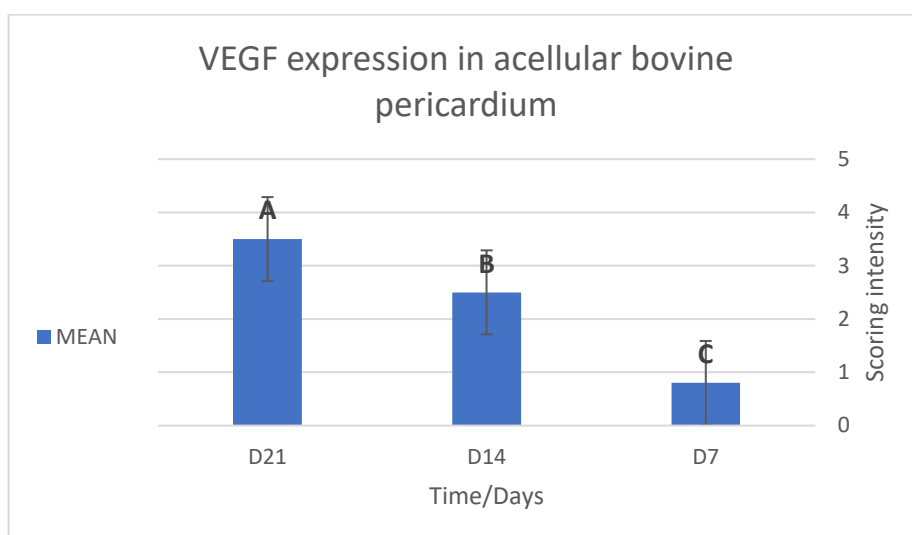


Figure 65: Diagrams show VEGF expression of wounds in second group on days 7, 14, 21 post dressing. Data were expressed as Means \pm S.E.M. Different letters indicate significant difference.

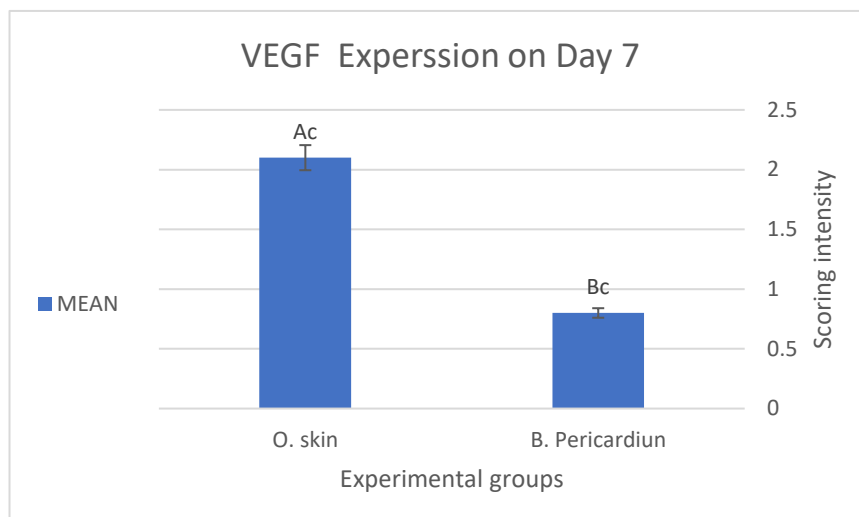


Figure 66: Diagrams show comparison of VEGF between first and second group on days 7 post dressing. Data were expressed as Means \pm S.E.M. Different letters indicate significant difference.

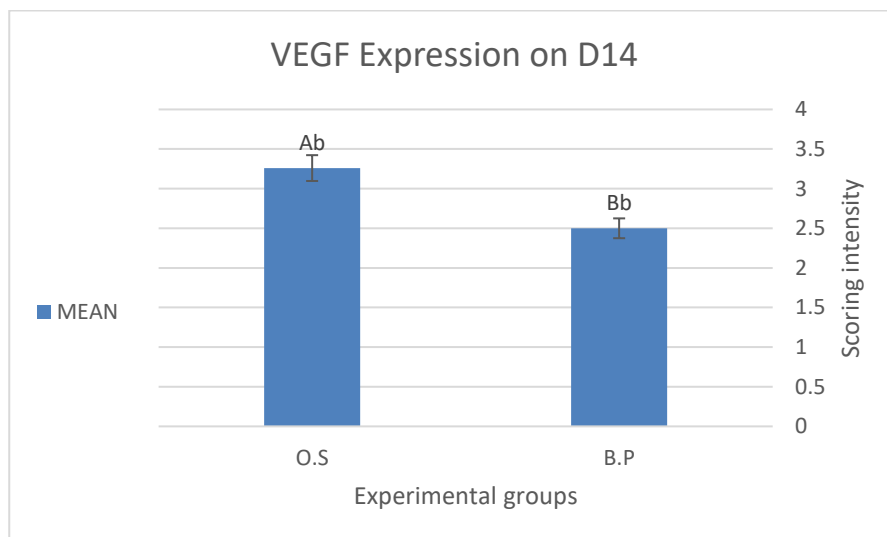


Figure 67: Diagrams show comparison of VEGF expression between first and second group on days 14 post dressing. Data were expressed as Means \pm S.E.M. Different letters indicate significant difference.

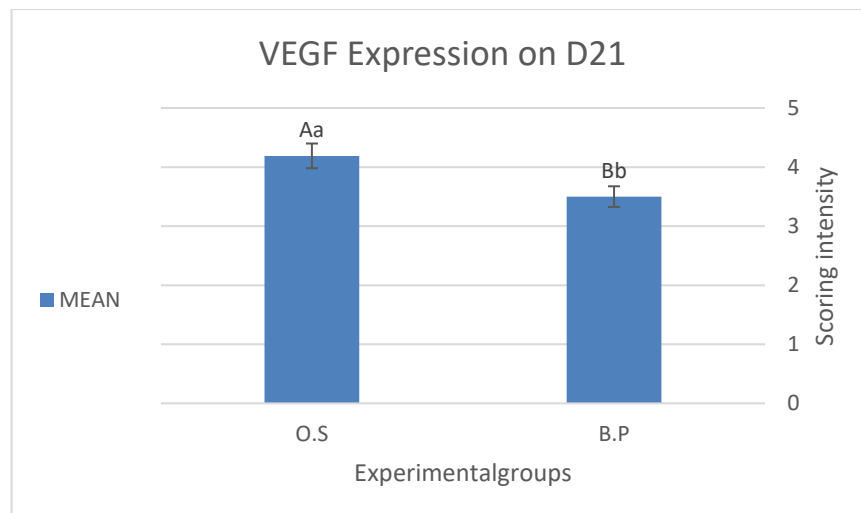


Figure 68: Diagrams show comparison of VEGF expression between first and second group on day 21 post dressing. Data were expressed as Means \pm S.E.M. Different letters indicate significant difference.

4-4: Physical Parameters

4-4-1: Doppler Ultrasound Results

The doppler ultrasound evaluation to detect cutaneous blood perfusion associated with using both xenografts for dressing of full-thickness started to be taken since day 12 post surgery to avoid the separation of the dressing from the underline bed. The doppler ultrasound examination exhibited presence of good cutaneous blood perfusion on day 12 1st acellular ovine skin, comparable to day 14 in acellular bovine pericardium (Figures 69- 74).

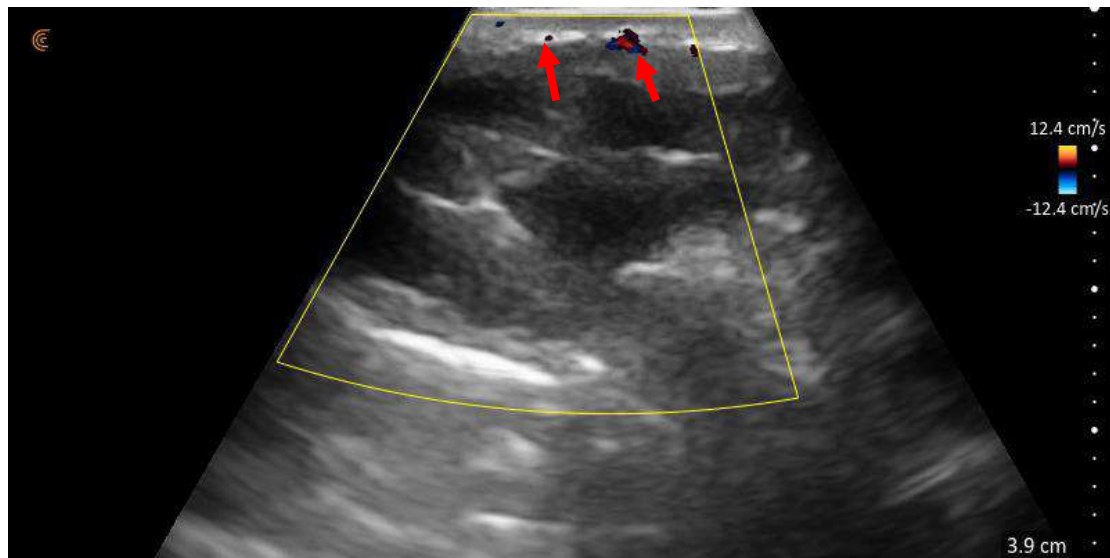


Figure 69: Ultrasonographic image for 1st group (AOS) after 12 days of dressing shows a presence of blood perfusion. Red color indicates blood flowing towards the beam while blue color indicates blood flowing away from the beam.

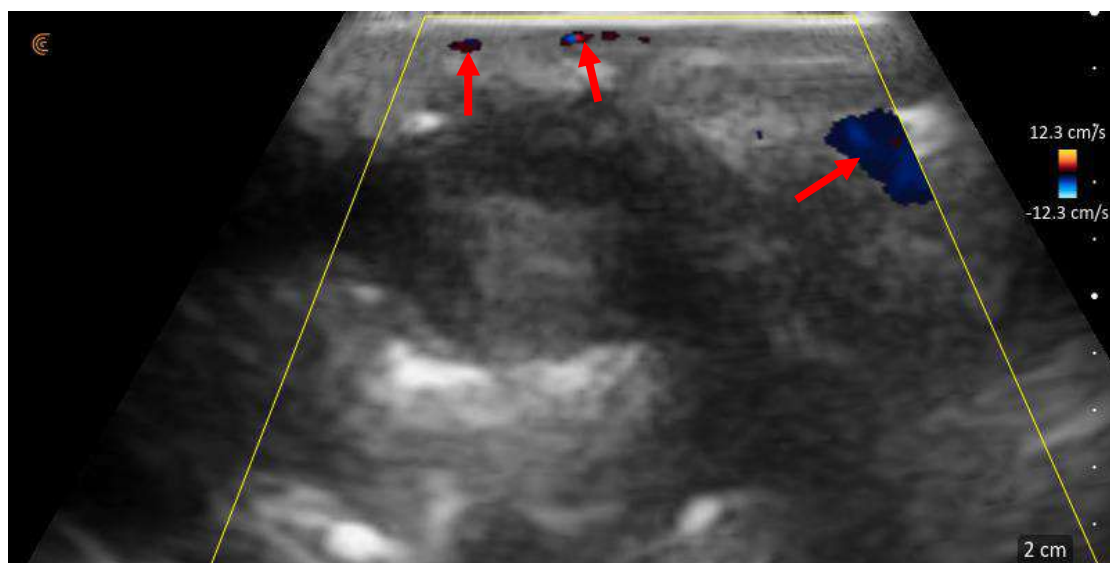


Figure 70: Ultrasonographic image for 1st group (AOS) after 14 days of dressing shows a presence of blood perfusion. Red color indicates blood flowing towards the beam while blue color indicates blood flowing away from the beam.

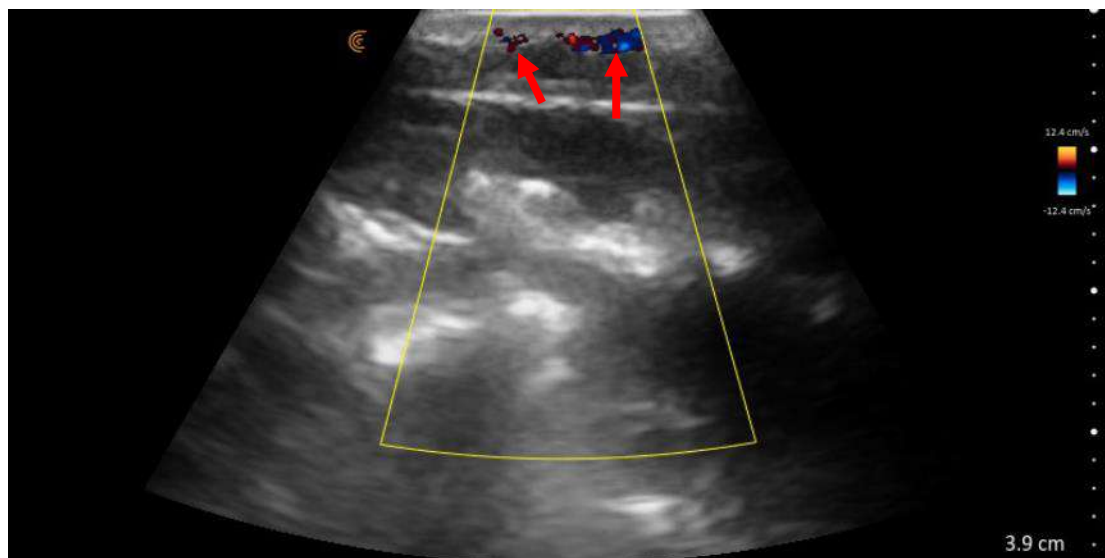


Figure 71: Ultrasonographic image for 1st group (AOS) after 18 days of dressing shows a presence of blood perfusion. Red color indicates blood flowing towards the beam while blue color indicates blood flowing away from the beam.

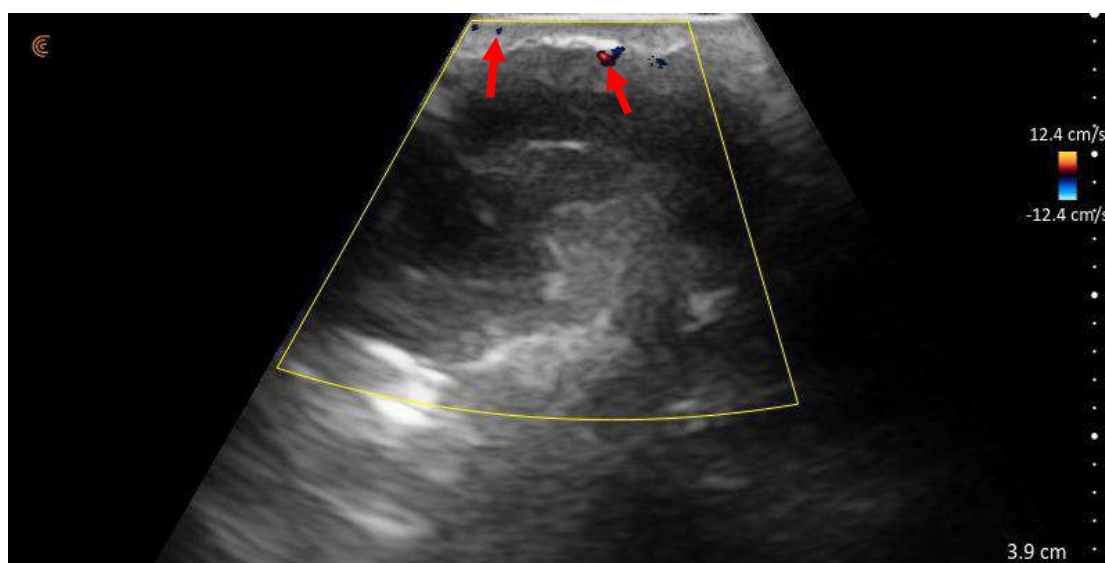


Figure 72: Ultrasonographic image for 2nd group (ABP) after 12 days of dressing shows a presence of blood perfusion. Red color indicates blood flowing towards the beam while blue color indicates blood flowing away from the beam.

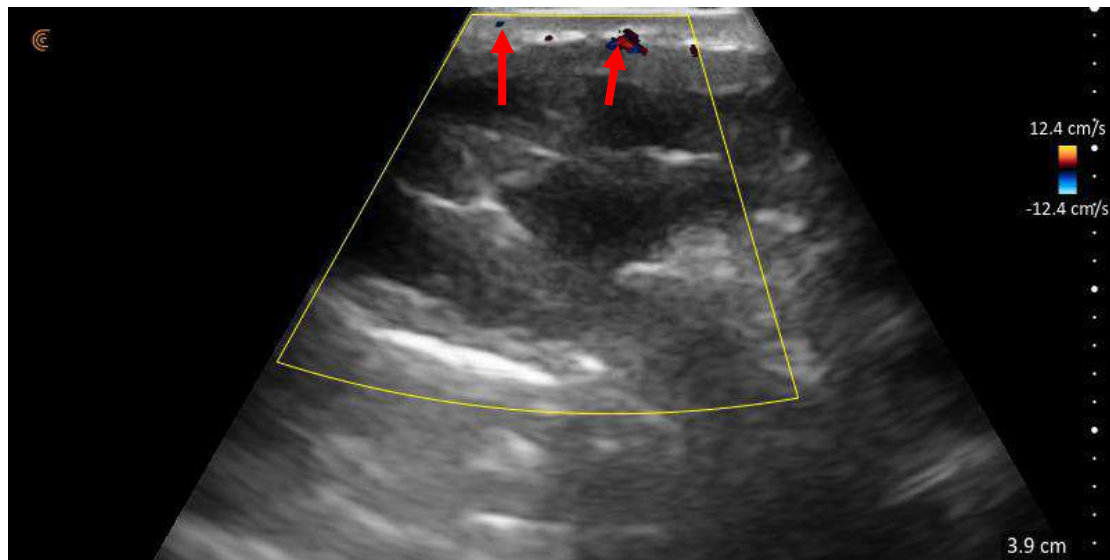


Figure 73: Ultrasonographic image for 2nd group (ABP) after 14 days of dressing shows a presence of blood perfusion. Red color indicates blood flowing towards the beam while blue color indicates blood flowing away from the beam.

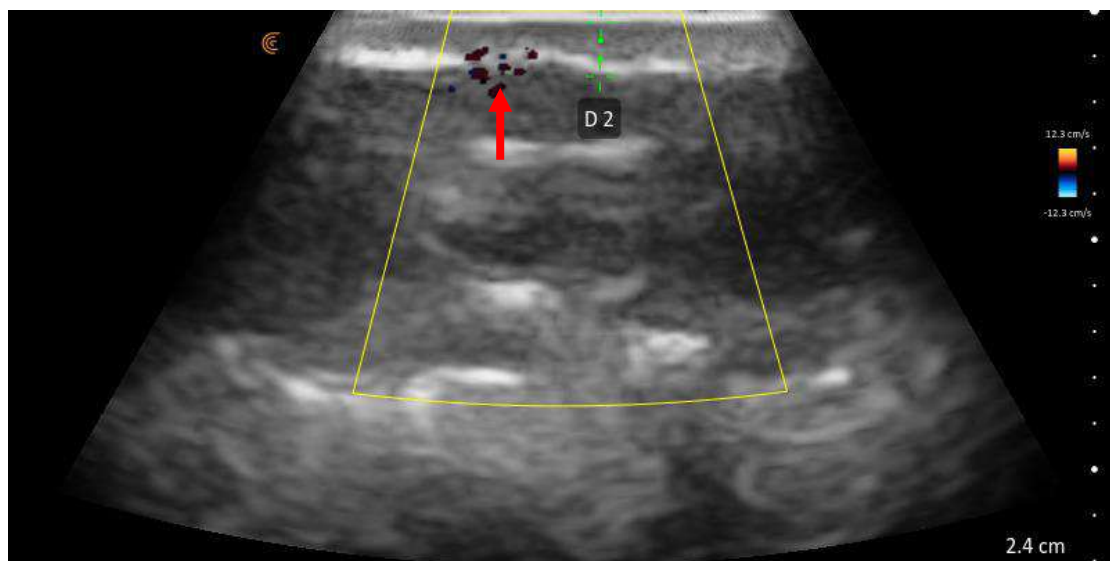


Figure 74: Ultrasonographic image for 2nd group (ABP) after 18 days of dressing shows a presence of blood perfusion. Red color indicates blood flowing towards the beam while blue color indicates blood flowing away from the beam.

Chapter Five

Discussion

Skin is the major and the uppermost organ of the body that make it very vulnerable structure. Its healthy continuity is of excessive importance, particularly in shielding the deeper tissues from microbes and other external factors (Bohling *et al.* (2006). Wound healing is a critical process for reestablishing skin integrity. It is an active process that happens according to the similar principle in all animals, but there are clinically significant differences between species especially with cats (Bohling *et al.* (2006); Cornell, 2012). The successful wound healing process requires the collaboration and coordination of three basic elements involving the extracellular matrix (ECM), cells, and growth factors (Gonzalez *et al.*, 2016; Rodrigues, *et al.*, 2019; Nikahval *et al.*, 2020; Kumar *et al.*, 2022).

This experimental study was achieved on 18 cats (n=9 for each group) to assess the macroscopical, physical, microscopical and the mechanical parameters associated with using of acellular ovine skin and acellular bovine pericardium for induced cutaneous wound in cats as healing of feline skin is not an easy process and much more challenging issue comparable with other animals because prolonged wound healing process, (indolent pocket) wounds and “pseudo-healing” that lead to complete wound dehiscence are much more predicted in cats rather than in rest of other species especially dogs (Perc & Erjavec 2022; Chatzimisios *et al.*, 2023).

In this study we used acellular xenografts derived from ovine skin and bovine pericardium as a compatible biological dressing due to their wide bioavailability, positive applicable history and relative less complicated preparation process (Nikahval *et al.*, 2020; Kumar *et al.*,

2022). The using of such biological implants has become as one of the most acceptable trends for regenerative biomedical applications as a result of their extracellular matrix (ECM) properties that possess the necessary dimensional architecture components to mimic the structural and functional properties of the native ECM besides acting as suitable environment for the host cells to invade and grow through it. These xenograft acellular implants when placed in the wound bed, their dimensional architecture will act as a temporary suitable scaffold that enable the host cells to invade, migrate and proliferate as well as to supported mechanical and functional performance that's in turn enhance the progress of healing process. Furthermore, these viable scaffolds have many vital proteins that do not only preserve the health of tissue differentiation, but also enable the host response to tissue damage that become an ideal option for replacement of the missing or damaged tissues (Xu *et al.*, 2020; Di Francesco *et al.*, 2022).

Our study based on using of bovine pericardium as a result of its inherent strength and biocompatibility, which is related with other studies around the world. In this respect, it becomes as one of the most usable biomaterial tissues for regenerative medicine for synthesizing numerous bio prostheses such as vascular stents and heart valves associated with lung and cardiovascular surgeries in addition to cardiac patches that are used to repair of several soft tissue deficiencies (Alizadeh *et al.*, 2019; Zhao *et al.*, 2021; Mendoza-Novelo *et al.*, 2011; Al-Saiegh *et al.*, 2024). Yet, biomaterials originated from sheep and goats are broadly accepted by all cultures and religious societies (Abdullah *et al.*, 2018; Silvipriya *et al.*, 2015). Besides, bovine pericardium is distinguished of its lower risk for disease transmission (Fauzi *et al.*, 2016; Caetano *et al.*, 2018).

To ascertain the complete a cellularity of our used ovine skin and bovine pericardium following decellularization processing, a histological

observation was performed and this examination revealed that the major tissue architecture was composed of ECM of collagen and elastic fibers with complete absence of any kind of cells within tissue section.

To eliminate immunogenicity that is usually associated with using xenografts implants, and thus preventing dress rejection. We mechanically and chemically processed bovine skin through a series of continues procedures using many chemical agents and protocols as mentioned previously as decellularization process reduces inflammatory and immunogenic responses associated with original tissues when implanted into recipient tissues (Hughes *et al.*, 2016; Wang *et al.*, 2023). Regeneration of any tissue through using decellularized materials requires keeping the original mechanical features of that tissue to ensure the correct performance. The most critical mechanical properties of attention include elastic modulus and tensile strength. Nevertheless, the most vital properties eventually based on the kind of function performed by the tissue or organ themselves. These mechanical properties are mostly ruled by the structural proteins of ECM, collagen, elastin, laminin and fibronectin (Gilpin and Yong, 2017). Therefore, it is significant to preserve ECM structures and elements in order to ensure the ideal performance of that tissue (Nelson and Bissell, 2006). In spite of the uniqueness of composition and architecture of any tissue (Gilbert, 2012). In our study, the microscopic examination of both xenografts following decellularization exhibited clearly the good preserving of the ECM structure especially the presence of collagen fiber bundles, which considered as the main controlling factor that is responsible for the biomechanical properties of any tissue (Basil-Jones *et al.*, 2011; Ribeiro *et al.*, 2013). The perfect preservation of ECM of both used xenografts in our work indicate the usefulness and success of our modified decellularization protocol that was adapted for both skin and pericardium. Since all authors and scientists has proved that

decellularization procedures and chemical used within are the most influencing factor in the obtained biochemical outcome data (Zhou *et al.*, 2010; Mendoza-Novelo *et al.*, 2011; O'Neill *et al.*, 2013; Syed *et al.*, 2014; Xing *et al.*, 2015).

What's more, our results associated with testing of mechanical properties of both a cellular ovine skin and a cellular bovine pericardium exhibited hug improvement in the mechanical characters of both used xenografts following decellularization. These obtained data could be due to the preservation of extra cellular matrix, which was so obvious by the microscopic examination of both dresses following decellularization. However, there was a significant difference between decellularized ovine skin and decellularized bovine pericardium in both examined mechanical criteria. The acellular bovine pericardium elasticity was much better comparable to acellular ovine skin. These variations in their mechanical properties belong to the differences in their histological components and even in their functions. Bovine pericardium is composed of layers of elastin and collagen fibers that make it acting as bio composite membrane with an inherent structural changeability and high rate of nonlinearity and elasticity in response to any great tension (Sánchez-Arévalo *et al.*, 2010) while skin lack this property. Furthermore, the crimp phenomena, which is the wavy structure of collagen fibrils is typically and hugely predominant in pericardium but not in the skin (Kayed *et al.*, 2015).

On the other side, the maximum load of decellularized ovine skin was much better than that of cellular bovine pericardium. This obvious phenomenon could be due to the skin collagen fibers are usually extended from the superficial levels to deeper layers, generating a three-dimensional network of oriented parallel intertwined collagen bundles (Ribeiro *et al.*, 2013). But pericardium is a planar fiber network consisted mainly of collagen type I fiber bundles that arranged with an irregular orientation

(Jaworska-Wilczynska *et al.*, 2016). It has been proved that collagen fibers orientation constitutes the chief structural factor responsible for biomechanical properties of any tissue (Sellaro *et al.*, 2007; Ribeiro *et al.*, 2013).

In addition, any minor alteration in the arrangement of the collagen fibers can modify significantly the biomechanical characters of any tissue (Kelly *et al.*, 2018). Besides, a strong correlation has been found between the tensile strength and the orientation of collagen microfibrils within tissue. Strong tensile strength is associated with presence of more fibrils aligned and parallel with the surface of the tissue with less crossover between layers, which is usually found within skin comparable to pericardium that has more irregular orientation of its collagen bundles (Basil-Jones *et al.*, 2011; Sizeland *et al.*, 2013). Too, mechanical properties of pericardium are dominated by other factors especially the non-collagenous tissue elements such as proteoglycans and glycosaminoglycans (Mirnajafi *et al.*, 2005). Monitoring cutaneous microcirculation can be achieved using many minimal non-invasive techniques that could be considered as a good indicator for wound healing (Varol and Anderson 2010; Merz *et al.*, 2010; Lima and Bakker 2012). It is an excellent technique for evaluating blood perfusion and neovascularization during healing (Stewart *et al.*, 2006; Lenasi *et al.*, 2017). Doppler ultrasonography is sensitive and easily applicable in clinical practice that can be used to assess perfusion of many vital organs such as kidney (Le Dorze *et al.*, 2012) or uterus (Campbell, 1990).

In this study, dressing bandage was used over the dressing patches (Coruh and Yontar, 2012) in order to immobilize the patches in situ, restrict shear forces, and to decline bacterial contamination leading to enhance the chance for successful dressing (Campbell, 2006), and thus yielding better results (Tsioli *et al.*, 2018).

In the present study, the back area of the cat was used as a site for experimental work in order to decline the possible access of cats that causing self-mutilation to the surgical site with their mouths besides dropping the dead space beneath the dressing patches as a result of the natural convexity of the dorsum (Vural *et al.*, 2010) in addition for being easily accessible position (Başaran *et al.*, 2006).

The clinical observations showed that the pliability of both acellular xenografts was not as the original native tissues and it became less pliable as compare with before decellularization, although pliability of acellular ovine skin was slightly better than acellular bovine pericardium. These observations could be due to the effect of decellularization procedure on the nature of these biomaterials, which in turn agree with (Xing *et al.*, 2014) who mentioned that decellularization procedures influenced on nature and the biomechanical properties of the natural tissue.

These obvious impacts of various decellularization methods on the nature of various biological tissues were also noticed with other works (Dau *et al.*, 2020; Bornert *et al.*, 2021; Franko *et al.*, 2023). Yet, the slight difference in degree of pliability between decellularized skin and pericardium could be due to the difference in their sources and histological structures especially collagen fiber contents and orientation, as the orientation of collagen fibers of any tissue is highly impact on its nature and properties (Ribeiro *et al.*, 2013). Besides, the collagen fibril orientation of ovine skin is completely different from that of bovine pericardium (Basil-Jones *et al.*, 2011; Basil-Jones *et al.*, 2013; Sizeland *et al.*, 2014; Whelan *et al.*, 2019). Too, the dressing of 1st group was derived from skin that suited well with external environment because skin is the upper most protective layer that always being in contact with external atmosphere while dressing of the 2nd group was derived from pericardium which had a completely different function and situation that did not accommodate well

with these external environment (Jaworska-Wilczynska *et al.*, 2016; Dąbrowska *et al.*, 2018).

Furthermore, the color of both acellular dressing was normal during the first week following application then started to change into more brown dark color. This could be due to the presence of well adhered with wound bed that preserved their moisture and nutrient supply as good adherence is considered as an important factor for progress of wound healing. Also, using of dressing, which is a crucial factor for typical wound care provided the dressing with the necessary moisture (Obagi *et al.*, 2019; Kus and Ruiz, 2020; Punjataewakupt and Aramwit, 2022).

In both groups, acellular dressing started to be partially and loosely adhered to the recipient bed on day 3 post dressing in all cats, which started to become stronger gradually, however, acellular ovine skin adhesion was much better than that of acellular bovine pericardium and continued until day 15, comparable to day 7 with pericardium group. This noticed feature could be due to the dryness of both dressing as a result of less blood circulation within cat skin (Volk and Bohling, 2013) that made these xenografts became hard and stiff and not unable to be part of wound beds and completely detached and peeled off (Chanda *et al.*, 1994). The less adherent ability of acellular bovine pericardium was also mentioned with other works, (Al-Falahi *et al.*, 2017) who mentioned that bovine pericardium was less adhered to the wound area comparison to amniotic membrane in their study about wounds skin healing in rabbits, furthermore (Albahrawy *et al.*, 2023) noticed that decellularized bovine pericardium exhibited shrinkage and change in color following its use for full-thickness cutaneous wound in donkeys. However, ovine skin continued for longer period than pericardium that could be due to the fact that processed ovine-based dressings hold the complex collagen structure of native tissue ECM

in addition to ECM-associated secondary particles, including fibronectin, laminin and glycosaminoglycans (Bohn *et al.*, 2016).

The results of physical planimetry measurements for the wound size that performed on days 0, 7, 14, and 21 following dressing exhibited presence of reduction in the wound size area in both groups over time in addition to the healing rate was significantly different. Further, the contraction percentage increased slowly to be reached up to 65% of wound size. While total wound healing percentage increased in both groups from day 0 to day 21, total wound healing reached high rates. These observed features exhibited clearly the beneficial synergistic effect of both dressing materials on wound healing progress that could enable them to be nominating as a very effective approach in accelerating the healing process of the experimentally induced full-thickness wounds in cats (Idrus *et al.*, 2014; Nikahval *et al.*, 2020; Subramaniam *et al.*, 2022). Nevertheless, these low rates of both contraction and total wound healing percentages obtained from this work were in agreement with other researchers works like (Bohling *et al.*, 2004; Bohling *et al.* 2006), and (Volk and Bohling 2013), who also documented the slow and poor rates as compared with other animals especially dogs because of poor inflammatory response, weakened granulation tissue formation and deprived blood vascularization (Pavletic *et al.*, 2018; Nolff *et al.*, 2017; Nolff. 2021) that leading to poor quality healing response.

The histopathological manifestations associated with using both acellular ovine skin and bovine pericardium for dressing of full-thickness skin wounds of cats revealed presence of significant differences in most of the studied histopathological parameters between them during the whole time period of study. The acellular ovine skin on day 7 following dressing was much better and exhibited presence of close contact and interwoven with the wound beds skin with less inflammatory response and infiltration

of polymorphonuclear and mononuclear inflammatory cells as compare with acellular bovine pericardium. This could due to fact that the dressing of the 1st group was derived from skin that resembles the cutaneous wound bed in its histology, anatomy and even physiology that enabled it to perfectly match the full-thickness wound and adhered well to it and to initiate less inflammatory reaction due to the presence of same tissue elements especially growth factors and cytokines, which can only display their action on a very precise cell surface receptors that later convey their growth signals as a result of these high attraction to a specific surface receptors (Rajkumar, 2001; Lau, 2016; Stone et al., 2017). All these factors enabled the acellular ovine skin to induce less inflammatory reaction when compared with a cellular bovine pericardium.

The histopathological manifestation associated with using both acellular tissue as a dressing xenogeneic cover of feline full-thickness cutaneous wounds showed sever infiltration of inflammatory cells especially mononuclear during the first two weeks, which indicate that both of them provoked more immunogenicity and less acceptance because both of them were derived from xenogeneic sources i.e. ovine and bovine (McGill *et al.*, 2018; Norte-Muñoz *et al.*, 2022). This intense spread of these inflammatory cells was also notice with the works of (Lu *et al.*, 2009), who noticed the severe mononuclear cells existence at day 14 during his work on transfer of peripheral nerve xenograft. Additionally, other inflammatory cells like polynuclear inflammatory cells were also recognized with both acellular tissues, which indicated the presence of foreign body reaction (Milde *et al.*, 2015).

Macrophages are mainly responsible cells for the innate immune system and thus during xenograft transplantation, they display phagocytic action and modify adaptive immunity through participating in cell recruitment and antigen exhibition (Vignery.,2005). Furthermore,

inflammatory reaction was less severe with acellular ovine skin comparable to acellular bovine pericardium, which in turn helped in the better performance of ovine skin dressing that made it keep its pliability to survive longer than bovine pericardium. This finding is in coincidence with findings of the work of (Yu *et al.*, 2014), who mentioned that skin allograft survival is greatly associated with the drops in its associated inflammatory infiltration. Besides, this intense inflammatory reaction showed an increase from day 0 to day 14 in both groups, then started to decline until day 21, which was in a great agreement with work of (Angelou *et al.*, 2022) that studied the cutaneous wound healing in cats.

Other histopathological indicator associated with application of both acellular tissues revealed presence of good blood perfusion and new blood vessels since day 14 following dressing although this blood perfusion was detected earlier since day 10-12 using doppler ultrasonography. Besides, this revascularization became more pronounced as healing process progresses forwards. It is considered as the foundation of the perfect healing process as blood perfusion. Also, the creation of new capillaries is the basic step within any normal tissue regeneration. This is due to the fact that these recently formed blood vessels would carry the essential nutrient elements with oxygen supply to the dynamically active renewing tissue, which is critical for biologic regeneration of the injured tissue because it needs an adequate huge vascular support. From this, many studies have found that blood perfusion is the key for wound repair that stimulate healing rates while its decline can impair healing rates (Guerra *et al.*, 2018; Veith *et al.*, 2019).

Finally, the existence of well-developed granulation tissue associated with acellular ovine skin group in comparison to a cellular bovine pericardium was evident since day 14 post dressing. Its rate and quantity are much lower than that, which is usually seen with other species

especially dogs because wound healing in cats is totally different from other animals that made all authors mentioned this cardinal phenomenon (lower granulation rate) as one of the very clear negative manifestations of wound healing (Bohling *et al.*, 2004; Bohling *et al.*, 2006; Volk and Bohling, 2013; Angelou *et al.*, 2022). This indicates that the ovine skin suited wounds bed tissue is much better than acellular bovine pericardium as the presence of granulation tissue with its all-histological elements such as inflammatory cell infiltration, proliferation of fibroblasts, endothelial cells and new thin-walled blood vessels is considered as the revealing parameters for the well progress of the repairing process within the dressed site (Häkkinen *et al.*, 2011; Jiang and Scharffetter-Kochanek, 2020). Moreover, granulation tissue was also observed with the work of (Costa *et al.*, 2009), who notices that the presence of granulation tissue associated with irregular blood perfusion invading the implant during his study with dogs for reduction of abdominal incisional using Nylon tissue mesh.

The presence of all these previously mentioned elements of perfect healing process associated with using of acellular ovine skin has led to the presence of the better histological appearance with good tissue architecture and structural integrity especially epidermal integrity and dermal - epidermal junction on the day 21 of experiment.

In the current study, the staining expression of VEGF in both experimental groups were inspected to assess the preserved tissue viability depending on their capacity to express this active growth factor that is crucial for success of any wound healing process. Blood perfusion is one of the major contributing factors in wound repair process and it is thought to enable the delivery of necessary nutrients and oxygen to the rapidly proliferating reparative cells at wound site. VEGF is the most substantial cellular mediator for wound blood perfusion and its manufacturing inspires new capillary growth to deliver satisfactory nutrients, oxygen, and

inflammatory cells. Many trainings have found that blood perfusion to be helpful for wound repair. Blood perfusion stimulation can stimulate healing rates while a decline in blood perfusion can impair healing rates (Guerra *et al.*, 2018; Veith *et al.*, 2019).

During wound healing process, new blood capillaries are produced into the wound bed in a gradual rate, leading to formation of a rich network of newly blood vessels that is even up to 10 times thicker than within normal tissue. The beginning of blood perfusion is completely controlled by several growth factors especially VEGF, which is the most leading proangiogenic element in healing wounds by acting as a powerful proangiogenic moderator that can also elevate vascular permeability that participating in wound edema (DiPietro, 2016).

The immunohistochemistry results of vascular endothelium growth factor expression detected that both exogenous dressings showed variable intensity expression and visualization of VEGF. This output data could be due to the presence of good preserved ECM within both decellularized ovine skin and bovine pericardium that indicated the efficiency of our decellularization protocol that preserves the intact tissue construction that made both of them still have the talent to express and deliver this vital growth factor. The presence of the well integral ECM within both xenograft dressing made these biomaterials still hold the aptitude to release growth factors and other cytokines to the wound area as this intact matrix in turn acts as a vital direct pool for various growth factors and other cytokines that enhance the healing process course (Olczyk *et al.*, 2014; Diller and Tabor, 2022).

The active connections between ECM and growth factors impact deeply on wound healing. These relations have many levels and forms that could be categorized into direct or indirect levels. The extra cellular matrix can directly connect to and secret certain growth factors that may help in

sequestering and keeping growth factors from breakdown and degradation or indirectly improve their activity (Schultz and Wysocki, 2009; Potekaev *et al.*, 2021). The presence of strong expression of VEGF as a regenerative indicator for degree of tissue viability is furtherly supported by other work achieved by (Landsman *et al.*, 2016) who mentioned that the VEGF is highly expressed during wound healing (Kumar *et al.*, 2009; Kameyama *et al.*, 2015).

On the other hand, the decellularized ovine skin displayed more staining intensity than decellularized bovine pericardium. Besides, statistical analysis showed significant difference in VEGF expression between them. This could be due to the difference in the type of tissue that is used as xenografts as biomaterial of the first group was taken from skin while the dressing of the second group was prepared from pericardium. This made ovine skin dressing biomaterial being more active in stimulating release of VEGF because it derived from the same tissue type i.e. skin, which is completely resembled the kind of tissue that has been injured. Yet, dressing biomaterial of second group was derived from pericardium, which is completely different from the anatomy, histology and even functions from the skin that is used to reconstruct it. In turn, this affects the proper functions of these tissue elements, especially the growth factors that can only be exhibited their action on very definite cell surface receptors, which later conduct their growth signals as a result of their big affinity to a specific surface receptor (Rajkumar, 2001; Stone *et al.*, 2017; Lau, 2016).

Moreover, the intensity of staining and expression was gradually increasing with time as a result of the progress in healing process that was in great agreement with (Khalaf *et al.*, 2019), who noticed the negative immunohistochemical staining of VEGF at early stages of wound healing (0-3 days) that then elevated in association with progress of wound healing in a time-dependent manner that can be even possible to suggested that

they would be useful indicators for the determination of wound age. Besides, following the injury, the levels of proangiogenic factors increase gradually in association with the progress of healing process then reaching a peak slightly and finally diminish (DiPietro, 2016).

Utilizing of doppler ultrasonography in this work was effective due to its practicability, non-invasiveness, repeatability (Schnell and Darmon 2015; Guven *et al.*, 2023). However, both blood speed and vessel width are serious elements that required to accurate determination of blood flow (Keymel *et al.*, 2010; Roustit and Cracowski 2012; Jarrett *et al.*, 2020).

The microcirculation contains capillaries, arterioles and venules that control microvascular blood flow, which in turn has a critical role in normal physiological processes of tissue nutritional and oxygenation exchange. Measurement of microcirculation can be applied on many organs in various pathological conditions (Eriksson *et al.*, 2014). Supply the tissues with oxygen for many organs especially skin surface, which is considered as one of the most preferred candidates for monitoring tissue microcirculation due to its easy access (Guven *et al.*, 2023). Ultrasound systems are usually used to detect the motion of blood in arteries, veins and even in the heart (Hoskins, 2019). Although, doppler ultrasound is not an actual measurement for the microcirculation blood flow, but a precise countenance of capillary blood flux (Cosgrove and Lassau 2010; Angelou *et al.*, 2022).

The doppler ultrasound evaluation to detect cutaneous blood perfusion associated with using both xenografts for dressing of full-thickness started to be taken since day 12 post surgery to avoid the separation of the dressing from the underline bed. The doppler ultrasound examination exhibited presence of good cutaneous blood perfusion since day 10 that became more detectable on day 12 in first group and day 14 in second experimental group, then continue to increase tile reached its peak

on day 21. These obtained results were in coinciding with (Bohling *et al.*,2004; Bohling *et al.*,2006), who noticed that cutaneous blood perfusion associated with wound healing in cat started within the first week then elevated until day 14 and then declining by day 21. Furthermore, (Angelou *et al.*,2022) noticed that the cutaneous blood perfusion was evident since day seven and continue gradually increasing until day 14.

Chapter Six

6-1: Conclusions

1. The new modified technique that was adapted for decellularization of bovine pericardium proved its efficiency in removing cells from pericardium and preserving its extra cellular matrix ECM.
2. Decellularization improved the mechanical properties (maximum load and modulus of elasticity) of both acellular tissue that could be recommended to be used with tissue under high tension and pressure
3. A cellular ovine skin is better than acellular bovine pericardium as dressing for extensive wound healing.
4. Cardinal manifestation of normal healing process especially granulation tissue formation, rates of wound contraction and re-epithelization are much lesser happening with cutaneous wound healing in cats.
5. Doppler ultrasound examination is an efficient tool to detect early blood perfusion.

6-2: Recommendations

1. Application of bioactive material such as platelet rich fibrine in combination with these dressing to produce better results.
2. Application of adhesive materials such as fibrin glue in combination with biological dressing
3. Using another biological dressing such as acellular fish skin
4. Comparison between fenestration and non-fenestration for acellular tissues.
5. Comparison between using antiseptic material such as tincture iodine and biological dressing for induce acutance wound in cat.
6. Studying Tensiometer of the wounds during the different healing period to assess its breaking strength associated with using various biomaterials.

References

- Abdulghani, S., and Mitchell, G. R. (2019). Biomaterials for in situ tissue regeneration: A review. *Biomolecules*. 9(11): 750.
- Abdullah, M. S. P., Noordin, M. I., Ismail, S. I. M., Mustapha, N. M., Jasamai, M., Danik, M. F., ... Shamsuddin, A. F. (2018). Recent advances in the use of animal-sourced gelatine as natural polymers for food, cosmetics and pharmaceutical applications. *Sains Malaysiana*. 47(2): 323-336.
- Affolter, V. K., & Moore, P. F. (1994). Histologie features of normal canine and feline skin. *Clinics in dermatology*, 12(4): 491-497.
- Agarwal, S., and Krishnamurthy, K. (2019). Histology, skin.
- Aisa, J., and Parlier, M. (2022). Local wound management: A review of modern techniques and products. *Veterinary Dermatology*. 33(5): 463-478.
- Albahrawy, M., Abouelnasr, K., Mosbah, E., Zaghloul, A., & Abass, M. (2023). Biostimulation effect of platelet-rich fibrin augmented with decellularized bovine pericardium on full-thickness cutaneous wound healing in Donkeys (*Equus asinus*). *BMC Veterinary Research*. 19(1): 166.
- Albahrawy, M., Abouelnasr, K., Mosbah, E., Zaghloul, A., and Abass, M. (2023). Acellular bovine pericardium as a biological dressing for treatment of cutaneous wounds of the distal limb in donkeys (*Equus Asinus*). *Veterinary Research Communications*. 47(2): 587-597.
- AL-Bayati, A. H., and Hameed, F. M. (2018). Effect of acellular bovine pericardium and dermal matrixes on cutaneous wounds healing in male rabbits: Histopathological evaluation. *J. Entomol. Zool. Stud.* (6): 1976-1986.
- Al-Falahi, N. H., Dhyaa. Ab. Abood and Dauood M.S. (2017). Comparative evaluation of bovine pericardial membrane and amniotic membrane in wounds skin healing in rabbits. *The Iraqi Journal of Veterinary Medicine*, 41(2):137-145.

- Alizadeh, M., Rezakhani, L., and Alizadeh, A. (2020). Characterization of the decellularized ovine pericardium for skin tissue engineering. *Journal of Shahrekord University of Medical Sciences*. 22(4): 173-180.
- Alizadeh, M., Rezakhani, L., Soleimannejad, M., Sharifi, E., Anjomshoa, M., & Alizadeh, A. (2019). Evaluation of vacuum washing in the removal of SDS from decellularized bovine pericardium: method and device description. *Heliyon*, 5(8).
- Al-Saiegh, A. M., Al-Hyani, O. H., & Alheyali, K. W. (2024). Using lyophilized bovine pericardium and acellular ovine esophageal mucosa to repair cerebral dura mater defect in dogs. *Iraqi Journal of Veterinary Sciences*, 38(2): 379-389.
- Angelou, V., Psalla, D., Dovas, C. I., Kazakos, G. M., Marouda, C., Chatzimisios, K., ... & Papazoglou, L. G. (2022). Locally injected autologous platelet-rich plasma improves cutaneous wound healing in cats. *Animals*, 12(15): 1993.
- Balsa, I. M., Culp, W.T. (2015). Wound care. *Veterinary Clinics: Small Animal Practice*, 45(5):1049-65.
- Başaran, Ö., Özdemir, H., Kut, A., Şahin, F. İ., Deniz, M., Sakallıoğlu, E. A., & Haberal, M. A. (2006). Effects of different preservation solutions on skin dress epidermal cell viability and dress performance in a rat model. *Burns*, 32(4): 423-429.
- Basil-Jones, M. M., Edmonds, R. L., Cooper, S. M., & Haverkamp, R. G. (2011). Collagen fibril orientation in ovine and bovine leather affects strength: a small angle X-ray scattering (SAXS) study. *Journal of agricultural and food chemistry*, 59(18): 9972-9979.
- Basil-Jones, M. M., Edmonds, R. L., Cooper, S. M., Kirby, N., Hawley, A., & Haverkamp, R. G. (2013). Collagen fibril orientation and tear strength across ovine skins. *Journal of agricultural and food chemistry*, 61(50): 12327-12332.

- Bermudez, D. M., Herdrich, B. J., Xu, J., Lind, R., Beason, D. P., Mitchell, M. E., ... & Liechty, K. W. (2011). Impaired biomechanical properties of diabetic skin: implications in pathogenesis of diabetic wound complications. *The American journal of pathology*, 178(5): 2215-2223.
- Bhoopathy, J., Prabakaran, L., Sathyaraj, W. V., Karthikeyan, R., & Senthil, R. (2024). A comprehensive review on natural therapeutics for Wound Treatment. *Regenerative Engineering and Translational Medicine*, 10(1): 34-45.
- Bianchera, A., Catanzano, O., Boateng, J., & Elviri, L. (2020). The place of biomaterials in wound healing. *Therapeutic dressings and wound healing applications*, 337-366.
- Bohling, M. W., Henderson, R. A., Swaim, S. F., Kincaid, S. A., & Wright, J. C. (2004). Cutaneous wound healing in the cat: a macroscopic description and comparison with cutaneous wound healing in the dog. *Veterinary Surgery*, 33(6): 579-587.
- Bohling, M. W., Henderson, R. A., Swaim, S. F., Kincaid, S. A., & Wright, J. C. (2006). Comparison of the role of the subcutaneous tissues in cutaneous wound healing in the dog and cat. *Veterinary Surgery*, 35(1): 3-14.
- Bohn, G., Liden, B., Schultz, G., Yang, Q., & Gibson, D. J. (2016). Ovine-based collagen matrix dressing: next-generation collagen dressing for wound care. *Advances in wound care*, 5(1): 1-10.
- Bornert, F., Herber, V., Sandgren, R., Witek, L., Coelho, P. G., Pippenger, B. E., & Shahdad, S. (2021). Comparative barrier membrane degradation over time: Pericardium versus dermal membranes. *Clinical and Experimental Dental Research*, 7(5): 711-718.
- Bradshaw, J. (2017). Behaviour of cats. *The ethology of domestic animals—an introductory text*. Glasgow: CABI, 241-254.
- Bradshaw, J. (2018). Normal feline behavior and why problem behaviors develop. *Journal of Feline Medicine and Surgery*, 20(5): 411-421.

- Butler, C. R., Hynds, R. E., Crowley, C., Gowers, K. H., Partington, L., Hamilton, N. J., ... & Janes, S. M. (2017). Vacuum-assisted decellularization: an accelerated protocol to generate tissue-engineered human tracheal scaffolds. *Biomaterials*, (124): 95-105.
- Caetano, P., Bettencourt, E. V., & Branco, S. (2018). Reviewing foot rot in sheep. *Journal of Veterinary Science & Animal Husbandry (Open Access)*, 6(4): 405-413.
- Cai, Z., Gu, Y., Xiao, Y., Wang, C., & Wang, Z. (2021). Porcine carotid arteries decellularized with a suitable concentration combination of Triton X-100 and sodium dodecyl sulfate for tissue engineering vascular grafts. *Cell and Tissue Banking*, (22): 277-286.
- Campbell, B. G. (2006). Dressings, bandages, and splints for wound management in dogs and cats. *Veterinary Clinics: Small Animal Practice*, 36(4): 759-791
- Campbell, S. (1990). New doppler technique for assessing uteroplacental blood flow. *Lancet*, (26): 675-67.
- Cao, D., & Ding, J. (2022). Recent advances in regenerative biomaterials. *Regenerative Biomaterials*, 9, rbac098.
- Cavanaugh, R. P. (2024). Postoperative Complications. *Techniques in Small Animal Wound Management*, 53-71.
- Chanda, J., Rao, S. B., Mohanty, M., Muraleedharan, C. V., Arthur, V. L., Bhuvaneshwar, G. S., & Valiathan, M. S. (1994). Use of glutaraldehyde-gentamicin-treated bovine pericardium as a wound dressing. *Biomaterials*, 15(1): 68-70.
- Chatzimisios, K., Tsioli, V., Brellou, G. D., Apostolopoulou, E. P., Angelou, V., Pratsinakis, E. D., ... & Papazoglou, L. G. (2023). Evaluation of the Effectiveness of Medical-Grade Honey and Hypericum Perforatum Ointment on Second-Intention Healing of Full-Thickness Skin Wounds in Cats. *Animals*, 14(1): 36.

- Choudhury, D., Yee, M., Sheng, Z. L. J., Amirul, A., & Naing, M. W. (2020). Decellularization systems and devices: State-of-the-art. *Acta biomaterialia*, (115): 51-59.
- Cornell K. Wound healing. In: Tobias KM, Johnston SA, editors. *Veterinary Surgery: Small Animal*. 2-volume set, 1st ed. Missouri: Elsevier Ltd., 2012: pp 125-132.
- Corr, S. (2009). Intensive, extensive, expensive: management of distal limb shearing injuries in cats.
- Coruh, A., & Yontar, Y. (2012). Application of split-thickness dermal grafts in deep partial-and full-thickness burns: a new source of auto-skin grafting. *Journal of Burn Care & Research*, 33(3): e95-e101
- Cosgrove, D., & Lassau, N. (2010). Imaging of perfusion using ultrasound. *European journal of nuclear medicine and molecular imaging*, (37): 65-85.
- Costa FR, Castro JR, Silva CB, Ávila DF, Faria MA, Dias TA, Eurides D. (2009). Abdominal Incisional Hernia Reduction in Dogs Using Nylon Tissue Fixed by Chromate Cat Gut Row Suture World Small Animal Veterinary Association World Congress Proceedings.
- Cramer, M. C., & Badylak, S. F. (2020). Extracellular matrix-based biomaterials and their influence upon cell behavior. *Annals of biomedical engineering*, 48(7): 2132-2153.
- Crapo, P. M., Gilbert, T. W., & Badylak, S. F. (2011). An overview of tissue and whole organ decellularization processes. *Biomaterials*, 32(12): 3233-3243.
- Crowell-Davis, S. L. (2007). Cat behaviour: social organization, communication and development. In *The welfare of cats* (pp. 1-22). Dordrecht: Springer Netherlands.
- Dąbrowska, A. K., Spano, F., Derler, S., Adlhart, C., Spencer, N. D., & Rossi, R. M. (2018). The relationship between skin function, barrier properties,

- and body-dependent factors. *Skin Research and Technology*, 24(2): 165-174.
- Das, S., & Baker, A. B. (2016). Biomaterials and nanotherapeutics for enhancing skin wound healing. *Frontiers in bioengineering and biotechnology*, (4): 82.
- Dau, M., Volprich, L., Grambow, E., Vollmar, B., Frerich, B., Al-Nawas, B., & Kämmerer, P. W. (2020). Collagen membranes of dermal and pericardial origin—In vivo evolvement of vascularization over time. *Journal of Biomedical Materials Research Part A*, 108(12): 2368-2378
- Davidson, J. R. (2015). Current concepts in wound management and wound healing products. *Veterinary Clinics: Small Animal Practice*, 45(3): 537-564.
- Deng, X., Gould, M., & Ali, M. A. (2022). A review of current advancements for wound healing: Biomaterial applications and medical devices. *Journal of Biomedical Materials Research Part B: Applied Biomaterials*, 110(11): 2542-2573.
- Dermisiadou, E., Panopoulos, I., Psalla, D., Georgiou, S., Sideri, A., Galatos, A., & Tsioli, V. (2023). Use of a semitendinosus myocutaneous flap for the coverage of hindlimb full-thickness skin defects in cats. *Journal of Veterinary Science*, 24(1).
- Di Francesco, D., Bertani, F., Fusaro, L., Clemente, N., Carton, F., Talmon, M., ... & Boccafoschi, F. (2022). Regenerative Potential of A Bovine ECM-Derived Hydrogel for Biomedical Applications. *Biomolecules*, 12(9): 1222.
- Diller, R. B., & Tabor, A. J. (2022). The role of the extracellular matrix (ECM) in wound healing: a review. *Biomimetics*, 7(3): 87.
- DiPietro, L. A. (2016). Angiogenesis and wound repair: when enough is enough. *Journal of Leucocyte Biology*, 100(5): 979-984.
- Doyle, G. R., & McCutcheon, J. A. (2015). *Wound Healing and Assessment*.

- Dzikiti, T. B., Chanaiwa, S., Mponda, P., & Sigauke, C. (2007). Comparison of quality of induction of anaesthesia between intramuscularly administered ketamine, intravenously administered ketamine and intravenously administered propofol in xylazine premedicated cats. *Journal of the South African Veterinary Association*, 78(4): 201-204.
- El Soury, M., García-García, Ó. D., Moretti, M., Perroteau, I., Raimondo, S., Lovati, A. B., & Carriel, V. (2021). Comparison of decellularization protocols to generate peripheral nerve grafts: a study on rat sciatic nerves. *International Journal of Molecular Sciences*, 22(5): 2389.
- Ellis, S., Lin, E. J., & Tartar, D. (2018). Immunology of wound healing. *Current dermatology reports*, (7): 350-358.
- Emami, A., Talaei-Khozani, T., Vojdani, Z., & Zarei Fard, N. (2021). Comparative assessment of the efficiency of various decellularization agents for bone tissue engineering. *Journal of Biomedical Materials Research Part B: Applied Biomaterials*, 109(1): 19-32.
- Epaulard, O., Adam, L., Poux, C., Zurawski, G., Salabert, N., Rosenbaum, P., ... & Martinon, F. (2014). Macrophage-and neutrophil-derived TNF- α instructs skin langerhans cells to prime antiviral immune responses. *The Journal of Immunology*, 193(5): 2416-2426.
- Eriksson, S., Nilsson, J., & Stureson, C. (2014). Non-invasive imaging of microcirculation: a technology review. *Medical Devices: Evidence and Research*, 445-452.
- Fadilah, N. I. M., Phang, S. J., Kamaruzaman, N., Salleh, A., Zawani, M., Sanyal, A., ... & Fauzi, M. B. (2023). Antioxidant biomaterials in cutaneous wound healing and tissue regeneration: A critical review. *Antioxidants*, 12(4): 787.
- Farrokhi, A., Pakyari, M., Nabai, L., Pourghadiri, A., Hartwell, R., Jalili, R., & Ghahary, A. (2018). Evaluation of detergent-free and detergent-based

methods for decellularization of murine skin. *Tissue Engineering Part A*, 24(11-12): 955-967.

Fauzi, M. B., Lokanathan, Y., Aminuddin, B. S., Ruszymah, B. H. I., & Chowdhury, S. R. (2016). Ovine tendon collagen: Extraction, characterisation and fabrication of thin films for tissue engineering applications. *Materials Science and Engineering: C* (68): 163-171.

Fedchenko, N., & Reifenrath, J. (2014). Different approaches for interpretation and reporting of immunohistochemistry analysis results in the bone tissue—a review. *Diagnostic pathology*, (9):1-12.

Fernández-Pérez, J., & Ahearne, M. (2019). The impact of decellularization methods on extracellular matrix derived hydrogels. *Scientific reports*, 9(1): 14933.

Foss, M. A., Stewart, N., & Swift, J. (2008). *Cat Anatomy and Physiology*. Rev. Edition. Washington State University (US).

Franko, R., Franko, Y., Martinez, E. R., Ferronato, G., Heinzelmann, I., Grechi, N., ... & Ferraz, M. D. A. M. M. (2023). Mechanical Properties of Native and Decellularized Reproductive Tissues: Insights for Tissue Engineering Strategies. *bioRxiv*, 2023-10.

Funamoto, S., Nam, K., Kimura, T., Murakoshi, A., Hashimoto, Y., Niwaya, K., ... & Kishida, A. (2010). The use of high-hydrostatic pressure treatment to decellularize blood vessels. *Biomaterials*, 31(13): 3590-3595.

Ghodbane, S. A., & Dunn, M. G. (2016). Physical and mechanical properties of cross-linked type I collagen scaffolds derived from bovine, porcine, and ovine tendons. *Journal of Biomedical Materials Research Part A*, 104(11): 2685-2692.

Gilbert, T. W. (2012). Strategies for tissue and organ decellularization. *Journal of cellular biochemistry*, 113(7): 2217-2222.

- Gilpin, A., & Yang, Y. (2017). Decellularization strategies for regenerative medicine: from processing techniques to applications. *BioMed research international*, 2017.
- Giraldo-Gomez, D. M., Leon-Mancilla, B., Del Prado-Audelo, M. L., Sotres-Vega, A., Villalba-Caloca, J., Garciadiego-Cazares, D., & Piña-Barba, M. C. (2016). Trypsin as enhancement in cyclical tracheal decellularization: morphological and biophysical characterization. *Materials Science and Engineering: C* (98): 930 -937.
- Goh, K. L., & Holmes, D. F. (2017). Collagenous extracellular matrix biomaterials for tissue engineering: lessons from the common sea urchin tissue. *International Journal of Molecular Sciences*, 18(5): 901.
- Goissis, G., de Fátima Giglioti, A., & Braile, D. M. (2011). Preparation and characterization of an acellular bovine pericardium intended for manufacture of valve bioprostheses. *Artificial organs*, 35(5): 484-489.
- Gonzalez, A. C. D. O., Costa, T. F., Andrade, Z. D. A., & Medrado, A. R. A. P. (2016). Wound healing-A literature review. *Anais brasileiros de dermatologia* (91): 614-620.
- Granick, M. S., Tran, B. N. N., & Alvarez, O. M. (2020). Latest Advances in Wound Debridement Techniques. *Surgical technology international*, 36, 37-40.
- Greco, K. V., Francis, L., Somasundaram, M., Greco, G., English, N. R., Roether, J. A., ... & Ansari, T. (2015). Characterisation of porcine dermis scaffolds decellularised using a novel non-enzymatic method for biomedical applications. *Journal of biomaterials applications*, 30(2): 239-253.
- Groves, R. (2012). Quantifying the mechanical properties of skin in vivo and ex vivo to optimise microneedle device design; PhD Thesis; Institute of Medical Engineering and Medical physics; School of Engineering; Cardiff University .

- Guerra, A., Belinha, J., & Jorge, R. N. (2018). Modelling skin wound healing angiogenesis: A review. *Journal of theoretical biology*, (459): 1-17.
- Guimaraes, A. B., Correia, A. T., Alves, B. P., Da Silva, R. S., Martins, J. K., Pêgo-Fernandes, P. M., ... & Cardoso, P. F. G. (2019, June). Evaluation of a physical-chemical protocol for porcine tracheal decellularization. In *Transplantation proceedings* (Vol. 51, No. 5, pp. 1611-1613). Elsevier.
- Gupta, A. and Kumar, P. (2015). Assessment of the histological state of the healing wound. *Plastic and Aesthetic Research*. (2): 239-242
- Gupta, Ankit. (2021). "Classification of Wounds and the Physiology of Wound Healing." *Wound Healing Research: Current Trends and Future Directions* (2021): 3-53.
- Gupta, B. S., & Edwards, J. V. (2019). Textile materials and structures for topical management of wounds. In *Advanced textiles for wound care* (pp. 55-104). Woodhead Publishing.
- Guven, G., Dijkstra, A., Kuijper, T. M., Trommel, N., van Baar, M. E., Topeli, A., ... & van der Vlies, C. H. (2023). Comparison of laser speckle contrast imaging with laser Doppler perfusion imaging for tissue perfusion measurement. *Microcirculation*, 30(1): e12795.
- Häkkinen, L., Larjava, H., & Koivisto, L. (2011). Granulation tissue formation and remodeling. *Endodontic Topics*, 24(1): 94-129.
- Hillebrandt, K. H., Everwien, H., Haep, N., Keshi, E., Pratschke, J., & Sauer, I. M. (2019). Strategies based on organ decellularization and recellularization. *Transplant International*, 32(6): 571-585
- Hollenbeck, D. L., Simon, B. T., Scallan, E. M., Thieman-Mankin, K. M., Miller, D. R., Dunn, A. K., & Dickerson, V. M. (2023). Sedation with dexmedetomidine decreases skin perfusion in cats. *American Journal of Veterinary Research*, 84(12).
- Hoskins, P. R. (2019). Principles of Doppler ultrasound. In *Diagnostic Ultrasound, Third Edition* (pp. 143-158). CRC Press.

- Hrebikova, H., Diaz, D., & Mokry, J. (2015). Chemical decellularization: a promising approach for preparation of extracellular matrix. *Biomed Pap Med Fac Univ Palacky Olomouc Czech Repub*, 159(1): 12-17.
- Hughes, O. B., Rakosi, A., Macquhae, F., Herskovitz, I., Fox, J. D., & Kirsner, R. S. (2016). A review of cellular and acellular matrix products: indications, techniques, and outcomes. *Plastic and Reconstructive Surgery*, 138(3S): 138S-147S.
- Idrus, R. B. H., Rameli, M. A. B. P., Cheong, L. K., Xian, L. J., Hui, C. K., Latiff, M. B. A., & Saim, A. B. (2014). Allogeneic bilayered tissue-engineered skin promotes full-thickness wound healing in ovine model. *Biomed Res India*, (25): 192-198.
- Irfan-Maqsood, M. (2018). Classification of wounds: know before research and clinical practice. *Journal of Genes and Cells*, 4(1): 1-4.
- Irvine, S. M., Cayzer, J., Todd, E. M., Lun, S., Floden, E. W., Negron, L., ... & May, B. C. (2011). Quantification of in vitro and in vivo angiogenesis stimulated by ovine forestomach matrix biomaterial. *Biomaterials*, 32(27): 6351-6361.
- Jarrett, C. L., Shields, K. L., Broxterman, R. M., Hydren, J. R., Park, S. H., Gifford, J. R., & Richardson, R. S. (2020). Imaging transcranial Doppler ultrasound to measure middle cerebral artery blood flow: the importance of measuring vessel diameter. *American Journal of Physiology-Regulatory, Integrative and Comparative Physiology*, 319(1): R33-R42.
- Jaworska-Wilczynska, M., Trzaskoma, P., Szczepankiewicz, A. A., & Hryniewiecki, T. (2016). Pericardium: structure and function in health and disease. *Folia histochemica et cytobiologica*, 54(3): 121-125.
- Jiang, D., & Scharffetter-Kochanek, K. (2020). Mesenchymal stem cells adaptively respond to environmental cues thereby improving granulation tissue formation and wound healing. *Frontiers in cell and developmental biology*, (8): 697.

- Kabashima, K., Honda, T., Ginhoux, F., & Egawa, G. (2019). The immunological anatomy of the skin. *Nature Reviews Immunology*, 19(1): 19-30.
- Kalra, A., Lowe, A., & Al-Jumaily, A. M. (2016). Mechanical behaviour of skin: a review. *J. Mater. Sci. Eng*, 5(4): 1000254.
- Kameyama, H., Udagawa, O., Hoshi, T., Toukairin, Y., Arai, T., & Nogami, M. (2015). The mRNA expressions and immunohistochemistry of factors involved in angiogenesis and lymphangiogenesis in the early stage of rat skin incision wounds. *Legal medicine*, 17(4): 255-260.
- Karnik, T., Dempsey, S. G., Jerram, M. J., Nagarajan, A., Rajam, R., May, B. C., & Miller, C. H. (2019). Ionic silver functionalized ovine forestomach matrix—a non-cytotoxic antimicrobial biomaterial for tissue regeneration applications. *Biomaterials Research*, 23(1): 6.
- Kaur, G., Narayanan, G., Garg, D., Sachdev, A., & Matai, I. (2022). Biomaterials-based regenerative strategies for skin tissue wound healing. *ACS Applied Bio Materials*, 5(5): 2069-2106.
- Kayed, H. R., Sizeland, K. H., Kirby, N., Hawley, A., Mudie, S. T., & Haverkamp, R. G. (2015). Collagen cross linking and fibril alignment in pericardium. *RSC advances*, 5(5): 3611-3618.
- Keane, T. J., Swinehart, I. T., & Badylak, S. F. (2015). Methods of tissue decellularization used for preparation of biologic scaffolds and in vivo relevance. *Methods*, (84): 25-34.
- Kelly, S., Edmonds, R., Cooper, S., Sizeland, K., Wells, H., Ryan, T., ... & Haverkamp, R. (2018). Mapping tear strength and collagen fibril orientation in bovine, ovine and cervine hides and skins. *Journal of the American Leather Chemists Association*, 113(01): 1-11.
- Keymel, S., Sichwardt, J., Balzer, J., Stegemann, E., Rassaf, T., Kleinbongard, P., ... & Lauer, T. (2010). Characterization of the non-invasive assessment

- of the cutaneous microcirculation by laser Doppler perfusion scanner. *Microcirculation*, 17(5): 358-366.
- Khalaf, A. A., Hassanen, E. I., Zaki, A. R., Tohamy, A. F., & Ibrahim, M. A. (2019). Histopathological, immunohistochemical, and molecular studies for determination of wound age and vitality in rats. *International Wound Journal*, 16(6): 1416-1425.
- Khavkin, J.; & Ellis, D. A. (2011). Aging skin: histology, physiology, and pathology. *Facial Plastic Surgery Clinics*, 19(2): 229-234.
- Khosravimelal, S., Momeni, M., Gholipur, M., Kundu, S. C., & Gholipourmalekabadi, M. (2020). Protocols for decellularization of human amniotic membrane. In *Methods in Cell Biology* (Vol. 157, pp. 37-47). Academic Press.
- Kierszenbaum, A. L., & Tres, L. (2015). *Histology and Cell Biology: an introduction to pathology E-Book*. Elsevier Health Sciences.
- Kim, J. J., & Evans, G. R. (2012). Applications of biomaterials in plastic surgery. *Clinics in Plastic Surgery*, 39(4): 359-376.
- Kim, J. K., Koh, Y. D., Kim, J. O., & Seo, D. H. (2016). Development of a decellularization method to produce nerve allografts using less invasive detergents and hyper/hypotonic solutions. *Journal of Plastic, Reconstructive & Aesthetic Surgery*, 69(12): 1690-1696.
- Kolarsick, P. A., BS, M. A. K., MSN, A. C., & Goodwin, C. (2011). APRN-BC. FNP, *Anatomy and Physiology of the Skin* | Top of Form *Journal of the Dermatology Nurses' Association*, 3(2): 1-2.
- Kolarsick, P. A., Kolarsick, M. A., & Goodwin, C. (2011). Anatomy and physiology of the skin. *Journal of the Dermatology Nurses' Association*, 3(4): 203-213.
- Koo, M. A., Jeong, H., Hong, S. H., Seon, G. M., Lee, M. H., & Park, J. C. (2022). Preconditioning process for dermal tissue decellularization using electroporation with sonication. *Regenerative Biomaterials*, (9), rbab071.

- Kožár, M., Hamilton, H., & Koščová, J. (2018). Types of wounds and the prevalence of bacterial contamination of wounds in the clinical practice of small animals. *Folia Veterinaria*, 62(4): 39-47.
- Kumar V, Kumar N, Mathew DD, Gangwar AK, Saxena AC, Remya V. (2013). Repair of abdominal wall hernias using acellular dermal matrix in goats. *Journal of applied animal research*. 1;41(1):117-20
- Kumar, I., Staton, C. A., Cross, S. S., Reed, M. W. R., & Brown, N. J. (2009). Angiogenesis, vascular endothelial growth factor and its receptors in human surgical wounds. *Journal of British Surgery*, 96(12): 1484-1491.
- Kumar, M. A. (2024). The skin. *Techniques in Small Animal Wound Management*, 1.
- Kumar, N., Purohit, S., Kumar, V., Gangwar, A. K., Shrivastava, S., Saxena, S., & Maiti, S. K. (2022). Tissue scaffolds derived from sheep skin. In *Tissue Scaffolds* (pp. 57-64). New York, NY: Springer US.
- Kus, K. J., & Ruiz, E. S. (2020). Wound dressings—a practical review. *Current Dermatology Reports*, 9, 298-308.
- Lam, C. X. F., Mo, X. M., Teoh, S. H., & Hutmacher, D. W. (2002). Scaffold development using 3D printing with a starch-based polymer. *Materials Science and Engineering: C*, 20(1-2): 49-56.
- Landsman, A., Rosines, E., Houck, A., Murchison, A., Jones, A., Qin, X., ... & Landsman, A. R. (2016). Characterization of a cryopreserved split-thickness human skin allograft—TheraSkin. *Advances in Skin & Wound Care*, 29(9): 399-406.
- Langley-Hobbs, S. J., Demetriou, J., & Ladlow, J. (Eds.). (2013). *Feline soft tissue and general surgery*. Elsevier Health Sciences. chapter 17 wound healing by M.W.Bohling pp171-174.
- Lau, L. F. (2016). Cell surface receptors for CCN proteins. *Journal of cell communication and signaling*, (10): 121-127.

- Le Dorze, M., Bouglé, A., Deruddre, S., & Duranteau, J. (2012). Renal Doppler ultrasound: a new tool to assess renal perfusion in critical illness. *Shock*, 37(4): 360-365.
- Lenasi, H., Potočnik, N., Petrishchev, N., Papp, M., Egorkina, A., Girina, M., ... & Kovaleva, A. (2017). The measurement of cutaneous blood flow in healthy volunteers subjected to physical exercise with ultrasound Doppler imaging and laser Doppler flowmetry. *Clinical Hemorheology and Microcirculation*, 65(4), 373-381.
- Levitan, D. M., Hitt, M., Geiser, D. R., & Lyman, R. (2021). Rationale for hyperbaric oxygen therapy in traumatic injury and wound care in small animal veterinary practice. *Journal of Small Animal Practice*, 62(9): 719-729.
- Li, M., Xia, W., Khoong, Y. M., Huang, L., Huang, X., Liang, H., ... & Zan, T. (2023). Smart and versatile biomaterials for cutaneous wound healing. *Biomaterials Research*, 27(1): 87.
- Lima, A., & Bakker, J. (2012). Noninvasive monitoring of peripheral perfusion. *Applied Physiology in Intensive Care Medicine 2: Physiological Reviews and Editorials*, 39-49.
- Linder, K. E. (2020). Structure and Function of the Skin. *Feline Dermatology*, 3-21
- Lu, L. J., Sun, J. B., Liu, Z. G., Gong, X., Cui, J. L., & Sun, X. G. (2009). Immune responses following mouse peripheral nerve xenotransplantation in rats. *BioMed Research International*, 2009(1): 412598.
- Lun, S., Irvine, S. M., Johnson, K. D., Fisher, N. J., Floden, E. W., Negron, L., ... & May, B. C. (2010). A functional extracellular matrix biomaterial derived from ovine forestomach. *Biomaterials*, 31(16): 4517-4529.
- Luze, H., Nischwitz, S. P., Smolle, C., Zrim, R., & Kamolz, L. P. (2022). The use of acellular fish skin grafts in burn wound management—a systematic review. *Medicina*, 58(7): 912.

- Maranduca, M. A., Hurjui, L. L., Branisteanu, D. C., Serban, D. N., Branisteanu, D. E., Dima, N., & Serban, I. L. (2020). Skin a vast organ with immunological function. *Experimental and therapeutic medicine*, 20(1): 18-23.
- McCrary, M. W., Vaughn, N. E., Hlavac, N., Song, Y. H., Wachs, R. A., & Schmidt, C. E. (2020). Novel sodium deoxycholate-based chemical decellularization method for peripheral nerve. *Tissue Engineering Part C: Methods*, 26(1): 23-36.
- McGill, T. J., Stoddard, J., Renner, L. M., Messaoudi, I., Bharti, K., Mitalipov, S., ... & Neuringer, M. (2018). Allogeneic iPSC-derived RPE cell graft failure following transplantation into the subretinal space in nonhuman primates. *Investigative Ophthalmology & Visual Science*, 59(3): 1374-1383.
- Mendoza-Novelo, B., Avila, E. E., Cauich-Rodríguez, J. V., Jorge-Herrero, E., Rojo, F. J., Guinea, G. V., & Mata-Mata, J. L. (2011). Decellularization of pericardial tissue and its impact on tensile viscoelasticity and glycosaminoglycan content. *Acta biomaterialia*, 7(3): 1241-1248.
- Merz, K. M., Pfau, M., Blumenstock, G., Tenenhaus, M., Schaller, H. E., & Rennekampff, H. O. (2010). Cutaneous microcirculatory assessment of the burn wound is associated with depth of injury and predicts healing time. *Burns*, 36(4): 477-482.
- Milde R, Ritter J, Tennent GA, Loesch A, Martinez FO, Gordon S, Pepys MB, Verschoor A, Helming L. Multinucleated giant cells are specialized for complement-mediated phagocytosis and large target destruction. *Cell reports*. 2015 Dec 1;13(9):1937-48.
- Miranda, C. M., Leonel, L. C., Cañada, R. R., Maria, D. A., Miglino, M. A., Del Sol, M., & Lobo, S. E. (2021). Effects of chemical and physical methods on decellularization of murine skeletal muscles. *Anais da Academia Brasileira de Ciências*, 93(2): e20190942.

- Mirani, B., Hadisi, Z., Pagan, E., Dabiri, S. M. H., van Rijt, A., Almutairi, L., ... & Akbari, M. (2023). Smart Dual-Sensor Wound Dressing for Monitoring Cutaneous Wounds. *Advanced Healthcare Materials*, 12(18): 2203233.
- Mirnajafi, A., Raymer, J., Scott, M. J., & Sacks, M. S. (2005). The effects of collagen fiber orientation on the flexural properties of pericardial heterograft biomaterials. *Biomaterials*, 26(7): 795-804.
- Moffat, D., Ye, K., & Jin, S. (2022). Decellularization for the retention of tissue niches. *Journal of tissue engineering*, 13, 20417314221101151.
- Moore, M. A., Samsell, B., Wallis, G., Triplett, S., Chen, S., Jones, A. L., & Qin, X. (2015). Decellularization of human dermis using non-denaturing anionic detergent and endonuclease: a review. *Cell and tissue banking*, 16(2): 249-259.
- Moura, B. S., Monteiro, M. V., Ferreira, L. P., Lavrador, P., Gaspar, V. M., & Mano, J. F. (2022). Advancing tissue decellularized hydrogels for engineering human organoids. *Advanced Functional Materials*, 32(29): 2202825.
- Neishabouri, A., Soltani Khaboushan, A., Daghigh, F., Kajbafzadeh, A. M., & Majidi Zolbin, M. (2022). Decellularization in tissue engineering and regenerative medicine: evaluation, modification, and application methods. *Frontiers in bioengineering and biotechnology*, (10): 805299.
- Nelson, C. M., & Bissell, M. J. (2006). Of extracellular matrix, scaffolds, and signaling: tissue architecture regulates development, homeostasis, and cancer. *Annu. Rev. Cell Dev. Biol.*, 22, 287-309.
- Niculescu, A. G., & Grumezescu, A. M. (2022). An up-to-date review of biomaterials application in wound management. *Polymers*, 14(3): 421.
- Nikahval, B., Oryan, A., Memarian, P., & Kamali, A. (2020). Use of ovine acellular peritoneal matrix combined with honey and ovine fetal skin

extract in the healing of full-thickness infected burn wounds in a rat model. In *Veterinary Research Forum*, 11(4): p. 355.

Nolff M. C., Albert R, Reese S, Meyer-Lindenberg A. (2018). Comparison of negative pressure wound therapy and silver-coated foam dressings in open wound treatment in dogs: a prospective controlled clinical trial. *Veterinary and Comparative Orthopaedics and Traumatology*. 31(04):229-38.

Nolff, M. C. (2021). Dress for Success–Auswahl der richtigen Wundauflage in der Kleintiermedizin. *kleintier konkret*, 24(05): 8-16.

Nolff, M. C., Fehr, M., Reese, S., & Meyer-Lindenberg, A. E. (2017). Retrospective comparison of negative pressure wound therapy and silver-coated foam dressings in open-wound treatment in cats. *Journal of feline medicine and surgery*, 19(6): 624-630.

Norte-Muñoz, M., Gallego-Ortega, A., Lucas-Ruiz, F., González-Riquelme, M. J., Changa-Espinoza, Y. I., Galindo-Romero, C., ... & Agudo-Barriuso, M. (2022). Immune recognition of syngeneic, allogeneic and xenogeneic stromal cell transplants in healthy retinas. *Stem cell research & therapy*, 13(1): 430.

Obagi, Z. A. I. D. A. L., Damiani, G., Grada, A., & Falanga, V. I. N. C. E. N. T. (2019). Principles of wound dressings: a review. *Surg Technol Int*, 35(5): 0-57.

Olczyk, P., Mencner, Ł., & Komosinska-Vassev, K. (2014). The role of the extracellular matrix components in cutaneous wound healing. *BioMed research international*, 2014.

Oliveira, A. C., Garzón, I., Ionescu, A. M., Carriel, V., Cardona, J. D. L. C., González-Andrades, M., ... & Campos, A. (2013). Evaluation of small intestine grafts decellularization methods for corneal tissue engineering. *PloS one*, 8(6): e66538.

O'Neill, J. D., Anfang, R., Anandappa, A., Costa, J., Javidfar, J., Wobma, H. M., ... & Vunjak-Novakovic, G. (2013). Decellularization of human and

- porcine lung tissues for pulmonary tissue engineering. *The Annals of thoracic surgery*, 96(3): 1046-1056.
- Onyekwelu, I., Yakkanti, R., Protzer, L., Pinkston, C. M., Tucker, C., & Seligson, D. (2017). Surgical wound classification and surgical site infections in the orthopaedic patient. *JAAOS Global Research & Reviews*, 1(3): e022.
- Parkale, R., Pulugu, P., & Kumar, P. (2021). Nanomaterials decoration on commercial cotton bandages for pain and infection management. *arXiv preprint arXiv:2105.10273*.
- Pavletic MM: (2018). Basic principles of wound healing. In: *Atlas of small animal wound management and reconstructive surgery*. (Pavletic, MM. Ed.), 4th ed., Wiley-Blackwell, Ames.; pp. 17-31.
- Pearson, R., Kurien, T., Shu, K., & Scammell, B. (2011). Histopathology grading systems for characterisation of human knee osteoarthritis—reproducibility, variability, reliability, correlation, and validity. *Osteoarthritis and Cartilage*, 19(3): 324-331.
- Perc, B., & Erjavec, V. (2022). Overview of wound healing differences between dogs and cats. *Proc. Socrat. Lect*, (7): 167-171.
- Percival, N. J. (2002). Classification of wounds and their management. *Surgery (Oxford)*, 20(5): 114-117.
- Perry, A. G.; Potter, P. A.; Ostendorf, W.; and Cobbett, S. (2019). *Canadian Clinical Nursing Skills and Techniques E-Book*. Elsevier Health Sciences.
- Phillips, M., Maor, E., & Rubinsky, B. (2010). Nonthermal irreversible electroporation for tissue decellularization.
- Pope, J. (2009). Wound aetiology and classification. In *BSAVA Manual of Canine and Feline Wound Management and Reconstruction* (pp. 15-24). BSAVA Library

- Potekaev, N. N., Borzykh, O. B., Medvedev, G. V., Pushkin, D. V., Petrova, M. M., Petrov, A. V., ... & Shnayder, N. A. (2021). The role of extracellular matrix in skin wound healing. *Journal of Clinical Medicine*, 10(24): 5947.
- Prete, S., Dattilo, M., Patitucci, F., Pezzi, G., Parisi, O. I., & Puoci, F. (2023). Natural and Synthetic Polymeric Biomaterials for Application in Wound Management. *Journal of Functional Biomaterials*, 14(9): 455.
- Punjataewakupt, A., & Aramwit, P. (2022). Wound dressing adherence: a review. *Journal of Wound Care*, 31(5): 406-423.
- Rabbani, M., Zakian, N., & Alimoradi, N. (2021). Contribution of physical methods in decellularization of animal tissues. *Journal of Medical Signals & Sensors*, 11(1): 1-11.
- Rahman, S., Griffin, M., Naik, A., Szarko, M., & Butler, P. E. (2018). Optimising the decellularization of human elastic cartilage with trypsin for future use in ear reconstruction. *Scientific reports*, 8(1): 3097.
- Rajkumar, T. (2001). Growth factors and growth factor receptors. *Current science*, 81(5).
- Ramm, R., Goecke, T., Theodoridis, K., Hoeffler, K., Sarikouch, S., Findeisen, K., ... & Hilfiker, A. (2020). Decellularization combined with enzymatic removal of N-linked glycans and residual DNA reduces inflammatory response and improves performance of porcine xenogeneic pulmonary heart valves in an ovine in vivo model. *Xenotransplantation*, 27(2): e12571.
- Rashtbar, M., Hadjati, J., Ai, J., Shirian, S., Jahanzad, I., Azami, M., ... & Sadroddiny, E. (2018). Critical-sized full-thickness skin defect regeneration using ovine small intestinal submucosa with or without mesenchymal stem cells in rat model. *Journal of Biomedical Materials Research Part B: Applied Biomaterials*, 106(6): 2177-2190.
- Ribeiro, J. F., dos Anjos, E. H. M., Mello, M. L. S., & de Campos Vidal, B. (2013). Skin collagen fiber molecular order: a pattern of distributional fiber

orientation as assessed by optical anisotropy and image analysis. *PLoS One*, 8(1): e54724.

- Riha, S. M., Maarof, M., & Fauzi, M. B. (2021). Synergistic effect of biomaterial and stem cell for skin tissue engineering in cutaneous wound healing: A concise review. *Polymers*, 13(10): 1546.
- Rodrigues, M., Kosaric, N., Bonham, C. A., & Gurtner, G. C. (2019). Wound healing: a cellular perspective. *Physiological reviews*, 99(1): 665-706.
- Rosselli, D. D. (2024). Wound Types and Terminology. *Techniques in Small Animal Wound Management*, p.73.
- Roustit, M., & CRACOWSKI, J. L. (2012). Non-invasive assessment of skin microvascular function in humans: an insight into methods. *Microcirculation*, 19(1): 47-64.
- Rowley, A. T., Nagalla, R. R., Wang, S. W., & Liu, W. F. (2019). Extracellular matrix-based strategies for immunomodulatory biomaterials engineering. *Advanced healthcare materials*, 8(8): 1801578.
- Sánchez-Arévalo, F. M., Farfán, M., Covarrubias, D., Zenit, R., & Pulos, G. (2010). The micromechanical behavior of lyophilized glutaraldehyde-treated bovine pericardium under uniaxial tension. *Journal of the Mechanical Behavior of Biomedical Materials*, 3(8): 640-646.
- Sarvazyan, N. (2020). Scaffolds and Tissue Decellularization. *Tissue Engineering: Principles, Protocols, and Practical Exercises*, 103-114.
- Schmidt, M. M., Dornelles, R. C. P., Mello, R. O., Kubota, E. H., Mazutti, M. A., Kempka, A. P., & Demiate, I. M. (2016). Collagen extraction process. *International food research journal*, 23(3): 913.
- Schnell, D., & Darmon, M. (2015). Bedside Doppler ultrasound for the assessment of renal perfusion in the ICU: advantages and limitations of the available techniques. *Critical ultrasound journal*, 7(1): 8.

- Schultz, G. S., & Wysocki, A. (2009). Interactions between extracellular matrix and growth factors in wound healing. *Wound repair and regeneration*, 17(2): 153-162.
- Schultz, G. S., Sibbald, R. G., Falanga, V., Ayello, E. A., Dowsett, C., Harding, K., ... & Vanscheidt, W. (2003). Wound bed preparation: a systematic approach to wound management. *Wound repair and regeneration*, (11): S1-S28.
- Sellaro, T. L., Hildebrand, D., Lu, Q., Vyavahare, N., Scott, M., & Sacks, M. S. (2007). Effects of collagen fiber orientation on the response of biologically derived soft tissue biomaterials to cyclic loading. *Journal of Biomedical Materials Research Part A: An Official Journal of The Society for Biomaterials, The Japanese Society for Biomaterials, and The Australian Society for Biomaterials and the Korean Society for Biomaterials*, 80(1): 194-205.
- Shi, J., Votrubia, A. R., Farokhzad, O. C., & Langer, R. (2010). Nanotechnology in drug delivery and tissue engineering: from discovery to applications. *Nano letters*, 10(9): 3223-3230.
- Sierad, L. N., Shaw, E. L., Bina, A., Brazile, B., Rierison, N., Patnaik, S. S., ... & Simionescu, D. T. (2015). Functional heart valve scaffolds obtained by complete decellularization of porcine aortic roots in a novel differential pressure gradient perfusion system. *Tissue Engineering Part C: Methods*, 21(12): 1284-1296.
- Silvipriya, K. S., Kumar, K. K., Bhat, A. R., Kumar, B. D., & John, A. (2015). Collagen: Animal sources and biomedical application. *Journal of Applied Pharmaceutical Science*, 5(3): 123-127.
- Singh, H., Purohit, S. D., Bhaskar, R., Yadav, I., Gupta, M. K., & Mishra, N. C. (2022). Development of decellularization protocol for caprine small intestine submucosa as a biomaterial. *Biomaterials and Biosystems*, (5), 100035.

- Sizeland, K. H., Basil-Jones, M. M., Edmonds, R. L., Cooper, S. M., Kirby, N., Hawley, A., & Haverkamp, R. G. (2013). Collagen orientation and leather strength for selected mammals. *Journal of agricultural and food chemistry*, 61(4): 887-892.
- Sizeland, K. H., Wells, H. C., Higgins, J., Cunanan, C. M., Kirby, N., Hawley, A., ... & Haverkamp, R. G. (2014). Age dependent differences in collagen alignment of glutaraldehyde fixed bovine pericardium. *BioMed research international*, 2014.
- Smandri, A., Nordin, A., Hwei, N. M., Chin, K. Y., Abd Aziz, I., & Fauzi, M. B. (2020). Natural 3D-printed bioinks for skin regeneration and wound healing: A systematic review. *Polymers*, 12(8): 1782.
- Sojo, K., Sawaki, Y., Hattori, H., Mizutani, H., & Ueda, M. (2005). Immunohistochemical study of vascular endothelial growth factor (VEGF) and bone morphogenetic protein-2, -4 (BMP-2, -4) on lengthened rat femurs. *Journal of Cranio-Maxillofacial Surgery*, 33(4), 238-245.
- Sokol, A. A., Grekov, D. A., Yemets, G. I., Galkin, A. Y., Shchotkina, N. V., Dovghaliuk, A. A., ... & Yemets, I. M. (2020). Comparison of bovine pericardium decellularization protocols for production of biomaterial for cardiac surgery. *Biopolymers & Cell*, 36(5): 392.
- Stavropoulos, A., Chiantella, G., Costa, D., Steigmann, M., Windisch, P., & Sculean, A. (2011). Clinical and histologic evaluation of a granular bovine bone biomaterial used as an adjunct to GTR with a bioresorbable bovine pericardium collagen membrane in the treatment of intrabony defects. *Journal of periodontology*, 82(3): 462-470.
- Stewart, C. J., Gallant-Behm, C. L., Forrester, K., Tulip, J., Hart, D. A., & Bray, R. C. (2006). Kinetics of blood flow during healing of excisional full-thickness skin wounds in pigs as monitored by laser speckle perfusion imaging. *Skin Research and Technology*, 12(4): 247-253.
- Stone, W. L., Leavitt, L., & Varacallo, M. (2017). Physiology, growth factor.

- Subramaniam, T., Hadi, N. S., Sulaiman, S., Fauzi, M. B., Idrus, R. B. H., Chowdhury, S. R., ... & Maarof, M. (2022). Comparison of three different skin substitutes in promoting wound healing in an ovine model. *Burns*, 48(5): 1198-1208.
- Sultana, J.; Molla, M.R.; Kamal, M.; Shahdullah, M.; Begum, F. and Bashir, M.A.(2009). Histological differences in wound healing in maxillofacial region in patients with or without risk factors. *Bangladesh Journal of Pathology*. 24(1):3-8
- Syed, O., Walters, N. J., Day, R. M., Kim, H. W., & Knowles, J. C. (2014). Evaluation of decellularization protocols for production of tubular small intestine submucosa scaffolds for use in oesophageal tissue engineering. *Acta biomaterialia*, 10(12): 5043-5054.
- Tan, J., Zhang, Q. Y., Huang, L. P., Huang, K., & Xie, H. Q. (2021). Decellularized scaffold and its elicited immune response towards the host: The underlying mechanism and means of immunomodulatory modification. *Biomaterials Science*, 9(14): 4803-4820.
- Tebyanian, H., Karami, A., Motavallian, E., Aslani, J., Samadikuchaksaraei, A., Arjmand, B., & Nourani, M. R. (2017). Histologic analyses of different concentrations of TritonX-100 and Sodium dodecyl sulfate detergent in lung decellularization. *Cellular and Molecular Biology*, 63(7): 46-51.
- Tsioli, V., Gouletsou, P. G., Galatos, A. D., Psalla, D., Lymperis, A., Papazoglou, L. G., & Karayannopoulou, M. (2016). Effects of two occlusive, hydrocolloid dressings on healing of full-thickness skin wounds in cats. *Veterinary and Comparative Orthopaedics and Traumatology*, 29(04): 298-305.
- Tsioli, V., Gouletsou, P. G., Galatos, A. D., Psalla, D., Lymperis, A., Sideri, A. I., & Papazoglou, L. G. (2018). The effect of a hydrocolloid dressing on second intention wound healing in cats. *Journal of the American Animal Hospital Association*, 54(3): 125-131

- Varol, A. L., & Anderson, C. D. (2010). A minimally invasive human in vivo cutaneous wound model for the evaluation of innate skin reactivity and healing status. *Archives of dermatological research*, (302): 383-393
- Veith, A. P., Henderson, K., Spencer, A., Sligar, A. D., & Baker, A. B. (2019). Therapeutic strategies for enhancing angiogenesis in wound healing. *Advanced drug delivery reviews*, (146): 97-125.
- Vignery A. (2005). Macrophage fusion: the making of osteoclasts and giant cells. *The Journal of experimental medicine* 1;202(3):337-40.
- Volk, S. W., & Bohling, M. W. (2013). Comparative wound healing—are the small animal veterinarian's clinical patients an improved translational model for human wound healing research? *Wound Repair and Regeneration*, 21(3): 372-381.
- Vural, E., Berbée, M., Acott, A., Blagg, R., Fan, C.-Y., & Hauer-Jensen, M. (2010). Skin Graft Take Rates, Granulation, and Epithelialization: Dependence on Myeloid Cell Hypoxia-Inducible Factor 1 α . *Archives of Otolaryngology–Head & Neck Surgery*, 136(7): 720-723
- Wang, B., Qinglai, T., Yang, Q., Li, M., Zeng, S., Yang, X., ... & Li, S. (2023). Functional acellular matrix for tissue repair. *Materials Today Bio*, (18): 100530.
- Wenger, M. P., Bozec, L., Horton, M. A., & Mesquida, P. (2007). Mechanical properties of collagen fibrils. *Biophysical journal*, 93(4): 1255-1263.
- Whelan, A., Duffy, J., Gaul, R. T., O'Reilly, D., Nolan, D. R., Gunning, P., & Lally, C. (2019). Collagen fibre orientation and dispersion govern ultimate tensile strength, stiffness and the fatigue performance of bovine pericardium. *Journal of the mechanical behavior of biomedical materials*, (90): 54-60.
- White, M. E. (2019). Genetic mapping of novel loci affecting clinical phenotypes of the domestic dog and cat

- Wickett, R. R., & Visscher, M. O. (2017). Structure and function of the epidermal barrier. *American Journal of Infection Control*, 34(10): S98–S110.
- Wilkins, R. G., & Unverdorben, M. (2013). Wound cleaning and wound healing: a concise review. *Advances in skin & wound care*, 26(4): 160-163.
- Windschnurer, I., Häusler, A., Waiblinger, S., & Coleman, G. J. (2022). Relationships between owner and household characteristics and enrichment and cat behaviour. *Applied Animal Behaviour Science*, (247): 105562.
- Wong, M. L., & Griffiths, L. G. (2014). Immunogenicity in xenogeneic scaffold generation: antigen removal vs. decellularization. *Acta biomaterialia*, 10(5): 1806-1816.
- Wong, R., Geyer, S., Weninger, W., Guimberteau, J. C., & Wong, J. K. (2016). The dynamic anatomy and patterning of skin. *Experimental dermatology*, 25(2): 92-98.
- Wu, J. Z., Cutlip, R. G., Welcome, D., & Dong, R. G. (2006). Estimation of the viscous properties of skin and subcutaneous tissue in uniaxial stress relaxation tests. *Bio-medical materials and engineering*, 16(1): 53-66.
- Xin, H., Ferguson, B. M., Wan, B., Al Maruf, D. A., Lewin, W. T., Cheng, K., ... & Clark, J. R. (2024). A Preclinical Trial Protocol Using an Ovine Model to Assess Scaffold Implant Biomaterials for Repair of Critical-Sized Mandibular Defects. *ACS Biomaterials Science & Engineering*.
- Xing, Q., Yates, K., Tahtinen, M., Shearier, E., Qian, Z., & Zhao, F. (2015). Decellularization of fibroblast cell sheets for natural extracellular matrix scaffold preparation. *Tissue Engineering Part C: Methods*, 21(1): 77-87.
- Xing, S., Liu, C., Xu, B., Chen, J., Yin, D., & Zhang, C. (2014). Effects of various decellularization methods on histological and biomechanical properties of rabbit tendons. *Experimental and Therapeutic Medicine*, 8(2): 628-634.

- Xu, A. T., Qi, W. T., Lin, M. N., Zhu, Y. H., & He, F. M. (2020). The optimization of sintering treatment on bovine-derived bone grafts for bone regeneration: in vitro and in vivo evaluation. *Journal of Biomedical Materials Research Part B: Applied Biomaterials*, 108(1): 272-281.
- Yadav, N., Parveen, S., Chakravarty, S., & Banerjee, M. (2019). Skin anatomy and morphology. *Skin Aging & Cancer: Ambient UV-R Exposure*, 1-10.
- Yamanaka, H., Morimoto, N., & Yamaoka, T. (2020). Decellularization of submillimeter-diameter vascular scaffolds using peracetic acid. *Journal of Artificial Organs*, (23):156-162.
- Yang, J., Dang, H., & Xu, Y. (2022). Recent advancement of decellularization extracellular matrix for tissue engineering and biomedical application. *Artificial organs*, 46(4): 549-567.
- Yousef H, Alhajj M, Sharma S. (2023). Anatomy, Skin (Integument), Epidermis. In: StatPearls. StatPearls Publishing, Treasure Island (FL); 2023. PMID: 29262154.
- Yu, Q., Chen, H., Sheng, L., Liang, Y., & Li, Q. (2014). Sodium tanshinone IIA sulfonate prolongs the survival of skin allografts by inhibiting inflammatory cell infiltration and T cell proliferation. *International immunopharmacology*, 22(1): 277-284.
- Zak, M., Kuropka, P., Kobielarz, M., Dudek, A., Kaleta-Kuratewicz, K., & Szotek, S. (2011). Determination of the mechanical properties of the skin of pig foetuses with respect to its structure. *Acta of Bioengineering and Biomechanics*, 13(2): 37-43
- Zhang, X., Chen, X., Hong, H., Hu, R., Liu, J., & Liu, C. (2022). Decellularized extracellular matrix scaffolds: Recent trends and emerging strategies in tissue engineering. *Bioactive materials*, (10):15-31.
- Zhao, Y., Li, Y., Peng, X., Yu, X., Cheng, C., & Yu, X. (2021). Feasibility study of oxidized hyaluronic acid cross-linking acellular bovine pericardium

with potential application for abdominal wall repair. *International Journal of Biological Macromolecules*, (184): 831-842.

Zhou, J., Fritze, O., Schleicher, M., Wendel, H. P., Schenke-Layland, K., Harasztosi, C., ... & Stock, U. A. (2010). Impact of heart valve decellularization on 3-D ultrastructure, immunogenicity and thrombogenicity. *Biomaterials*, 31(9): 2549-2554.

Zouhair, S., Dal Sasso, E., Tuladhar, S. R., Fidalgo, C., Vedovelli, L., Filippi, A., ... & Iop, L. (2020). A comprehensive comparison of bovine and porcine decellularized pericardia: new insights for surgical applications. *Biomolecules*, 10(3): 371.

الخلاصة

تم تخطيط هذه الدراسة لمقارنة جلد الاغنام اللاخوي وتامور الابقار اللاخوي كضمادات بيولوجية لأصلاح الجروح الجلدية الكبيرة المستحدثة في القطط. تم تقسيم حيوانات التجربة الثمانية عشر من القطط البالغة من السلالة المحلية إلى مجموعتين متساويتين. تم إنشاء جروح جلدية كاملة السماكة بأبعاد 4×4 سم على ظهور جميع القطط. في المجموعة الأولى، تم استخدام جلد الاغنام اللاخوي برفعة 3×3 سم لتضميد هذه الجروح الظهيرية كاملة السماكة بينما تم استخدام تامور الابقار اللاخوي بنفس الحجم لتغطية هذه الجروح المستحدثة في المجموعة الثانية. بشكل عام، تم تقييم التئام الجروح يوميًا بعد التضميد في كلتا المجموعتين، بالإضافة إلى الفحص النسيجي المرضي والدراسة المناعية الكيميائية والموجات فوق الصوتية في الأيام 7 و 14 و 21. كما تم الاعتماد على الخواص الميكانيكية لكل من الضمادات البيولوجية قبل وبعد إزالة الخلايا.

أظهرت نتائج الفحوصات السريرية وجود فرق كبير ($P < 0.05$) بين المجموعتين في مرونة ولون ومدى التصاق الضمادة البيولوجية بفراش الجرح السفلي. وأظهرت نتائج قياسات التخطيط الفيزيائي لحجم الجرح التي أجريت في الأيام 0 و 7 و 14 و 21 بعد الضمادة وجود انخفاض في منطقة حجم الجرح خاصة في المجموعة الأولى مقارنة بالمجموعة الثانية. بالإضافة إلى ذلك، زادت نسبة الانكماش ووصلت إلى 65% من حجم الجرح. كما زادت نسبة التئام الجروح الكلية من اليوم 0 إلى اليوم 21 حيث وصلت إلى أكثر من 85%.

بينت المظاهر النسيجية المرضية وجود اختلافات كبيرة في معظم المعايير النسيجية المرضية الملاحظة بين المجموعتين طوال فترة الدراسة. في المجموعة الأولى، كان تضميد الجروح بجلد الاغنام اللاخوي في اليوم السابع أفضل بكثير والذي تميز بوجود نسيج حبيبي متطور جيدًا وتكوين الأوعية الدموية الجيد واستجابة التهابية أقل وتسلسل للخلايا الالتهابية متعددة النوى وأحادية النواة مقارنة بتضميد الجروح بتامور الابقار اللاخوي في المجموعة الثانية. إلى جانب ذلك، كشف فحص الموجات فوق الصوتية دوبلر عن وجود تدفق دم جيد منذ اليوم العاشر والذي أصبح أكثر قابلية للكشف في اليوم الثاني عشر في المجموعة الأولى واليوم الرابع عشر في المجموعة الثانية، ثم استمر في الزيادة حتى وصل إلى ذروته في اليوم الحادي والعشرين.

أظهرت نتائج الكيمياء المناعية لقياس شدة تفاعل عامل نمو بطانة الأوعية الدموية وجود شدة تفاعل جيدة ومتفاوتة لـ VEGF في كلتا المجموعتين. إلا أن ذلك التفاعل في المجموعة الأولى والتعبير عن VEGF وشدته كان أكثر من المجموعة الثانية. علاوة على ذلك، أظهر اختبار

ب

الخصائص الميكانيكية لكلا الأنسجة اللاخلوية تحسناً كبيراً في خصائصها الميكانيكية بعد إزالة الخلايا وخاصة الحمل الأقصى ومعامل المرونة. باختصار، كان جلد الأغنام اللاخلوي أفضل بكثير من تامور البقري اللاخلوي كضمانة بيولوجية لألتئام الجروح الواسعة النطاق في القطط.

مقارنة بين ضمادتين بايولوجية لألتئام الجروح الجلدية المستحدثة في القطط

رساله تقدم بها

مصطفى محمد زكي دنون

الى

مجلس كلية البيطري في جامعة الموصل
في اختصاص الطب البيطري / الجراحة البيطرية
وهي جزء من متطلبات نيل شهادة الماجستير

بإشراف

الأستاذ المساعد الدكتور

سحر محمد أبراهيم



جامعة الموصل
كلية الطب البيطري

مقارنة بين ضمادتين بايولوجية لألتئام الجروح الجلدية المستحدثة في القطط

مصطفى محمد زكي ذنون

رسالة ماجستير

في اختصاص الطب البيطري / الجراحة البيطرية

بإشراف

الأستاذ المساعد الدكتور

سحر محمد أبراهيم